# The Role of WT1 and GATA4 during Gonad Development in Mice

Inaugural-Dissertation

to obtain the academic degree

Doctor rerum naturalium (Dr. rer. nat.)

submitted to the Department of Biology, Chemistry and Pharmacy

of Freie Universität Berlin


by

Lucas Johannes Rudigier

from Hard am Bodensee

2015

The doctoral thesis was performed in the laboratory and under the supervision of Prof. Dr. Holger Scholz in the Institute for Vegetative Physiology at the Charité -Universitätsmedizin Berlin - between September 2011 and March 2015.

1st Reviewer: Prof. Dr. Holger Scholz

2nd Reviewer: Prof. Dr. Christian Freund

date of defence: 22.07.2015

“Take the risk of thinking for yourself,
much more happiness, truth, beauty,
and wisdom will come to you that way.“

*Christopher Hitchens*
*(13 April 1949 – 15 December 2011), engl. author*

# Acknowledgements

This work would not have been possible without the help of many people. Foremost, I am grateful to Holger Scholz who gave me the opportunity to perform this project in his lab and I am thankful for his supervision. His constant support and encouragement was endless and I am much obliged for the freedom he granted me to bring in my own ideas in order to pursue this project.

I express my gratitude to Karin Kirschner for her supervision and fruitful discussions that contributed immensely to the final outcome of the project. Not only was she there to debate theoretical issues but also when technical problems arose Karin had an open ear. Moreover, I am in debt of gratitude to Ulrike Neuman for her technical support and her problem solving abilities. It would not have been as much fun without you and thanks for the time being there to chit-chat. A special thank you goes to Anja Persson, for being there to help with bureaucracy and writing related matters. Thank you to the lab's former technicans Mrs. Inge Graetsch and Mrs. Angelika Richter. I would also like to thank all of the other lab members for their support.

In addition, I am very grateful to have spent this time with some people who made this time as enjoyable as it was and therefore I can't take credit for it all. Cheers Matthias Münzner, Philip Prince, Mads Danger, Daniela Ellinger, Ruben Aubrecht, Maria Anwander, Antje Krüger, Tracie Pennimpede, Benedikt Schwartz, Arica Beisaw and Eu-han Shin.

Finally, thanks to all of my friends back in Austria and a special thank you goes out to my parents - Annemarie and Werner Rudigier - my sister Christina and my brother Sebastian without their constant support this would not have been possible.

# Contents

# List of Figures

# List of Tables

## LIST OF ABBREVIATIONS

# List of Abbreviations

| | |
|---|---|
| **3'UTR** | 3' untranslated region |
| **aa** | amino acid |
| **AD** | activation domain |
| **Amh** | anti-Müllerian hormone |
| **Amhr2** | anti-Müllerian hormone receptor, type II |
| **APS** | ammoniumperoxodisulfat |
| **Bmp** | bone morphogenetic protein |
| **bp** | base pairs |
| **BrdU** | 5-bromo-2'-deoxyuridine |
| **CBP** | CREB-binding protein |
| **CBX2** | chromobox homolog 2 |
| **cDNA** | complementary DNA |
| **ce** | coelomic epithelium |
| **ChIP** | chromatin immunoprecipitation |
| **ChIP-chip** | chromatin immunoprecipitation - DNA microarray |
| **CITED2** | Cbp/p300-interacting transactivator, with Glu/Asp-rich carboxy-terminal domain, 2 |
| **CRISPR/Cas9** | clustered regularly interspaced short palindromic repeats/ CRISPR associated nuclease 9 |
| **Ct** | cycle threshold |

| | |
|---|---|
| **Ctnnb1** | catenin - cadherin-associated protein-beta 1 |
| **DAPI** | 4',6-diamidino-2-phenylindole |
| **Dax1** | dosage-sensitive sex reversal, adrenal hypoplasia critical region, on chromosome X, gene 1 |
| **DBD** | DNA binding domain |
| **DHH** | desert hedgehog homolog |
| **DNA** | deoxyribonucleic acid |
| **DP** | prostaglandin D2 receptor |
| **dpc** | days post conception |
| **DSDs** | developmental sexual disorders |
| **DTT** | dithiothreitol |
| **EDTA** | ethylenediaminetetraacetic acid |
| **EMSA** | electrophoretic mobility shift assay |
| **EMX2** | empty spiracles homeobox 2 |
| **ESR1** | estrogen receptor 1 |
| **EtOH** | ethanol |
| **FBS** | fetal bovine serum |
| **FGF9** | fibroblast growth factor 9 |
| **FGFR2** | fibroblast growth factor receptor 2 |
| **Foxl2** | forkhead box protein L2 |
| **Fst** | follistatin |
| **GADD45G** | growth arrest and DNA-damage-inducible protein 45 gamma |
| **Gapdh** | glyceraldehyde-3- phosphate dehydrogenase |
| **Gata4** | GATA binding protein 4 |
| **Gsk3$\beta$** | glycogen synthase kinase 3 beta |

| | |
|---|---|
| **IB** | immunoblot |
| **IGFR** | insulin-like growth factor 1 receptor |
| **IHC** | immunohistochemistry |
| **IR** | insulin receptor |
| **IRR** | insulin receptor-related receptor |
| **JMJD1** | lysine (K)-specific demethylase 3A |
| **Kdm5d** | lysine-specific demethylase 5D |
| **KTS** | lysine, threonin, serin |
| **LHX9** | LIM homeobox 9 |
| **LiCl** | lithiumchloride |
| **MAPK** | mitogen-activated protein kinases |
| **Mism** | mismatch |
| **MO** | morpholino |
| **mRNA** | messenger RNA |
| **NKX2.5** | NK2 homeobox 5 |
| **NLS** | nuclear localization signal |
| **p21** | cyclin-dependent kinase inhibitor 1A |
| **p27** | cyclin-dependent kinase inhibitor 1B |
| **p38** | p38 mitogen-activated protein kinases |
| **p53** | tumor protein p53 |
| **p57** | cyclin-dependent kinase inhibitor 1C |
| **PBS** | phosphate-buffered saline |
| **PCR** | polymerase chain reaction |
| **Pdgfra** | platelet-derived growth factor receptor |
| **PGC** | primordial germ cells |

| | |
|---|---|
| **PGD2** | prostaglandin D2 |
| **Pgds** | prostaglandin synthase |
| **PTM** | peritubular myoid cells |
| **RA** | retinoic acid |
| **RD** | repression domain |
| **RNA** | bibonucleic acid |
| **RT-qPCR** | reverse transcription quantitative polymerase chain reaction |
| **SAD** | self association domain |
| **SC35** | spliceosome component of 35kDa |
| **Sdha** | succinate dehydrogenase |
| **SDS** | sodiumdodecylsulfat |
| **Sf1** | steroidogenic factor 1 |
| **SF2** | splice factor 2 |
| **siRNA** | short interfering RNA |
| **SIX1/SIX4** | sine oculis-related homeobox 1 / 4 |
| **Sox9** | sex determining region Y-box 9 |
| **Sry** | sex determining region Y |
| **Star** | steroidogenic acute regulatory protein |
| **TBST** | tris buffered saline tween |
| **tc** | testicular cords |
| **TEMED** | tetramethylethylendiamin |
| **TESCO** | testis-specific enhancer of Sox9 core |
| **TGF** | transforming growth factor |
| **ts** | tail somites |
| **U1-70K** | U1 small nuclear ribonucleoprotein-70K |

| | |
|---|---|
| **U2AF65** | U2 small nuclear ribonucleoprotein auxiliary factor 65kDa |
| **Vegf** | Vascular endothelial growth factor |
| **WAGR** | wilms tumour, aniridia, genitourinary anomalies, retardation |
| **Wt1** | Wilms' tumuor suppressor |

# 1

# Introduction

## 1.1 Gonad development: an overview

The decision of whether an individual becomes a female or a male is well-founded on the fact that at the time of fertilisation either an X or the Y-chromosome is inherited paternally and sets the direction of sex-development (1). Is the genotype of XX – a girl develops – if the Y-chromosome is passed onwards, hence the genotype XY – a boy develops (2; 3). The inheritance of the sex chromosomes, as important and essential it is, provokes downstream effects that are not only intertwined but at the same time rely on a tight network of factors that have to act in a precise spatiotemporal manner (1; 4). These factors fine-tune and regulate pathways that eventually culminate in the proper development of the sexes (1). Is this process perturbed, severe consequences follow that appear as disorders of sexual development (DSDs), and patients suffer from both physiological and psychological health issues (5; 6). The organ that propagates the development of either sex is called the gonad. Throughout the process of embarking into either direction, the gonad – within a narrow window of time – undergoes major molecular changes that can be distinguished as the processes of sex-determination and sex-differentiation (7; 8; 9). The former is driven by genetic cues and the latter is the result of a hormonal response that dictates the progression of the anatomical configuration of the reproductive tract (1).

## 1.2 Sex-determination and -differentiation: signals that drive testis or ovary development

### 1.2.1 The bipotential gonad and the morphology of a testis and an ovary

The undifferentiated or bipotential gonad is different from other organs as it can bring about two divergent structures, namely either testes or ovaries. It is compelling to understand how this organ initially arises and during the course of development differentiates into either one of the fates. The gonad initially arises from the intermediate mesoderm and becomes visible at about 10.5 dpc above the mesonephros as a result of the thickening of the coelomic epithelium at the ventromedial midline on either side (Figure 1.1 A) (10; 11). What renders the bipotential gonad so unique, is that precursor cells within the gonad are able to differentiate – dependent on the genetic signature – into either direction (12). Crucial for the decision to embark towards one of the fates is the underlying sex genotype that is either XY or XX. The Y-chromosome linked gene termed sex-determining region Y, in short *Sry*, shifts the fate of the bipotential gonad towards the male direction as shown by previous experiments (3; 13). Along these lines, given precursor cells in the bipotential gonad are capable of differentiating into the Sertoli cell lineage in the presence of SRY activity and in response to certain signalling cues (14). During the progression of male gonadal development Sertoli cells become rearranged and form in conjunction with peritubular myoid (PTM) cells and the basal lamina the characteristic features of a testis, the testicular cords, which first appear at around 12.5 dpc (15; 16). These cell types bestow the structural integrity of the testicular cords, which enclose germ cells that eventually undergo spermatogenesis (17; 18). Furthermore, Sertoli cells provide a nutrient source for the germ cells (1). An additional major cell lineage within the testis are the Leydig cells. These cells are located within the interstitium of the gonad and produce testosterone, which supports the progression of the Wolffian duct (Figure 1.1 B) (1). The Wolffian duct eventually gives rise to the male reproductive tract, encompassing the rete testis, efferent ducts, epididymis, vas deferens, and seminal vesicles (Figure 1.2 B). On the other hand, during ovarian development given precursor cells within the bipotential gonad differentiate into the granulosa cell lineage due to the exposure of ovarian promoting signals in the absence of the Y-chromosome, hence lack of SRY activity (Figure 1.3) (19; 20). The granulosa cell type is the female counterpart to the Sertoli cell lineage and both originate from a common precursor cell type dependent on the underlying signalling cues (14; 21). The second main cell lineage that the ovary constitutes are the theca cells, the counterpart to the Leydig cells (22). These cells are implicated in estrogen biosyntheses

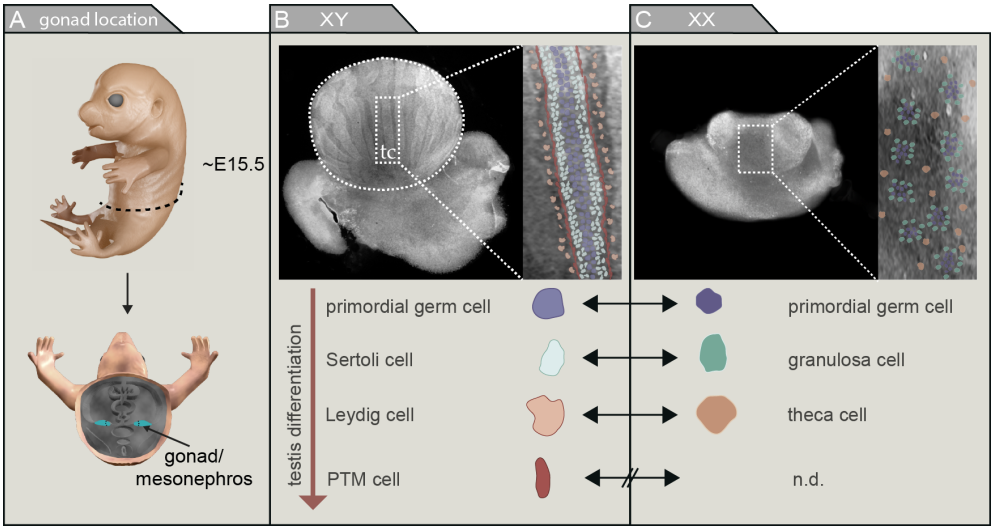


**Figure 1.1: Cell biology of the gonad.** (A) A 3D model (Autodesk Maya - Student version 2015) of an ∼15.5 dpc embryo is shown and illustrates the location of the gonad in cyan within the body cavity. (B) Left: The top panel shows a testis with the testicular cords (tc). A higher magnification of the inset is illustrated to its right and depicts the major cell types within a testis. (C) Left: The ovary is shown and a region is highlighted as an inset to its right, which illustrates the major cell types comprising an ovary. The bottom panel on either side (B,C) pinpoints the major cell types in the gonad and stresses the point that PGC (primordial germ cells), Sertoli, granulosa, Leydig, and theca cells originate from a common precursor. A defined counterpart in the ovary to the PTM cells in the testis has not been identified yet (26; 27). n.d.: not defined.

by producing adrogens which are converted to estrogen by the granulosa cells (23). However, the origin of the theca cell lineage is not clear yet (24). This particular ovarian environment eventually drives the development of the female reproductive tract. In the ovary, the Wolffian duct degenerates but at the same time the Müllerian duct differentiates into the ovidicut, uterus, cervix, and vagina (Figure 1.2 C) (25). The ovarian morphological characteristics are merely reflected by the development of the primordial follicles into the primary follicles. This process occurs shortly after birth and the morphological characteristics appear less prominent when compared to the testis morphology (1; 12). During this process, oocytes are layered by granulosa cells which in turn are encompassed by theca cells (24). Thereby granulosa cells and theca cells provide a nourishing source for the germ cells and assuring their structural integrity (Figure 1.1 C) (24).

In order to guarantee the proper development of either fate the precise regulation of various factors within a narrow time window is required. A number of factors have been identified that are essential for the development of the bipotential gonad, i.e., SIX1/SIX4 (29), IGF1R/IRR/IR (30), SF1 (31), WT1 (32), LHX9 (33), M33 (34), EMX2 (35), and GATA4 (36; 37) (Figure 1.3). All of these factors are rather essential in the maintenance of the developmental process of the gonad compared to the initiation

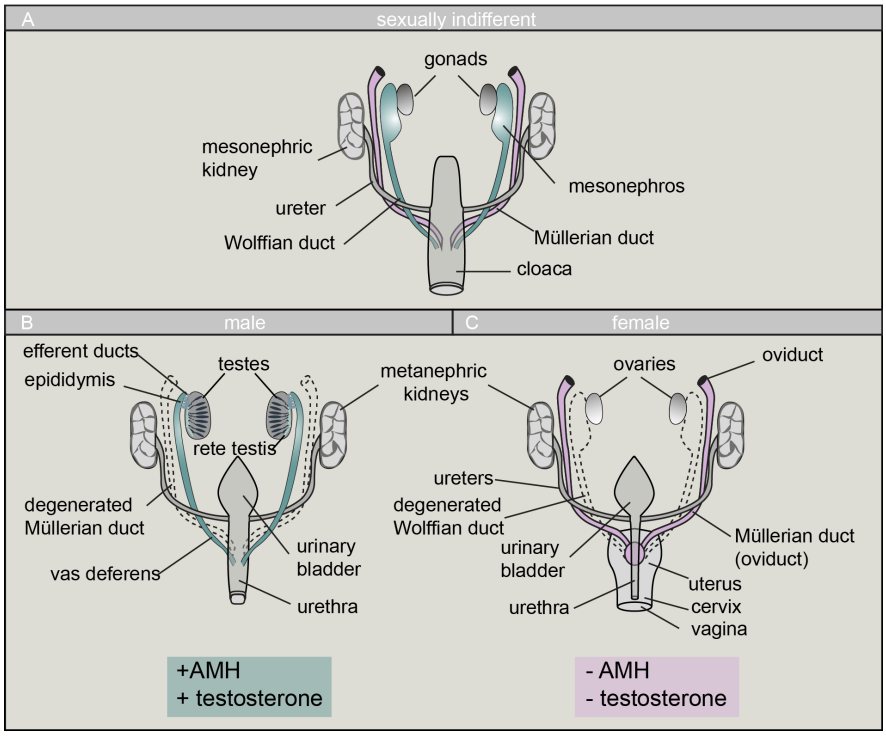


**Figure 1.2: The development of the female and male reproductive organs.** (A) At the sexually indifferent stage both duct systems - the Wolffian duct (cyan) and the Müllerian duct (magenta) - are present, which give rise to the reproductive tract in males and females. The gonads are connected to the mesonephros and shown in grey. (B) MALE: The presence of testosterone propagates the differentiation of the Wolffian duct into the rete testis which is connected via the efferent ducts to the epididymis. Adjacent to the epididymis are the seminal vesicles (not illustrated) and the vas deferens. AMH induces the regression of the Müllerian duct. (C) FEMALE: The local absence of testosterone leads to the regression of the Wolffian duct. At the same time the absence of AMH prevents the regression of the Müllerian duct which is capable of differentiating into the oviduct, uterus, cervix, and the vagina. Figure is modified from (28)

phase. The exception states GATA4. Hu *et al.* (37) reported that GATA4 has a crucial role in the initial step of the formation of the bipotential gonad. GATA4 is expressed in an anterior to posterior wave like-pattern and induces the thickening of the coelomic epithelium. Mice lacking GATA4 do not initiate the development of the gonad (37).

### 1.2.2 Sex-determination: testis development

#### 1.2.2.1 SRY: the master regulator

In the early nineties an approach was performed that focused on screening for conserved sequences – in four sex reversed males – which led to the identification of the *Sry* gene (3). *Sry* was subsequently proven to be the initial driving force that dictates male development (13). *Sry* expression is confined to a particular precursor cell type that

eventually differentiates into the Sertoli lineage (Figure 1.4 A) (14). Furthermore, *Sry* expression is restricted within a given window of time and its expression pattern occurs in a centre-to-pole fashion (38; 39). It is first detected by 10.5 dpc in the central region of the gonad and by 11.5 dpc the whole gonad is under SRY influence but by 12.5 dpc the expression is shut down (38; 40; 41; 42). A delay in *Sry* expression for a couple of hours is associated with XY to XX sex reversal and reveals the importance of the *Sry* expression pattern (43). This requires that the expression of *Sry* underlies a tight regulatory system that ensures its correct spatiotemporal expression. Evidence exists for three transcription factors that are implicated in *Sry* expression: namely, SF1, WT1, and GATA4 (44). However, also upstream events of these factors contribute to the correct expression of *Sry* (Figure 1.3 A). SF1 is able to bind to the *Sry* promoter (45) and there is evidence that SF1 synergizes with a factor called CITED2 in the activation of the *Sry* gene (46). WT1 has been shown to be required for the proper development of the gonad (32) and upon deletion of the WT1(+KTS) isoform, *in-vivo*, a reduction in *Sry* transcript levels was observed (47). The role of WT1 in regulating *Sry* expression is supported by a bulk of *in-vitro* data, comprising co-transfection, EMSA, and ChIP experiments (Figure 1.3 A) (47; 48; 49; 50). Interestingly, at least *in-vitro*, WT1 acts in a cooperative manner with GATA4 to activate the pig and mouse *Sry* gene (49). Moreover, *in-vitro* experiments revealed that GATA4 is involved in the direct transcriptional regulation of *Sry* (Figure 1.3 A) (49; 51). To this end, the initial process of male development is illustrated by the complex regulation of *Sry* expression, not only in a direct but also in an indirect manner in order to provoke the precise transcriptional activation.

#### 1.2.2.2 SOX9: the downstream target of SRY

SRY was discovered in the early nineties as the male determining factor (3; 13) and only recently *Sox9* was identified as the first SRY target that is activated in a cooperative manner with SF1 (54). A number of experiments revealed the importance of SOX9 during gonadal development, which has been shown, when mutated, to be associated with male to female sex reversal in humans (55). Deletion of *Sox9* in a XY mouse leads to the development of females (56; 57) and the ectopic expression of *Sox9* in XX females leads to a sex reversed phenotype (58; 59). Moreover, expression of *Sox9* is elevated as soon as SRY activity is present and this expression is confined to the Sertoli cell lineage (39). This line of evidence supports the concept that the main action of *Sry* relies in the purpose to elevate SOX9 levels above a certain threshold (60) that in turn is capable of stimulating the differentiation of precursor cells towards the Sertoli cell fate. Importantly, the generation of the testicular cords (tc) (Figure 1.1 B) depends on

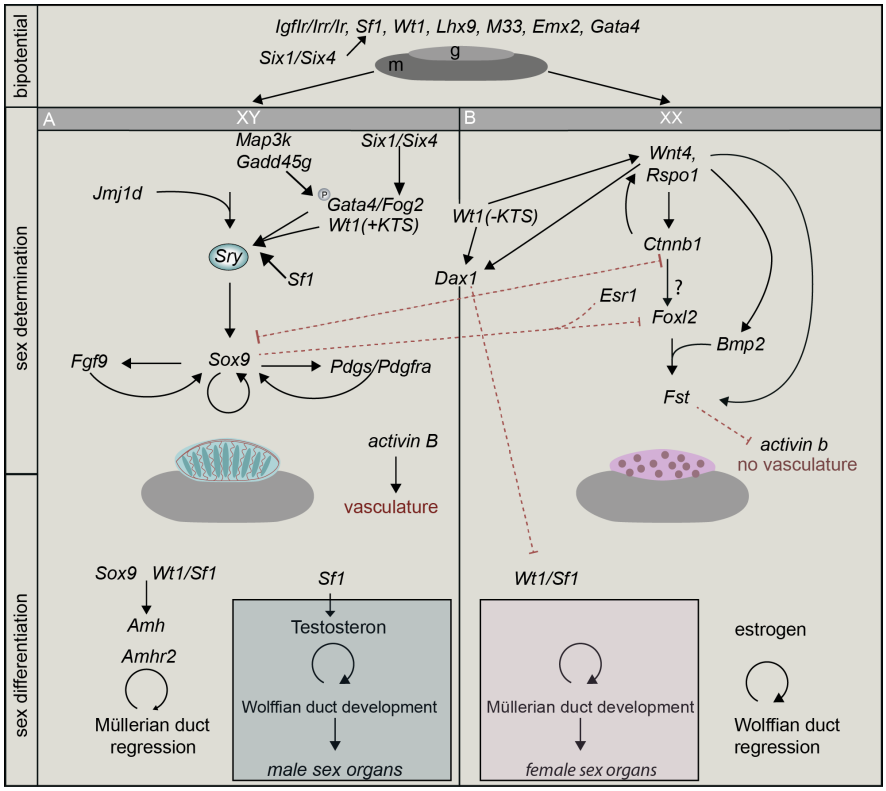


**Figure 1.3: The genetic network of sex determination and sex differentiation.** Various genes have been identified that are pivotal in the development of the bipotential gonad, such as *Six1/Six4, Igfr/Irr/Ir, Sf1, Wt1, Lhx9, M33, Emx2*, and *Gata4*. (A) In the presence of SRY the gonad embarks on the male route. JMJ1D modulates the Y-chromatin region (52) in order to provide access for the transcriptions factors SF1, WT1, and GATA4 to activate *Sry* expression. SRY initiates the expression of *Sox9*. SOX9 activity is maintained by three possible mechanisms: an SOX9 auto-regulatory loop, via FGF9, and PDG2 signalling. These signalling events culminate in the differentiation of the gonad into the male fate and finally provoke the development of the male sex organs. (B) In the absence of SRY the gonad embarks on the female pathway and certain factors become up-regulated such as WNT4, RSPO1, and DAX1. These provoke downstream effects, e.g., stabilisation of $\beta$-CATENIN or the inhibition of WT1/SF1 and thereby repressing the activation of AMH. Finally, these events contribute to ovarian development as characterised by a less pronounced vasculature, the presence of the respective cell types and eventually the appearance of the female reproductive tract. Figure is modified from (53)

the differentiation of precursor cells into Sertoli cells. These precursor cells originate from SF1 positive cells that migrate from the coelomic epithelium into the gonad and additionally, they also generate interstitial cells (Figure 1.4 B)(12; 61). Sertoli cell differentiation is elevated via positive feed forward loops: SRY leads to the activation of SOX9 which in turn activates FGF9 and PDG2 that are capable of binding to the corresponding receptors on precursor cells and enable *Sox9* expression which in turn provokes the differentiation of precursor cells into the Sertoli cell lineage (Figure 1.3, Figure 1.4 B) (24; 62; 63; 64). Furthermore, once SRY levels decline to undetectable levels – how this occurs is still a matter of debate (44) - SOX9 is capable of driving its

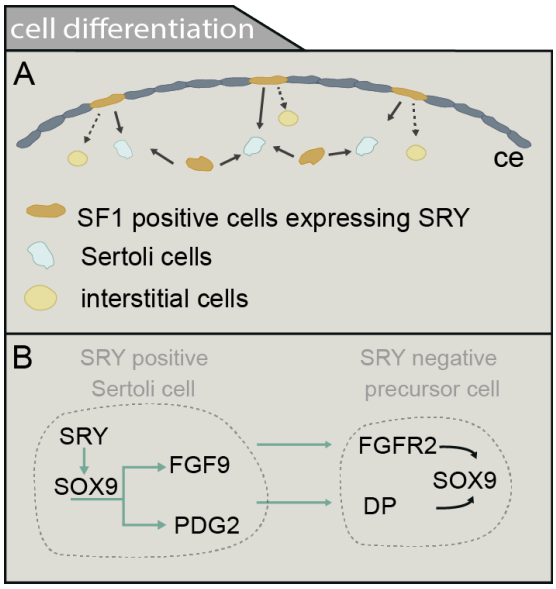


**Figure 1.4: The differentiation into the Sertoli cell lineage** (A) SF1 positive cells from the coelomic epithelium (ce) give rise to Sertoli cells between 11.2 dpc-11.4 dpc. Otherwise - when *Sf1* expression ceases these cells contribute to the interstitial cell population. Sertoli cells can also originate from precursor cells residing inside the gonad (12; 62). Figure is modified from (60). (B) To ensure a certain threshold number of Sertoli cells a variety of mechanism exists. Sertoli cells express *Sry* which activates *Sox9* expression. SOX9 is capable of activating *Fgf9* which in turn initiates a positive feed forward loop: FGF9 binds to its corresponding receptor FGFR2 which sustains *Sox9* expression in neighbouring cells. Further, SOX9 initiates *Pdg2* expression which is capable of binding its receptor on neighbouring cells in order to initiate *Sox9* expression. Figure is modified from (24)

own transcription in a cooperative manner with SF1. In this constellation both factors bind to a binding site, named TESCO, and initiate *Sox9* transcription (54). All of these mechanisms sustain *Sox9* expression and thus contribute to downstream effects such as differentiation of Sertoli cells and testicular cord formation. Concomitantly of driving the male pathway, ovarian promoting genes within the testis have to be turned off and there is evidence that SOX9 together with SRY is involved in this process (Figure 1.3) (65).

#### 1.2.2.3 Sex-differentiation and downstream events of SOX9

There is a set of striking features that sets aside the testis from the ovary. The two most prominent characteristics are the morphological appearance of the testicular cords or seminiferous tubules and a pronounced vasculature of the gonad. The testis adopts gross morphological changes during foetal development, starting from 11.5 dpc that are manifested by the appearance of testicular cords at around 12.5 dpc (16; 66; 67; 68). The testicular cords arise via a tubulogenesis process that is unique in its way and different from those occurring in other organs such as kidney or lung (15; 19). The outer layer of a testicular cord is composed of PTM and Sertoli cells with the basal lamina in between (Figure 1.1 B) (17). Germ cells originate outside the gonad at the allantois, starting to migrate at 7.5 dpc through the hindgut and mesonephros and arrive in the gonad by around 10.5 dpc (19). Leydig cells and a variety of other cell types such as, endothelial cells, macrophages and nerve cells constitute the interstitium (Figure 1.1) (19). However, still an ongoing issue today is the clarification of what causes the initiation of

testicular cord development in the first place and whether this process can be linked to a sole factor (19). A second prominent morphological event that occurs in the testis is the generation of an intertwined complex vasculature system. This is generated through a novel mechanism that comprises the break down of the pre-existing vasculature system at the gonad/mesonephros border. Cells contributing to the vasculature system migrate through the gonad, reassemble at the outer layer and in between the testicular cords, and rearrange in order to build up a vast network that is required for circulating nutrients and testosterone (69; 70). Involved within the generation of such a complex vascularisation system are a number of factors such as inhibin B, WNT4, and FST (71). Also indications exist towards the signalling cascade through Vegf (Figure 1.5) (15). It has been shown by *in-vivo* studies that inhibin B plays a major role in the establishment of the vasculature network within the testis. The same study revealed that the down regulation of *Wnt4* and its downstream gene *Fst* is required for the proper development of a vasculature system in the XY gonad, as *Wnt4* deficient XX gonads exhibit a similar vasculature as XY gonads (71). Furthermore, Ross *et al.* demonstrated that XX gonads treated with AMH and BMP2 acquire a male specific vasculature phenotype (72). A third issue worth mentioning is the differentiation of the Leydig cells which contribute to the proper development of the male pathway. The Leydig cell lineage is implicated

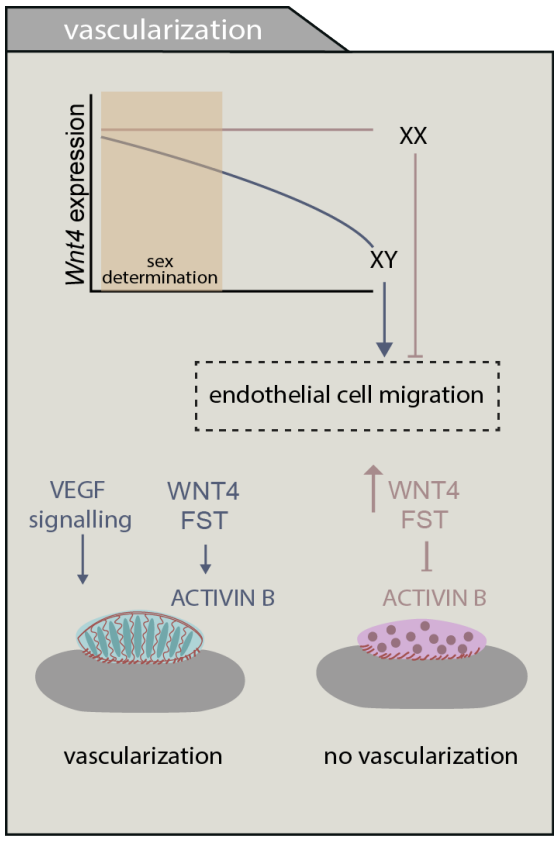


**Figure 1.5:** The testis exhibits a more pronounced vasculature compared to the ovary. Within this process two main factors are involved: WNT4 and FST. *Wnt4* expression starts to decline during gonadal development in the testis which leads to the migration of endothelial cells into the gonad which in turn contribute to vascularisation of the testis via ACTIVIN B and downstream TGF-$\beta$ signalling together with VEGF signalling. *Wnt4* expression levels are sustained in the ovary though, which hinders endothelial cells to migrate into the gonad thereby leading to an elevated ACTIVIN B level. Hence vascularisation is inhibited. Figure is modified from (24).

in the process of sex differentiation by regulating steroidogenesis. In particular, they produce testosterone which provokes the development of the Wolffian duct (73). Along this line, Sertoli cells produce AMH, which is a SOX9 target and a TGF-$\beta$ ligand that signals through its receptor AMHR2 and thereby initiates the regression of the Müllerian duct in males (74). On the other hand the Wolffian duct persists and progresses in the presence of testosterone into the rete testis, efferent ducts, epididymis, vas deferens, and seminal vesicles, thus building the anatomical structures of the male genitalia (73; 75) (Figure 1.3 A and Figure 1.2 B).

### 1.2.3 Sex-determination and -differentiation: ovary development

#### 1.2.3.1 An overview of ovary development

Unlike the XY gonad, a sole factor that drives ovarian development has not been identified up to now and controversial discussions were a matter of debate whether such a factor exists at all (76). However, today the general view is that the ovarian process is rather a counterbalancing act between a set of factors (11; 77; 78). In the absence of SRY, hence at low SOX9 levels, a specific set of factors, e.g., FOXL2, WNT4, RSPO1, FST, and $\beta$-CATENIN becomes up-regulated and promotes the differentiation of precursor cells to embark on the female route (9; 79) (Figure 1.3 B). Ablation of any of these factors results in perturbed ovarian development (71; 80; 81; 82; 83). The ovarian pathway is considered the default pathway as the absence of *Sry* culminates in the development of the ovary. But, one should bear in mind that passive must not be equated with the absence of active signalling cues. It is rather the case that ovarian development is as alike an active process as testis development (44; 84). Importantly in the absence of SRY, given precursor cells within the gonad are capable of differentiating into the granulosa cell lineage or the theca cell lineage, the two most prominent cell types that make up an ovary (Figure 1.1 C) (14; 24).

#### 1.2.3.2 The molecular network that drives ovary development

The proper development of the ovary, particularly the differentiation of the respective cell types depends on a variety of factors ranging from transcription factors to signalling molecules, such as FOXL2, WNT4, RSPO1, FST, and $\beta$-CATENIN (Figure 1.3 B) (20; 24). It has been shown that, *Foxl2* ablation in the foetal embryo results in premature ovarian failure which is associated with defects in granulosa cell differentiation (80). Conditional deletion of *Foxl2* in the adult ovary provokes the transdifferentiation of granulosa cells into Sertoli cells and theca cells into Leydig cells. Moreover, evidence was also provided that FOXL2 is able, synergistically with ESR1, to repress the transcription

of *Sox9* (Figure 1.3 B). The study concludes that FOXL2 is required to maintain the ovarian phenotype throughout life time (81). The question that still remains elusive is how *Foxl2* expression is regulated on the transcriptional level. Indications pinpoint the transcription factor GATA4 as a potential regulator of *Foxl2* expression as $Gata4^{ki/ki}$ mice show diminished *Foxl2* transcript levels (36). Moreover, DNA methylation and miRNA binding to the 3'UTR are other possible regulatory circuits that have been shown to be associated with *Foxl2* expression (85; 86). Despite these open questions it is now grounded knowledge that *Foxl2* is a crucial factor for ovarian development (87). WNT signalling is considered as a hallmark of ovary development, as exemplified by the involvement of factors such as RSPO1, WNT4 and $\beta$-CATENIN (Figure 1.3 B) (88). RSPO1 has been shown to be an essential factor for ovary development as a 2752 bp deletion within the *RSPO1* locus results in XX to XY sex reversal (89). Follow-up experiments in mice revealed that RSPO1 is capable of activating the WNT pathway and *Rspondin-1* ablation results in a XX to XY sex reversed phenotype in mice (90). Second, WNT4 is another agonist that is implicated in activating canonical WNT signalling in the gonad (91). Mutations in the human *WNT4* gene are associated with SERKAL syndrome and result in XX to XY sex reversal (92). Interestingly, both factors play a role in cell proliferation at an early stage in the XY gonad (82). However, as development proceeds WNT4 is turned off in the testis via FGF9 signalling (78; 93). Reduced levels of WNT4 enable endothelial cells to migrate into the gonad and contribute to vessel formation. High levels of WNT4 inhibit endothelial cell migration into the female gonad and thereby contributing together with its downstream target *Fst* to the inhibition of the vasculature formation (Figure 1.5) (71). The expression of *Fst* has been shown to be regulated by FOXL2 cooperatively with BMP2 and WNT4 in a developmental stage dependent manner (79). Furthermore, transcript levels of *Wnt4* and *Fst* are alike in terms of displaying a dimorphic expression pattern, with higher levels in the female gonad (9; 79).

To this end, the ovarian driving force encompasses the absence in SRY-SOX9 activity but the presence of ovarian promoting factors such as FOXL2, WNT4, RSPO1, FST, and $\beta$-CATENIN (Figure 1.3 B). All of these factor contribute to the differentiation of the respective cell types that make up an ovary and these cells provide the proper environment and eventually drive the development of the reproductive female tract. In addition, the absence of AMH and diminished levels of testosterone (94) prevents the regression of the Müllerian duct in the ovary, which is then capable of developing into the oviduct, uterus, cervix, and vagina. The Wolffian duct on the other hand is subject to regression (Figure 1.3 B) (25).

## 1.3 The functional relevance of WT1 and GATA4

### 1.3.1 WT1 and its role in mouse gonad development

Initially, the *Wt1* gene was identified as a tumour suppressor gene that is associated with children suffering from kidney tumours – known as Wilms' tumour (95; 96). Mutations or deletions in *Wt1* are the cause of a variety of syndromes such as WAGR, Frasier, and Denys-Drash syndrome, comprising abnormalities like urogenital deformations and patients are prone to cancer progression (96). *Wt1* is expressed throughout development in various tissues/organs in particular the kidney, gonad, spleen, epicardium, retina, thymus, brain, and mesothelium (97). The biological significance of WT1 during embryonic development was demonstrated by the generation of germline *Wt1* deficient mice (32). These mice lack kidneys and gonads, and exhibit concomitant spleen, lung, and heart defects of which the latter is most probably the cause for the lethal phenotype observed between 13.0 dpc and 15.0 dpc (32). Although, this demonstrates that WT1 is required for the proper development, knowledge of the precise mechanism of how WT1 functions remains elusive. This is most likely attributed to the fact that WT1 is able to act in a tissue dependent context as a transcriptional repressor or an activator, e.g., in the regulation of the *Wnt4* gene (98). In the kidney, WT1 interacts with cofactors such as CBP and p300 which provokes the activation of *Wnt4*. In the epicardium – WT1 interacts with a co-repressor BASP1 and shuts down the expression of *Wnt4* (98). The *Wt1* gene consists of 10 exons and is located on mouse chromosome 2. The *Wt1* gene encodes for at least 24 different splice variants that posses different functions (47; 99). Responsible for this vast number of splice variants are mechanisms ranging from the usage of different start codons to alternative splicing to RNA editing. The best studied *Wt1* splice variants, namely *WT1(+KTS)* and *WT1(-KTS)*, are the result of an alternative splicing event between zinc finger three and four that either leads to an additional insertion of three amnio acids – lysine, threonine, serine (+KTS) – or a lack thereof (-KTS) (Figure 1.6 A) (100). It is the general view based on accumulated evidence that WT1(+KTS) has a higher RNA binding affinity, whereas WT1(-KTS) preferentially binds to DNA and functions as a transcription factor (101). Similar to the Frasier syndrome in humans mice lacking the *Wt1(+KTS)* isoform exhibit a sex reversed phenotype (47). This study not only describes the crucial role of WT1 in terms of sex determination by revealing an *in-vivo* link to the *Sry* gene – mice lacking WT1(+KTS) show reduced *Sry* expression – but the experiments also demonstrate that different splice variants could act in a different manner (47). It is well described that WT1 is implicated in the regulation of the *Sry* gene (49; 50). Furthermore, WT1 is also capable of acting on the post-translational level by interacting with various co-factors

involved in splicing such as U170K, SF2, SC35, and U2AF65 (102). This illustrates that WT1 engages a role in RNA processing.
Previous studies revealed that WT1 is implicated in the regulation of a number of genes such as *Dax1* (103), *Sox9*, (104) *Sf1* (31), *Amhr2* (105), *Star* (106), *Ctnnb1* (107), *Gata4* (108), and *Amh* (109), which play a crucial role in the development of the gonad. Evidence that supports a functional link derives in most cases (*Dax1, Gata4, Amhr2, Amh*) from *in-vitro* assays such as reporter gene assays in combination with EMSA or ChIP as well as siRNA knockdown approaches in cell culture models (103; 105; 108; 109). In addition, for the genes *Star* and *Ctnnb1* data retrieved from *in-vivo* models suggest a direct or indirect role in the regulation for WT1 (106; 107). *In-vivo* evidence that demonstrates a direct functional link to WT1 was provided for the *Sf1* gene by Wilhelm *et al.* (31). This study showed in transgenic mice, which express the reporter gene *lacZ* under the control of the *Sf1* promoter, that when the WT1 binding sites within the *Sf1* promoter are mutated the reporter *lacZ* is not expressed (31). To this end, whether WT1 regulates these genes directly needs to be yet investigated. In addition it would be interesting whether the regulation by WT1 occurs in a sex-specific manner or independent of the embryonic sex.

### 1.3.2 GATA4 and its role in mouse gonad development

The mouse transcriptome encodes for a total of 6 GATA factors that all have in common to bind to the same consensus sequence in the context of (A/T)GATA(A/G) via two zinc-finger domains. GATA proteins can be classified into two groups: the first group, consists of GATA-1, -2, and -3, which are primarily involved in haematopoiesis. The second group consists of GATA-4, -5, and -6, which are crucial for proper development of the heart and the gonad (110). Of particular interest herein is GATA4, which fulfils essential roles throughout gonadal development (111). The *Gata4* gene comprises 6 exons and is located on mouse chromosome 14. The start codon ATG is located within exon 2. The *Gata4* gene encodes for a protein that is 441 aa in length and contains two activation domains (AD), a DNA binding domain (DBD) and a nuclear localisation signal (NLS) (Figure 1.6 B). *Gata4* expression is detected in the liver, heart, adrenal cortex, ovary, and testis (112). Furthermore, the essential function of GATA4 for proper development has been demonstrated by ablation of the gene *in-vivo*. Within this line, homozygous $Gata4^{-/-}$ null mice die between 8.5 dpc and 10.5 dpc due to heart defects and intestine abnormalities, whereas heterozygous $Gata4^{+/-}$ mice develop normally (113; 114). Recently Hu *et al.* could show that GATA4 is expressed at the onset of gonad formation by around 9.5 dpc to 9.75 dpc and expressed in an anterior-posterior wave pattern. The authors could pinpoint *Gata4* as a gene that is crucial for the initial

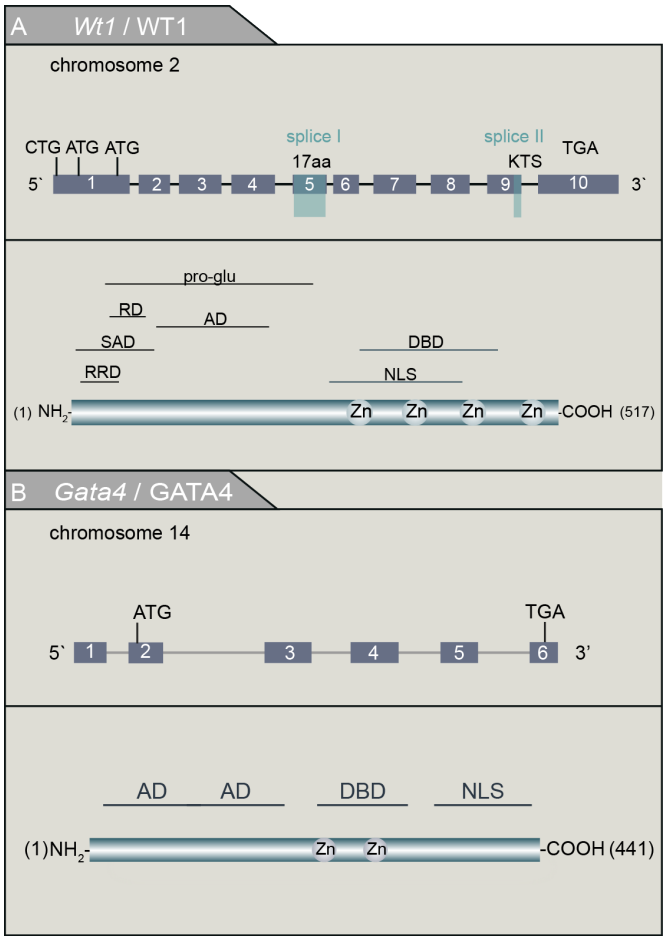


**Figure 1.6:** (A) top: The murine *Wt1* gene resides on chromosome 2 and is made up of 10 exons and contains 3 transcriptional start codons. Two major splice sites within the *Wt1* gene are the cause of alternative isoforms. The first, in exon 5 introduces additional 17 amino acids (aa) and the second, in exon 9, leads to the incorporation of three additional amino acids: lysine, threonine, and serine (KTS). bottom: The WT1 protein is depicted and spans over 517 amino acids comprising different domains: activation domain (AD), repression domain (RD), self association domain (SAD), proline-glutamine rich region, RNA recognition domain, nuclear localisation signal (NLS), and DNA binding domain (DBD), which constitutes 4 zinc fingers. (B) top: The murine *Gata4* gene resides on chromosome 14 and contains a start codon within exon two and spans over 3374 bp with a total of 6 exons. bottom: It encodes for a Zn-finger transcription factor that is 441 amino acids in length. The N-terminal part contains two activation domains (AD) and the C-terminus harbours a nuclear localisation signal (NLS) and a DNA binding domain (DBD) that enables the interaction with DNA.

thickening stage of the gonad – ablation of *Gata4* results in thickening effects with no gonads formed (37). Although the biological function of GATA4 has been well described (115), the transcriptional regulation of the *Gata4* gene however, still remains poorly understood. Recent studies have shown that the expression of *Gata4* in various organs is driven by distinct enhancer elements (116; 117; 118; 119). Another study describes that the proximal promoter directs *Gata4* expression to the Sertoli cell lineage (120). As it has been shown previously that *Gata4* expression appears at the onset of gonadal formation it is not surprising that GATA4 is also involved in the transcriptional regulation of important genes during gonadal development (37; 115). Foremost, the transcriptional regulation of two genes, namely *Star* (121; 122) and *Amh* (49; 123; 124; 125) requires the activity of GATA4. Notable is that Miyamoto *et al.* revealed that GATA4 and WT1 interact with each other and that the *Sry* and *Amh* promoters were activated in a synergistic manner by both transcription factors (49). A functional link referring to the expression of *Sox9, Foxl2* and *Fst* is suggested from the analysis of a transgenic mouse

model that exhibits a mutation, which abrogates the interaction of GATA4 with FOG2 (124). Moreover, the expression of *Foxl2* and *Fst*, was down-regulated in the ovary as observed in a different mouse model, in particular *Sf1-Cre; Gata4*$^{flx/flx}$. Although, a direct link still remains to be proven (125). It might as well be interesting whether WT1 and GATA4 share other common target genes within the context of sex differentiation.

## 1.4 Vivo-morpholinos: a tool to assess gene function

In order to study the function of a gene, the general approach is to disrupt the gene's function and assess for downstream effects comprising, e.g., phenotypic analysis or changes in gene expression. One way to achieve this is the generation of germline or conditional knock-out mice (126). An alternative strategy is provided by the use of antisense oligonucleotides (127). Initially, morpholinos were developed in the mid-90s by James Summerton (128; 129). The chemistry behind the generation of morpholinos and vivo-morpholinos is described in more detail by Moulton *et al.* (130). Notable though is the unique chemical composition of morpholino antisense oligonucleotides. Compared to DNA, a morpholino unit exhibits two distinct and unique properties: an uncharged backbone, consisting of a phosphorodiamidate unit, and a morpholino ring structure to which either one of the purines or pyrimidines is attached (Figure 1.7 A). Vivo-morpholinos contain in addition a delivery moiety that consists of a linker molecule that holds eight guanidinium groups (131) (Figure 1.7). Due to this delivery moiety no transfection reagents are needed in order to conduct the cell transfection procedure (131; 132). Once inside the cell, vivo-morpholinos are capable of binding to complementary RNA molecules and interfere with translation (Figure 1.7 B) (130). A number of recent reports have successfully applied vivo-morpholinos in murine organ culture systems (133; 134; 135; 136).

## 1.5 Hypothesis and aim

Within the cascade of sex determination and sex differentiation two prominent transcription factors WT1 and GATA4 play a crucial and essential role. The main scope of this thesis is to examine the interplay of WT1 and GATA4 during murine gonadal development and to what extend they contribute to the proper development of the gonad in either sex. Furthermore, as WT1 and GATA4 interact with each other and cooperatively activate common target genes (49) a particular interest of this study was to examine to what extent both factors contribute to the regulation of gene expression in a sex specific manner. In order to address this question, I studied the relevance of

WT1 during sex differentiation by assessing gene expression levels in germline *Wt1*$^{-/-}$ deficient mice. Within the analysis I focused on sex-specific differences by distinguishing between XX and XY gonads. Furthermore, I developed a novel approach by combining a hanging droplet culture technique together with the application of vivo-morpholino antisense oligonucleotides. This system allows me to conduct experiments that address the following questions: (i) what is the impact of WT1 during sex differentiation in either sex (ii) to what extend does GATA4 contribute to the sex differentiation process and is this contribution sex specific, and (iii) do WT1 and GATA4 share common target genes. The final aim of this thesis is to provide novel insights in terms of the functional relationship between WT1 and GATA4 during gonadal development.

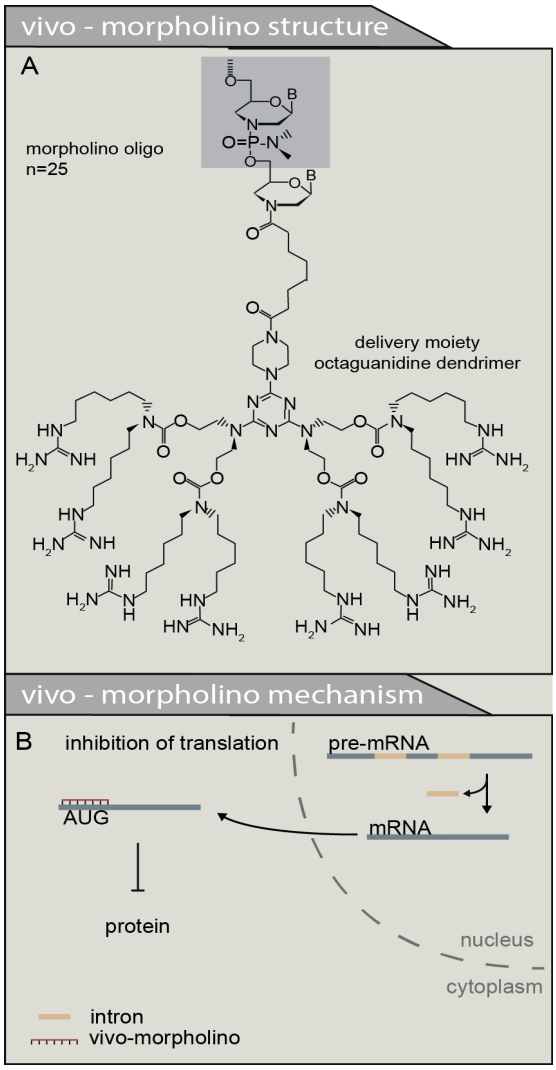


**Figure 1.7:** (A) Vivo-morpholinos are composed of a delivery moiety and typically a 25 morpholino oligomere. One oligomere is composed of a ring structure with a nitrogen that is located para to an oxygen and linked to the next oligomere via a non-ionic phosphorodiamidate group. The delivery is an octaguanidine dendrimer that enables entry into cells. The structure was modified from http://www.gene-tools.com/vivomorpholinos. (B) Vivo-morpholinos are capable of interfering with translation by masking the start codon of the gene of interest and thus leading to the knockdown of the protein (130).

# 2

# Results

## 2.1 Analysis of *Wt1* deficient mice

To provide additional biological insight into the functional relevance of WT1 during gonad development, the morphology and the gene expression status were examined in $Wt1^{-/-}$ deficient mice compared to wild type $Wt1^{+/+}$ embryos. Gene expression analysis was studied in more detail on given genes, to which a profound role during the development of the ovary, e.g., *Foxl2, Fst* (71; 80), and *Ctnnb1* (83), and testis, e.g., *Sf1, Sox9, Amh, Amhr2* (31; 104; 105; 137), and *Star* (138), was ascribed to. In addition, two genes *Dax1* and *Gata4* were as well subject to analysis, as they are implicated in gonadal development of both sexes (36; 139). Genotyping of the *Wt1* locus was determined by PCR analysis, using genomic DNA isolated from embryonic tails. Wild type $Wt1^{+/+}$ embryos give rise to a band at 150bp and $Wt1^{-/-}$ deficient mice lead to the appearance of a band at 220bp (Figure 2.1 A). The sex-genotype was assessed by PCR amplification of the *Kdm5d* gene. This yields a visible band at 331bp in case of the XX genotype. XY gonads give rise to two bands, one at 331bp and at 302bp (Figure 2.1 B). Genotyping of the sex allows for the comparison of female and male gonads in terms of morphology and gene expression status. Next, the morphology was analysed by microscopy (Figure 2.1 C, D) and gene expression by RT-qPCR (Figure 2.2). Therefore, the gonad/mesonephroi anlagen were dissected at 13.5 dpc, from $Wt1^{+/+}$ and $Wt1^{-/-}$ littermates.

### 2.1.1 Morphological analysis of *Wt1* deficient gonads

Kreidberg *et al.* reported that the homozygous deletion of *Wt1* leads to the lack of kidneys and gonads in addition to concomitant lung and heart defects (32). The latter is most likely the cause of lethality between 13.0 dpc and 15.0 dpc (32). Whether

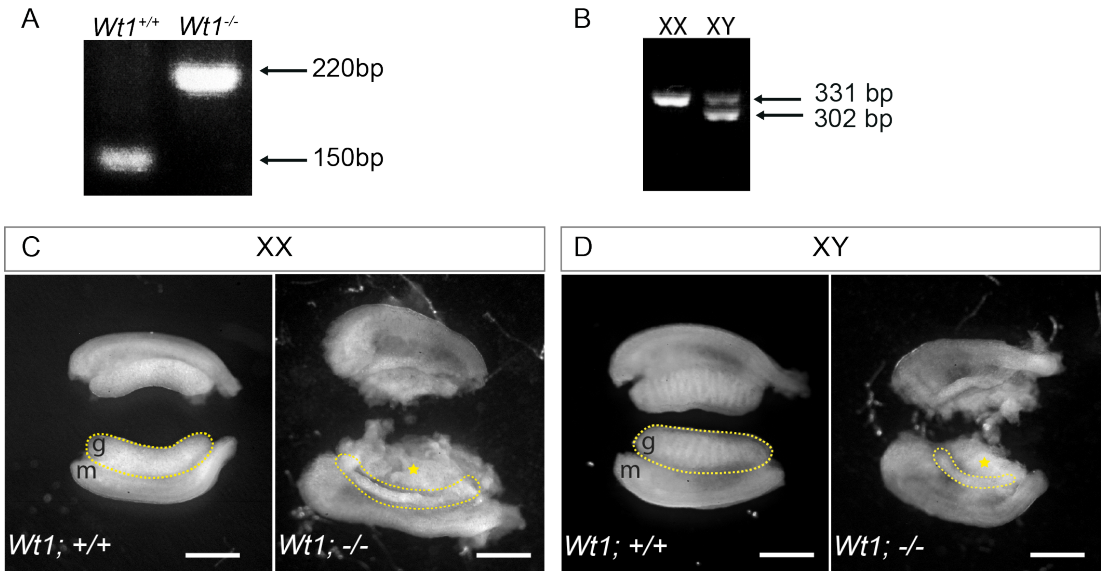


**Figure 2.1: Comparison of the morphology of $Wt1^{+/+}$ to $Wt1^{-/-}$ gonads at stage 13.5 dpc**. (A) Genotyping of wild type $Wt1^{+/+}$ and $Wt1^{-/-}$ deficient mice is shown. (B) Amplification of the *Kdm5d* gene was used for sex-genotyping (140) (C) $Wt1^{+/+}$ ovaries allow a clear distinction between the mesonephros and the ovary. $Wt1^{-/-}$ ovaries exhibit an enlarged mesonephros and the gonad morphology is disrupted. (D) In $Wt1^{+/+}$ testis a distinction between testis and the mesonephros is possible. Note the striated appearance of the $Wt1^{+/+}$ testis reflecting the presence of seminiferous tubules. $Wt1^{-/-}$ XY gonads are smaller in size and seminiferous tubules are absent. The mesonephros appears enlarged and the overall morphology is disrupted. The yellow dashed line represents the gonad (g) with the mesonephros (m) underneath. The asterisk indicates tissue oedema. scale bar: 500$\mu$m

WT1 exerts a sex specific function has not been studied in detail yet, as previous reports did not differentiate between the sexes within the same model system used (32; 104; 108; 141). Therefore, it was tempting to hypothesise whether WT1 acts in a sex specific manner and whether this becomes apparent in the morphology of the gonads. In order to address this issue, gonads of wild type $Wt1^{+/+}$ mice were compared to $Wt1^{-/-}$ deficient mice of either sex in respect to the morphology (Figure 2.1 C, D). By comparing $Wt1^{+/+}$ to $Wt1^{-/-}$ ovaries, the gonadal and mesonephric structure of the mutant ovaries are not clearly delimited. In addition, the mutant ovaries are smaller in size, which is consistent with a recent report (141), and are linked to an enlarged mesonephros and tissue oedema (Figure 2.1 C). In $Wt1^{+/+}$ testis, the seminiferous tubules are observed, a well known feature of testis development (15). These notable structures are absent in the *Wt1* deficient testes, in addition to their smaller size and tissue oedema (Figure 2.1 D). In conclusion, the results herein show that WT1 has an essential role in the development of the morphological features of the gonads in either sex.

### 2.1.2 Genes important for gonadal development are regulated in a dimorphic or non-dimorphic manner by WT1 in female and male gonads

Although previous studies provided important insights into the functional relevance of WT1, however, a comparative approach between males and females has not been addressed yet within the same model system (32; 104; 108; 141). Taking this into account, together with the importance of WT1 for the proper development of the morphological features in either sex (seen in Figure 2.1), it was tempting to hypothesise whether the underlying gene expression signature in either the ovary or testis is perturbed upon the loss of WT1. The analysis was aimed towards a set of genes that have a prominent role during sex determination and differentiation, as described above. In order to address this issue gonad/mesonephroi anlagen were dissected by 13.5 dpc, from $Wt1^{+/+}$ and $Wt1^{-/-}$ littermates. RNA from $Wt1^{+/+}$ and $Wt1^{-/-}$ derived gonads was isolated, reverse transcribed into cDNA and used for RT-qPCR. The experimental set-up focused on a distinction between female and male sexes. Overall, two specific expression patterns were observed in $Wt1^{-/-}$ deficient gonads. The first group encompasses genes, i.e., *Dax1, Sf1, Amhr2, Star*, and *Gata4* whose expression pattern is reduced in $Wt1^{-/-}$ deficient gonads independent of the sex. The second group consists of genes, i.e., *Ctnnb1, Fst, Foxl2, Sox9*, and *Amh* whose expression pattern is regulated in a sex-specific manner (Figure 2.2). The mean, as illustrated within the box plots (Figure 2.2), by the white rectangle, is listed as $\Delta CT$ value in the Appendix. The fold increase from the raw value was calculated and presented as percent (Table 5.1).

The first group contains genes, i.e., *Dax1, Sf1, Amhr2, Star*, and *Gata4* whose expression is reduced in $Wt1^{-/-}$ compared to wild type $Wt1^{+/+}$ littermates. This reduction in mRNA expression is independent of the embryos sex. In greater detail, *Dax1* mRNA transcripts were significantly down regulated to 8.7% and 8.6% in $Wt1^{-/-}$ ovaries and testes, as opposed to the corresponding $Wt1^{+/+}$ littermates. In terms of *Sf1* expression, mRNA transcripts were significantly reduced to 1.7% and 0.4% in the $Wt1^{-/-}$ ovaries and testes as opposed to the corresponding wild type littermates. Moreover, *Amhr2* transcripts were significantly diminished to 0.3% and 0.5% in $Wt1^{-/-}$ ovaries and testes, when compared to their wild type littermates. *Star* transcripts were significantly reduced to 13.5% and 25.0% in the $Wt1^{-/-}$ ovaries and testes as opposed to their respective wild type littermates. Last, comparing $Wt1^{-/-}$ ovaries and testes to their $Wt1^{+/+}$ littermates, *Gata4* mRNA transcripts were significantly reduced to 16.7% and 12.5%.

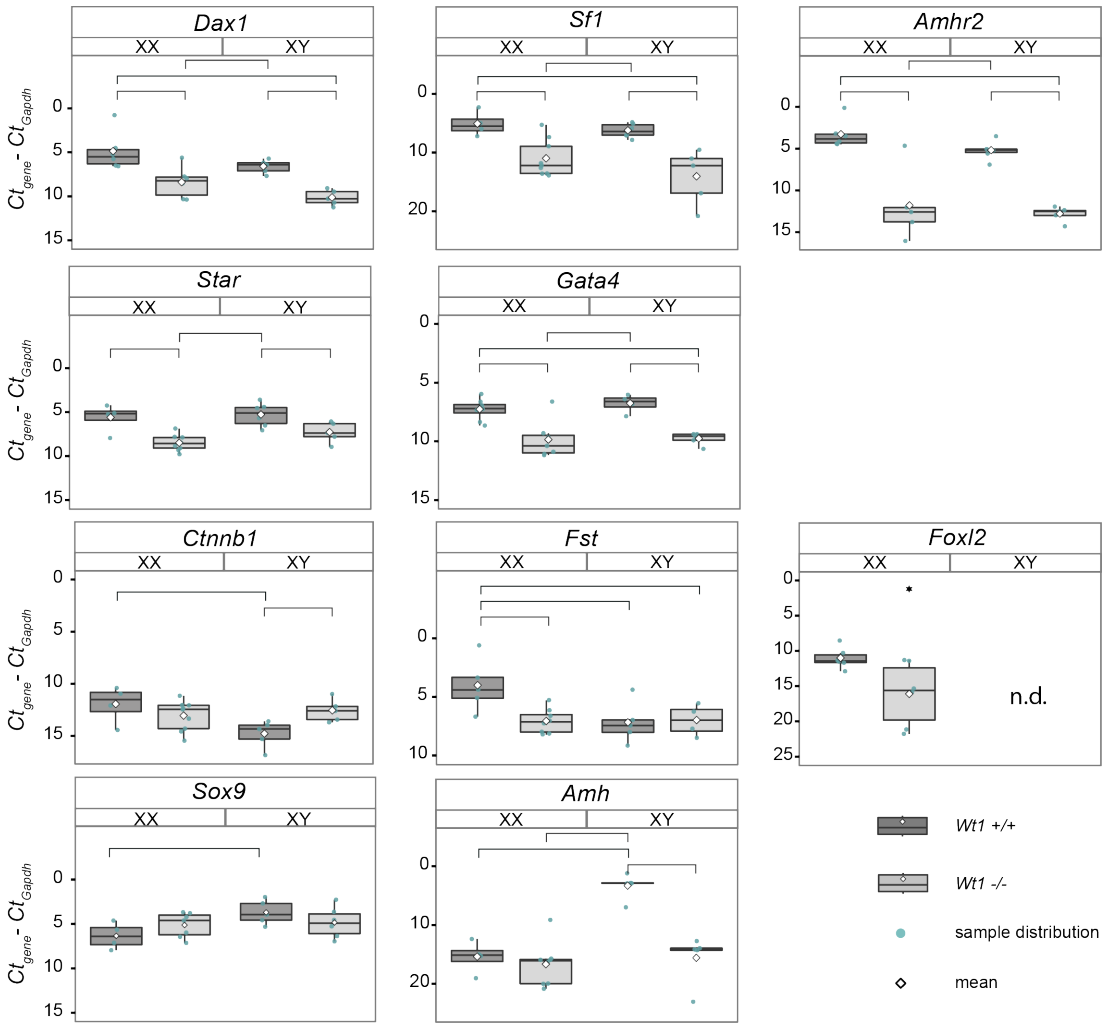


**Figure 2.2: Gene expression analysis in gonads of 13.5 dpc wild type littermates compared to female and male *Wt1* deficient embryos**. (A) RT-qPCR analysis of 13.5 dpc gonad/mesonephros anlagen is shown for genes as indicated on top of each panel. mRNA levels were normalised to *Gapdh* mRNA and normalised Ct values are visualised as Tukey box plots. Statistical comparison was performed by an ANOVA test and Tukey post-hoc test. In terms of *Foxl2*, a student's t-test was performed. The significance is indicated by brackets (*p<0.05, t-test). n.d.: not detectable.

The second group comprises the following genes: *Ctnnb1, Fst, Foxl2, Sox9*, and *Amh*, which show changes in gene expression that occur in a sex-specific manner. Interestingly, *Ctnnb1* transcript levels were significantly up regulated to approximately 4.7 fold in $Wt1^{-/-}$ testes compared to their wild type $Wt1^{+/+}$ counterpart. Expression of *Fst* was significantly reduced to 12.1% in $Wt1^{-/-}$ ovaries compared to their wild type littermates. Notable is the significant lower level of *Fst* mRNA expression within wild type testes, when compared to wild type ovaries. Within the same line *Foxl2* transcripts are significantly down regulated to 2.9% in $Wt1^{-/-}$ ovaries as opposed to their wild

type counterpart. *Foxl2* mRNA transcripts were undetectable within the testes, as shown also by others (79; 142). On the other hand, *Sox9* mRNA levels showed a significant increase in expression to 5.3 fold in $Wt1^{+/+}$ testes compared to $Wt1^{+/+}$ ovaries, this dimorphic pattern was also observed by others (9). The expression of *Amh* is, as previously shown, pivotal for duct development in the male gonad in terms of inducing the regression of the Muellerian duct (137). *Amh* expression is clearly detectable in $Wt1^{+/+}$ testes compared to $Wt1^{+/+}$ ovaries. However, in $Wt1^{-/-}$ testes, *Amh* transcripts were significantly reduced to 0.01% compared to the wild type. In summary, the data herein show that WT1 is necessary to maintain a sex-specific gene expression pattern in the developing gonads.

## 2.2 siRNA knockdown of *Wt1* and *Gata4* in a mesonephric cell line – M15

### 2.2.1 *Wt1* siRNA knockdown

The results under section 2.1 and 2.2 describe WT1 as a crucial factor for the establishment of a sex specific signature in testes and in ovaries. It has been shown that WT1 acts either together with GATA4, at least *in-vitro*, or alone on the activation of the *Sry* gene (49; 50). Therefore the observed effects (Figure 2.1 and Figure 2.2), could be a consequence of reduced SRY activity and thus secondary to the WT1 loss. Furthermore, gene expression analysis was possibly compromised by the structural changes in $Wt1^{-/-}$ deficient gonads. In the gonads a heterogenous cell population exists which makes the interpretation of the results (Figure 2.2) rather difficult. Therefore it was tempting and necessary to search for an alternative cell culture model. The M15 mesonephric cell line, which is of XX genotype (143), seemed to be suitable for mediating the *Wt1* siRNA knockdown as endogenous WT1 is expressed at a high level. The knockdown of WT1 was efficient as determined by immunoblot analysis (Figure 2.3 A). Genes subject to analysis are illustrated in Figure 2.3 B. Transcript levels of *Amhr2* and *Star* were significantly down regulated to 15.4% and 68.5%, respectively. Other genes did not show any significant changes in the expression levels upon the WT1 knockdown. In conclusion, these results did not confirm the expression data gathered from *WT1* deficient mice, with the exception of *Star* and *Amhr2*, known downstream targets of WT1 (105; 106).

### 2.2.2 *Gata4* siRNA knockdown

The results of the WT1 knockdown in M15 cells contradicts previous studies, although different model systems have been used. For example, the transcriptional regulation of

*Sf1* and *Sox9* by WT1 was addressed using *in-vivo* models (31; 104). In case of the *Amh* gene the HeLa cell line was used (49). Additionally, results gathered from *WT1* deficient mice (Figure 2.2) were not in line with the siRNA knockdown results (Figure 2.3 A, B). However, to finally validate M15 cells as a tool to study gene regulation

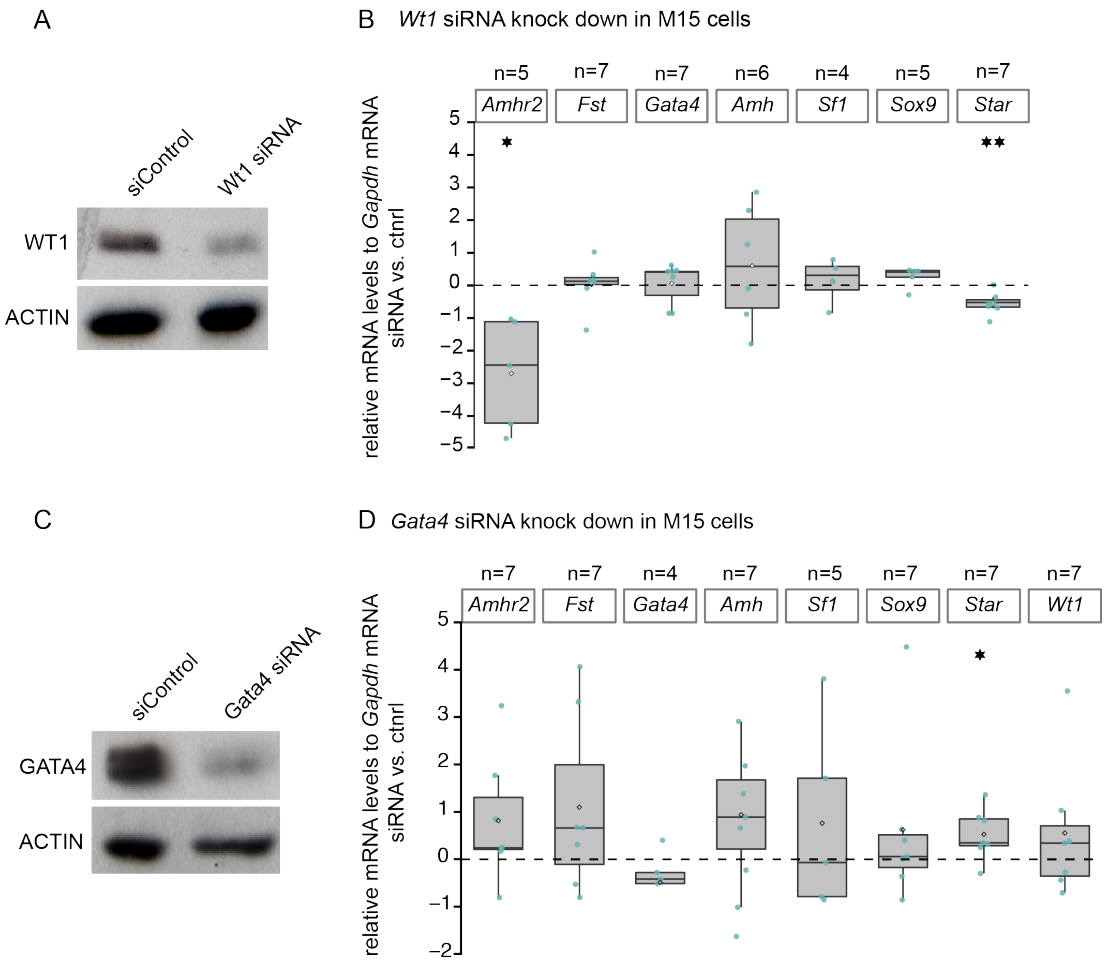


**Figure 2.3: siRNA knockdown of WT1 and GATA4 in the mesonephric cell line M15.** Knockdown was performed using a pool of four different siRNAs against the *Wt1* or *Gata4*. The respective control samples were transfected with a non-targeting control siRNA. The knockdown efficiency is indicated by immunoblotting in (A) for WT1 and (C) for GATA4 by using 20$\mu$g of total protein isolated from M15 cells. WT1 and GATA4 were detect using specific antibodies, C-19 WT1 and C-20 GATA4. ACTIN was used as a loading control. (B) Shown is RT-qPCR analysis of *Wt1*-siRNA knockdown in M15 cells. Briefly, no gross changes of the analysed genes were observed upon the knockdown of WT1, except for *Amhr2* and *Star*. (D) Shown is RT-qPCR analysis of *Gata4*-siRNA knockdown in M15 cells. mRNA levels were normalised to *Gapdh* mRNA and the normalised Ct values are visualised on Tukey box plots. The siControl was set to zero, which is represented by the black dashed line. At the top of each panel the sample number is shown and the cyan points illustrate the distribution of the samples. The white rectangle within the boxplot refers to the mean and the black line depicts the median value. Statistical significances are indicated by asterisks: *p<0.05, **p<0.01 and were determined by using a paired student's t-test.

during gonadal development *GATA4* siRNA knockdown was performed, as GATA4 is an essential transcription factor during gonadal development (36). The GATA4 knockdown was efficient as determined by immunoblot analysis (Figure 2.3 C). The results show that genes subject to analysis display no overall changes in the expression levels, with the exception of *Star*, which shows a significant up regulation to 143.9% (Figure 2.3 D). Concluding from this, the knockdown of GATA4 led to no relevant significant changes, of genes that have previously been shown to be regulated by GATA4 (122; 123). Therefore, the M15 cell line is not a suitable model system to assess gene expression in terms of gonadal development.

## 2.3 Establishment of an *ex-vivo* organ culture system: hanging droplet culture combined with vivo-morpholino knockdown

Due to the embryonic lethality of *Wt1* deficient mice at around 13.0 dpc (32), later developmental stages are unapproachable for analysis. As a consequence of the $Wt1^{-/-}$ phenotype that includes the loss of kidneys and the absence of gonads (32), the interpretation of the described effects, herein observed by RT-qPCR might be tampered by a mere decline or the absence of particular cell types. This is based on the notion that gonadal cells undergo apoptosis in *Wt1* deficient mice (47). Moreover, results gathered from analysis of *Wt1* deficient mice revealed the deregulation of a particular set of genes. However, it cannot be excluded that this is a consequence of the diminished SRY level as it has been shown previously that WT1 regulates the expression of *Sry* (48; 49; 50) Lastly, the M15 cell line turned out to be unsuitable to study gene expression in this context. In order to address the question of whether WT1 is involved in the regulation of a sex specific gene expression pattern, after the decline of SRY activity, a different system needed to be established. Consequently, an *ex-vivo* organ culture system of isolated gonads at 12.5 dpc was set up and combined with an oligo-antisense knockdown strategy by using vivo-morpholinos against sole *Wt1* and/or *Gata4*.

### 2.3.1 Design of antisense vivo-morpholinos for the gene of interest and knockdown efficiency

The sequence of the *Wt1* vivo-morpholino has previously been published (133) Figure 2.4 B). In case of the *Gata4* transcript, the vivo-morpholino was designed as a complementary 25-mer oligonucleotide that is capable of masking the start codon. Into its

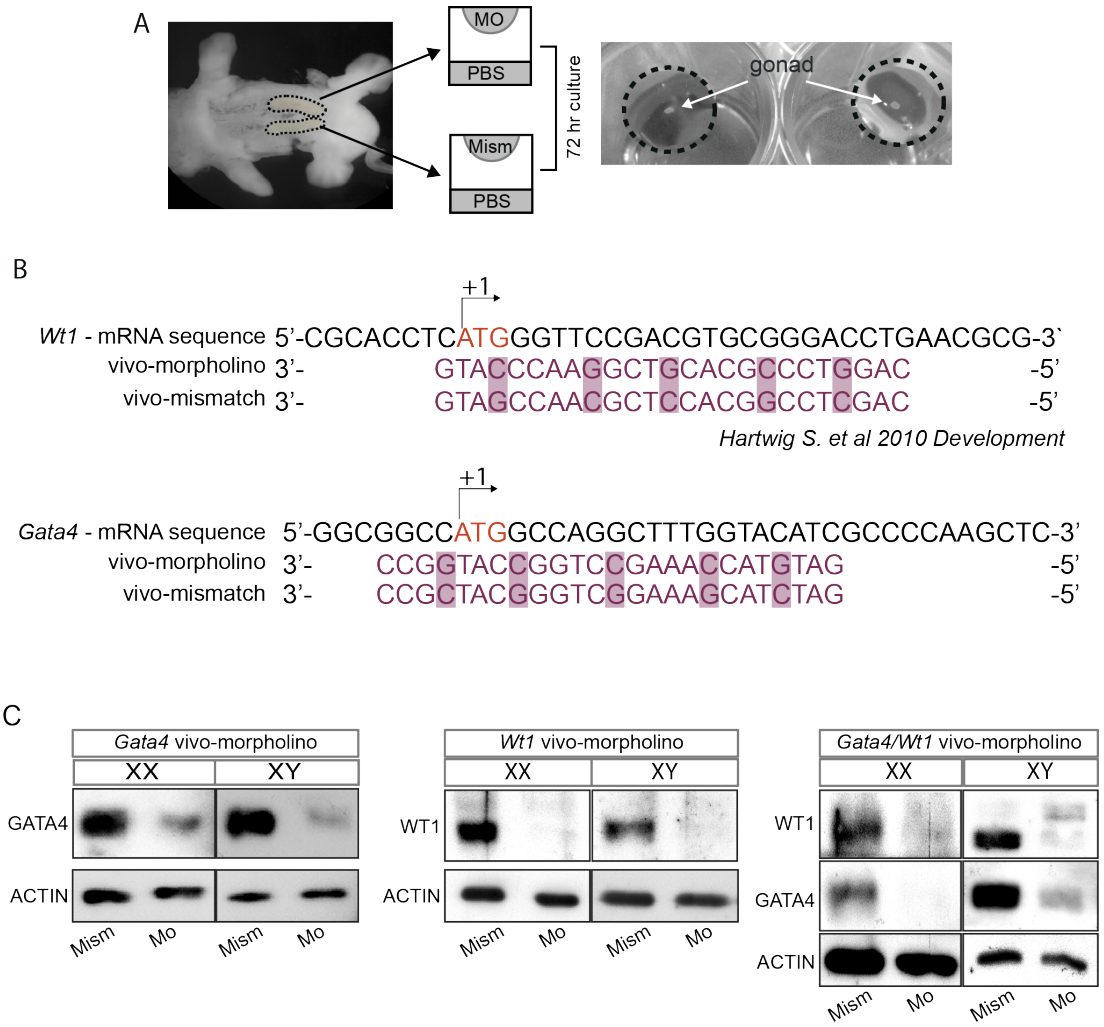


**Figure 2.4: Immunoblot analysis of vivo-morpholino mediated gene knockdown in testes and ovaries**. (A) An embryo at 12.5 dpc is shown with gonads on either side. The gonads were dissected and placed into 40$\mu$l droplets containing either a vivo-morpholino against the gene of interest or the respective mismatch control. (B) The sequence of the *Wt1* (133) and *Gata4* gene is shown with the designed vivo-morpholinos spanning the transcriptional start site. Based on their backbone composition the translational machinery is not able to convert the information into a protein, thus leading to the knockdown of the protein. (C) The knockdown efficiency is shown by immunoblotting. Total protein of single organs were loaded and WT1 and GATA4 were detected using specific antibodies. Actin was used as a loading control.

corresponding control oligomer, namely the mismatch control, five mismatches were introduced that are unable to undergo watson-crick base pairing with its complementary base pairs (Figure 2.4 B). The gonads were dissected at stage 12.5 dpc and embryos were sex-genotyped, as described before (Figure 2.1 B). One gonad was subjected to the knockdown by placing it into a 40$\mu$l droplet containing the vivo-morpholino. The contra-lateral gonad served as a control and was placed into a 40$\mu$l droplet contain-

ing the mismatch vivo-morpholino. The organ cultures were incubated for 72 hours in total. The knockdown efficiency was determined by immunoblotting (Figure 2.4 C). Gonads of either sex were used for a single or combined knockdown approach (Figure 2.4 C). The left panel shows the immunoblot of a testis and an ovary treated with *Gata4* vivo-morpholino. In both, testis and ovary the GATA4 knockdown was efficient. The middle panel illustrates the knockdown of WT1 in the testis and the ovary. An efficient knockdown of WT1 is visible in both, testis and ovary upon *Wt1* vivo-morpholino treatment compared to the mismatch control. The right panel demonstrates the knockdown efficiency upon combined inhibition of *Wt1* and *Gata4* in the testis and the ovary. The double knockdown approach was efficient in both organs (Figure 2.4 C). In conclusion, the *ex-vivo* organ culture system was successfully set up in terms of culturing the gonads for 72 hours in hanging droplets and mediating the knockdown of the protein of interest. This system is subsequently used for morphological analysis and assessing gene expression patterns in the testis and ovary.

### 2.3.2 *Wt1* vivo-morpholino knockdown leads to the degeneration of the gonadal duct system

Sainio *et al.* reported that WT1 influences the development of the mesonephric duct system in particular the development of the caudal mesonephric tubules. While cranial and caudal tubules are present in 11.0 dpc $Wt1^{+/+}$ mice, only the cranial tubules develop in $Wt1^{-/-}$ mice (144). Thus, it was tempting whether the knockdown using *Wt1* vivo-morpholinos exerts an effect at later stages of caudal mesonephric tubule development. To address this question, gonad/mesonephros anlagen were dissected at 12.5 dpc. One gonad was cultivated *ex-vivo* in the presence of the *Wt1* vivo-morpholino. The contralateral gonad was cultivated in the presence of the *Wt1* vivo-morpholino mismatch control. The gonads were visualised by staining of GATA4 (Cy3, magenta) and the mesonephric tubular system was stained for PAX2 expression (Dye-488, cyan) (Figure 2.5). In respect to the XY gonad the results show the degeneration of the caudal tubules, whereas the cranial tubules are present, although at a lower density number. In terms of the XX gonad the same effect was observed: the cranial tubules develop rather normally whereas the caudal mesonephric tubules degenerate (asterisks in Figure 2.5). The results suggest that WT1 is involved not only in the initial phase of caudal tubular development (144) but also in the maintenance of the caudal tubular structures.

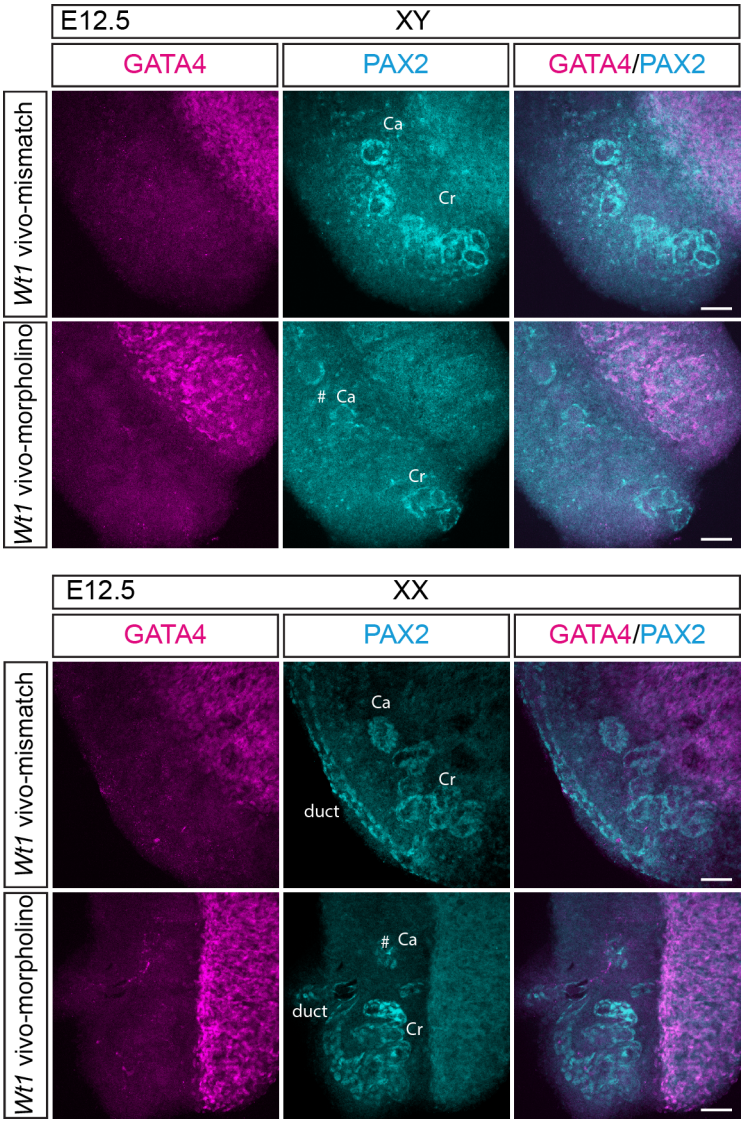


**Figure 2.5: *Wt1* vivo-morpholino treatment leads to the deformation of the duct system in XX and XY gonads.** Gonad/mesonephroi anlagen were dissected at 12.5 dpc. One gonad of the embryo was used for the WT1 knockdown ( *Wt1* vivo-morpholino) and the respective contralateral gonad served as the control ( *Wt1* vivo-morpholino mismatch). Organs were cultivated for a total of 72 hours in a 40$\mu$l droplet using the *ex-vivo* droplet culture technique. Cultured gonads were used for whole mount immunofluorescence staining. Primary antibodies against GATA4 and PAX2 were used. Cy3-(GATA4) and Dye488-(PAX2) secondary antibodies were used to visualise the primary antibody. The top panel shows representative images performed using a confocal microscope (LeicaDM2500) of the XY gonad and the bottom panel of the XX gonad. Note in the *Wt1* vivo-morpholino samples the defects in the caudal mesonephric tubules indicated by #. Ca: caudal; Cr: cranial; scale bar: 75$\mu$m. n=3

### 2.3.3 Gene expression analysis in *ex-vivo* cultured gonads

In order to gain novel insight into the molecular mechanisms of sex differentiation, the role of WT1 and GATA4 are studied in detail in terms of gene expression and synergistic effects. To address this issue the *ex-vivo* organ culture system, at stage 12.5 dpc, was utilised in order to knockdown WT1 or GATA4, or both.

The results upon the vivo-morpholino mediated knockdown of WT1 (Figure 2.4 C), revealed that genes can be grouped within two classes: first, genes that show a sex-specific gene expression pattern in either testes- (*Sf1, Sox9, Amh, Gata4*) or ovaries (*Dax1, Foxl2*). Second, genes whose expression level changes in both sex (*Amhr2, Star*) (Figure 2.6). Genes comprising the first group, i.e., *Sf1, Sox9, Gata4* and *Amh*, were

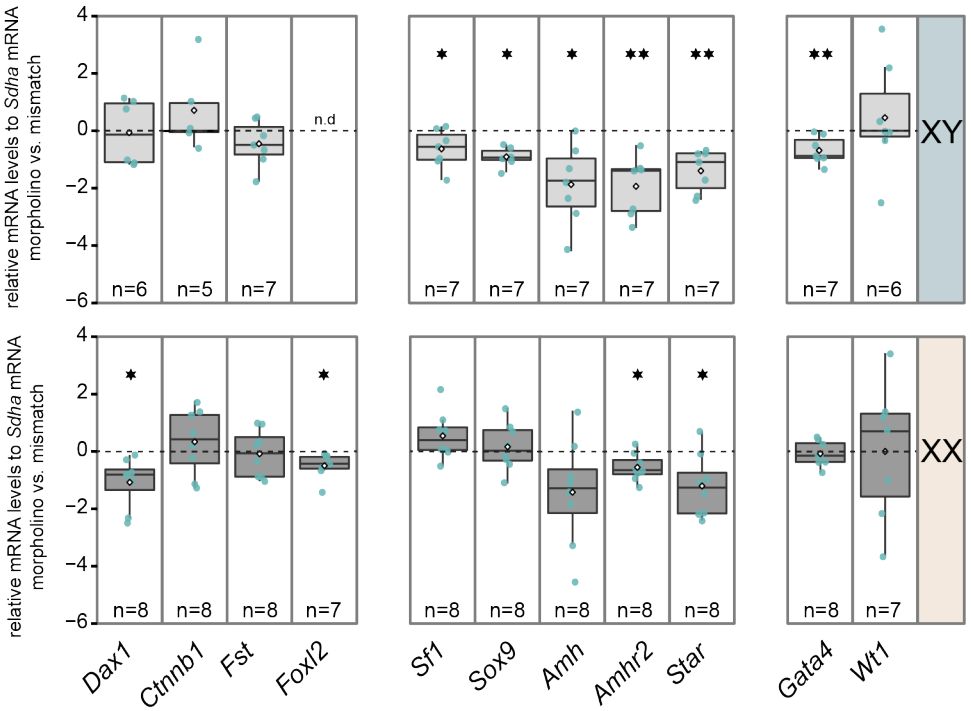


**Figure 2.6: Gene expression analysis of the *Wt1*-vivo-morpholino knockdown in testes and ovaries.** Genes are arranged with respect to female promoting, i.e., *Dax1, Ctnnb1, Fst*, and *Foxl2*) and male specific, i.e., *Sf1, Sox9, Amh, Amhr2*, and *Star*, and those implicated in both sexes, i.e., *Wt1* and *Gata4*. Gonads were dissected from mice at stage 12.5 dpc. One gonad of the embryo was used for the WT1 knockdown and the contra-lateral gonad served as the control (vivo-morpholino mismatch). Organs were cultivated for a total of 72 hours in a 40$\mu$l droplet using the *in-vitro* droplet culture technique and were then subjected to RT-qPCR analysis. mRNA levels were normalised to *Sdha* mRNA (145) and normalised Ct values are visualised on Tukey box plots. The vivo-morpholino-mismatch control was set to zero, which is represented as the black dashed line. At the bottom of each panel the sample number is shown and the cyan points illustrate the distribution of the samples. The white rectangle within the boxplot refers to the mean and the black line represents the median value. The results are visualised as fold differences between vivo-morpholino vs mismatch treated organ cultures. Statistical significances are determined by using a paired student's t-test and shown as asterisks: *p$<$0.05, **p$<$0.01. n.d.: not detectable.

significantly down regulated to 64.6%, 53.4%, 62.3% and 27.3% only in testes without significant changes in ovaries. In ovaries, genes like *Dax1* and *Foxl2* showed a significant down regulation in their transcript levels to 47.5% and 70.9%, respectively. Of note, *Foxl2* transcripts were undetectable in the testes. Within the second group, *Star* and *Amhr2* transcripts were significantly down regulated in either sex. *Star* transcripts were reduced to 43.5% in ovaries and to 38.0% in the testes. *Amhr2* transcripts declined to 68.2% in the ovaries and to 26.2% in the testes.

A previous report has provided evidence for a synergistic link between WT1 and GATA4 (49). Based on this rationale I first studied the effect of sole *Gata4* vivo-morpholino treatment (Figure 2.7) and thereafter a combined approach of *Wt1* and *Gata4* silencing was conducted (Figure 2.8). The knockdown was successful as shown by immunoblot-

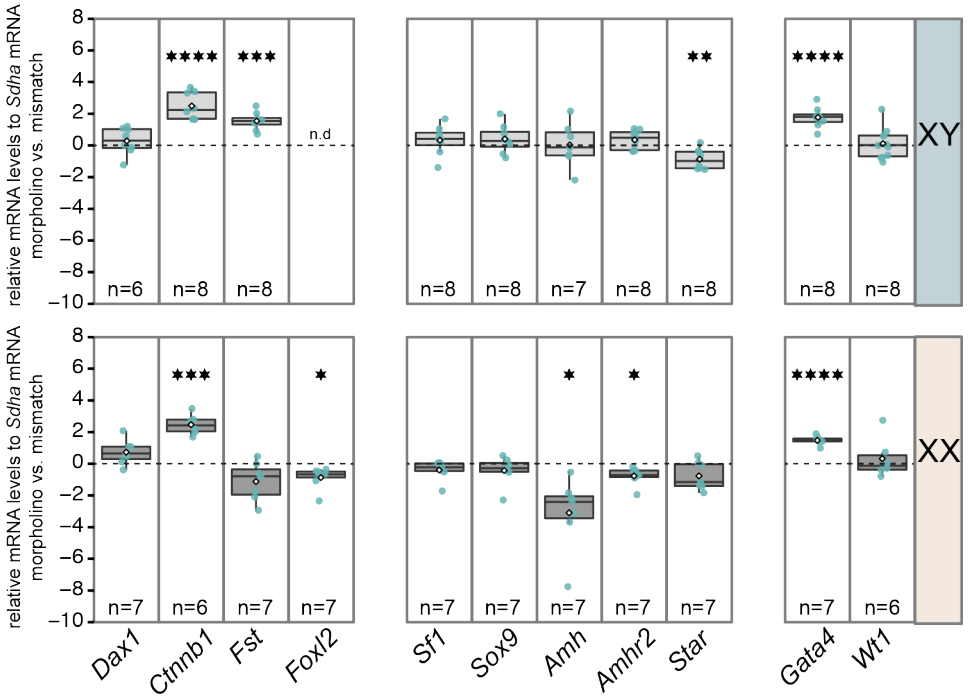


**Figure 2.7: Gene expression analysis of the *Gata4*-vivo-morpholino knockdown in testes and ovaries.** Genes are arranged with respect to female promoting, i.e., *Dax1, Ctnnb1, Fst*, and *Foxl2*) and male specific, i.e., *Sf1, Sox9, Amh, Amhr2*, and *Star*, and those implicated in both sexes, i.e., *Wt1* and *Gata4*. Gonads were dissected from mice at stage 12.5 dpc. One gonad of the embryo was used for the Gata4 knockdown and the contralateral gonad served as the control (vivo-morpholino mismatch). Organs were cultivated for a total of 72 hours in a 40$\mu$l droplet using the *in-vitro* droplet culture technique and were then subjected to RT-qPCR analysis. mRNA levels were normalised to *Sdha* mRNA (145) and normalised Ct values are visualised on Tukey box plots. The vivo-morpholino-mismatch control was set to zero, which is represented as the black dashed line. At the bottom of each panel the sample number is shown and the cyan points illustrate the distribution of the samples. The white rectangle within the boxplot refers to the mean and the black line represents the median value. The results are visualised as fold differences between vivo-morpholino vs mismatch treated organ cultures. Statistical significances are determined by using a paired student's t-test and shown as asterisks: *p<0.05, **p<0.01, ***p<0.001, ****p<0.0001. n.d.: not detectable.

ting (Figure 2.4 C). Genes subject to analysis can be grouped in two classes: first, given genes that show a sex-specific expression pattern in respect to the testes, i.e., (*Fst, Star*), or ovaries, i.e., (*Foxl2, Amh, Amhr2*). The second group comprises genes whose transcript levels were modulated sex-independently (*Ctnnb1, Gata4*). In detail, within testes transcript levels of *Fst* were up regulated 2.9-fold, whereas *Star* transcript levels were reduced to 58.9%. In ovaries a significant reduction of *Foxl2, Amh* and *Amhr2* to 54.9%, 11.7%, and 58.7% was observed. *Foxl2* transcripts were undetectable within the testes. Genes of the second group, in particular, *Ctnnb1* transcripts were up regulated 5.5-fold in ovaries and 5.6-fold in testes. *Gata4* transcripts increased 2.8-fold in ovaries and 3.4-fold in testes. As a subsequent step, the combined knockdown of WT1 and

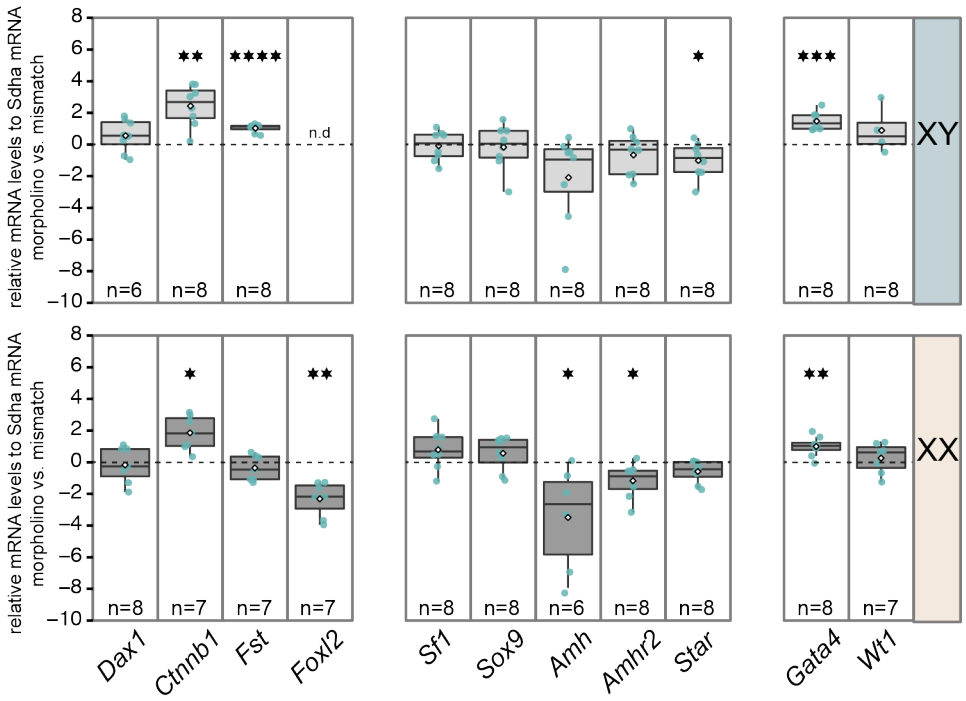


**Figure 2.8: Gene expression analysis of the *Wt1/Gata4*-vivo-morpholino knockdown in testes and ovaries.** Genes are arranged with respect to female promoting, i.e., *Dax1, Ctnnb1, Fst*, and *Foxl2*) and male specific, i.e., *Sf1, Sox9, Amh, Amhr2*, and *Star*, and those implicated in both sexes, i.e., *Wt1* and *Gata4*. Gonads were dissected from mice at stage 12.5 dpc. One gonad of the embryo was used for the Wt1/Gata4 knockdown and the contra-lateral gonad served as the control (vivo-morpholino mismatch). Organs were cultivated for a total of 72 hours in a 40$\mu$l droplet using the *in-vitro* droplet culture technique and were then subjected to RT-qPCR analysis. mRNA levels were normalised to *Sdha* mRNA (145) and normalised Ct values are visualised on Tukey box plots. The vivo-morpholino-mismatch control was set to zero, which is represented as the black dashed line. At the bottom of each panel the sample number is shown and the cyan points illustrate the distribution of the samples. The white rectangle within the boxplot refers to the mean and the black line represents the median value. The results are visualised as fold differences between vivo-morpholino vs mismatch treated organ cultures. Statistical significances are determined by using a paired student's t-test and shown as asterisks: *p<0.05, **p<0.01, ***p<0.001, ****p<0.0001. n.d.: not detectable.

GATA4 was analysed (Figure 2.8). The efficient knockdown of both proteins is shown by immunoblotting (Figure 2.4 C). Based on the results, the combined knockdown of GATA4 and WT1 caused similar changes in mRNA levels as sole GATA4 silencing. Therefore, the first group comprises genes that show a sex-specific expression pattern in either testes (*Fst, Star*) or ovaries (*Foxl2, Amh, Amhr2*). Genes within the second group display significant changes independent of their sex (*Ctnnb1, Gata4*). In detail, transcript levels of *Fst* were significantly up regulated 2-fold and *Star* transcripts were reduced to 49.7% only in testes. In terms of ovarian specific changes, the transcript levels of *Foxl2, Amh* and *Amhr2* were reduced to 20.1%, 8.9% and 44.2%, respectively. Transcript levels of *Ctnnb1, Gata4* were modulated in either sex. *Ctnnb1* was up regulated 3.6-fold in ovaries and 5.4-fold in testes. *Gata4* transcripts were increased 1.9-fold in ovaries and 2.8-fold in testes. It is interesting to note that in case of *Sf1, Sox9, Amh*, and *Amhr2* expression the combined approach prevented the decrease in their expression by sole *Wt1* antisense silencing. On the other hand all genes influenced by sole *GATA4* knockdown still show the same pattern in the combined approach. Although both WT1 and GATA4 proteins were reduced efficiently as shown by the immunoblot (Figure 2.4 C).

Inhibition of GATA4 protein translation was efficient (Figure 2.4 C), *Gata4* mRNA transcripts were significantly upregulated in both sexes (Figure 2.7 and Figure 2.8). A regulatory feedback mechanism regarding *Gata4* has previously been pointed out in different model systems (146). Mazaut-Guittot *et al.* reported that in gonads two alternative *Gata4* transcripts, namely *Gata4 E1a* and *E1b*, are expressed and involved in this regulatory feedback mechanism (147). In the gonads both transcripts are expressed at similar high levels (147). Notable, *Gata4* deficient mice express elevated *Gata4 E1b* transcripts, whose promotor is normally repressed by GATA4 itself (148). Therefore it was tempting to assess which alternative transcript, *Gata4 E1a* or *Gata4 E1b*, is up regulated upon *Gata4* vivo-morpholino silencing. RT-qPCR was performed with specific primers against either isoform. The results show that upon *Gata4* silencing the transcript, *Gata4 E1a*, is up regulated 2-fold in either sex. However, in the testis, the *Gata4 E1b* transcript is up regulated 5-fold (Figure 2.9).
In conclusion, the results first describe the successful establishment of the *ex-vivo* organ culture and second that WT1 and GATA4 are implicated, in a complex manner, in the proper regulation of genes involved in gonadal sex differentiation. Analysis gathered from these experiments could identify *Foxl2* as a potential new WT1 target gene, which is regulated most likely in a synergistic manner with GATA4. Furthermore, the *Gata4* vivo-morpholino mediated knockdown, could identify *Ctnnb1* and *Fst* as potential new GATA4 target genes.

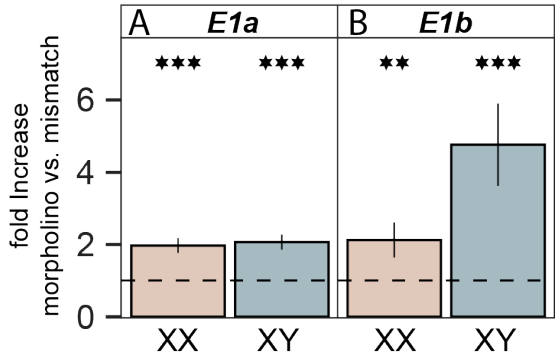


**Figure 2.9: Gene expression analysis of the alternative splice variants *Gata4* E1a and E1b in *Gata4*-vivo-morpholino mediated knockdown.** In (A) the *Gata4 E1a* and in (B) the *Gata4 E1b* alternative transcript is shown. mRNA levels were normalised to *Sdha* mRNA (145). Ct values are represented as fold increase between vivo-morpholino vs mismatch treated organ cultures. The vivo-morpholino-mismatch control was set to 1, which is represented as the black dashed line. Statistical differences are indicated by asterisks: **p<0.01, ***p<0.001, paired student's t-test. n=4

#### 2.3.3.1 Co-expression analysis of WT1 and GATA4

In the context of assessing gene regulation (Figure 2.6, Figure 2.7 and Figure 2.8), it is essential that WT1 and GATA4 are co-expressed within the same cells in the gonad in order to propose that both transcription factors act on the same promoters of given target genes. To address, whether WT1 and GATA4 are co-expressed within the gonad, gonads of different developmental stages were subject to whole mount immunofluorescence staining.

At the bipotential stage by 11.5 dpc, WT1 and GATA4 are co-expressed within cells that are scattered throughout the gonad. No gross morphological differences at this stage were observed in neither the testis nor the ovary (Figure 2.10 A,B), consistent with previous reports (reviewed in 12). By 13.5 dpc the ovary appears to be reduced in size (149) and starts to adopt a more roundish shape compared to the testis. Co-expression of WT1 and GATA4 is detected within the ovary (Figure 2.10 C). In the testis, note the presence of the testicular cords (tc), a characteristic feature of testis development (15) (Figure 2.10 D). Furthermore, the confocal image scan allows to confine co-expression within the cells towards a particular compartment. GATA4 is scattered throughout the gonad, within the interstitium as well as in cells that make up the seminiferous tubules. On the contrary, WT1 was undetected within cells of the interstitium but present in cells of the seminiferous tubules. Hence, GATA4 and WT1 are co-expressed within cells of the seminiferous tubules (Figure 2.10 D), which has been also shown by Natoli *et al.* (150). By 15.5 dpc, the ovary has developed into a more roundish shape and is linked to a more pronounced underlying mesonephros. GATA4 and WT1 are co-expressed within the gonad (Figure 2.10 E). Within the testis, co-expression of WT1 and GATA4 is noticed within the cells that make up the outer wall of the seminiferous tubules (Figure 2.10 F). By 18.5 dpc the ovary is surrounded by the adjacent tissue and GATA4 and WT1 are co-expressed within gonadal cells (Figure 2.10 G). In the testis, WT1 expression is restricted to cells that build up the testicular cords and GATA4 is

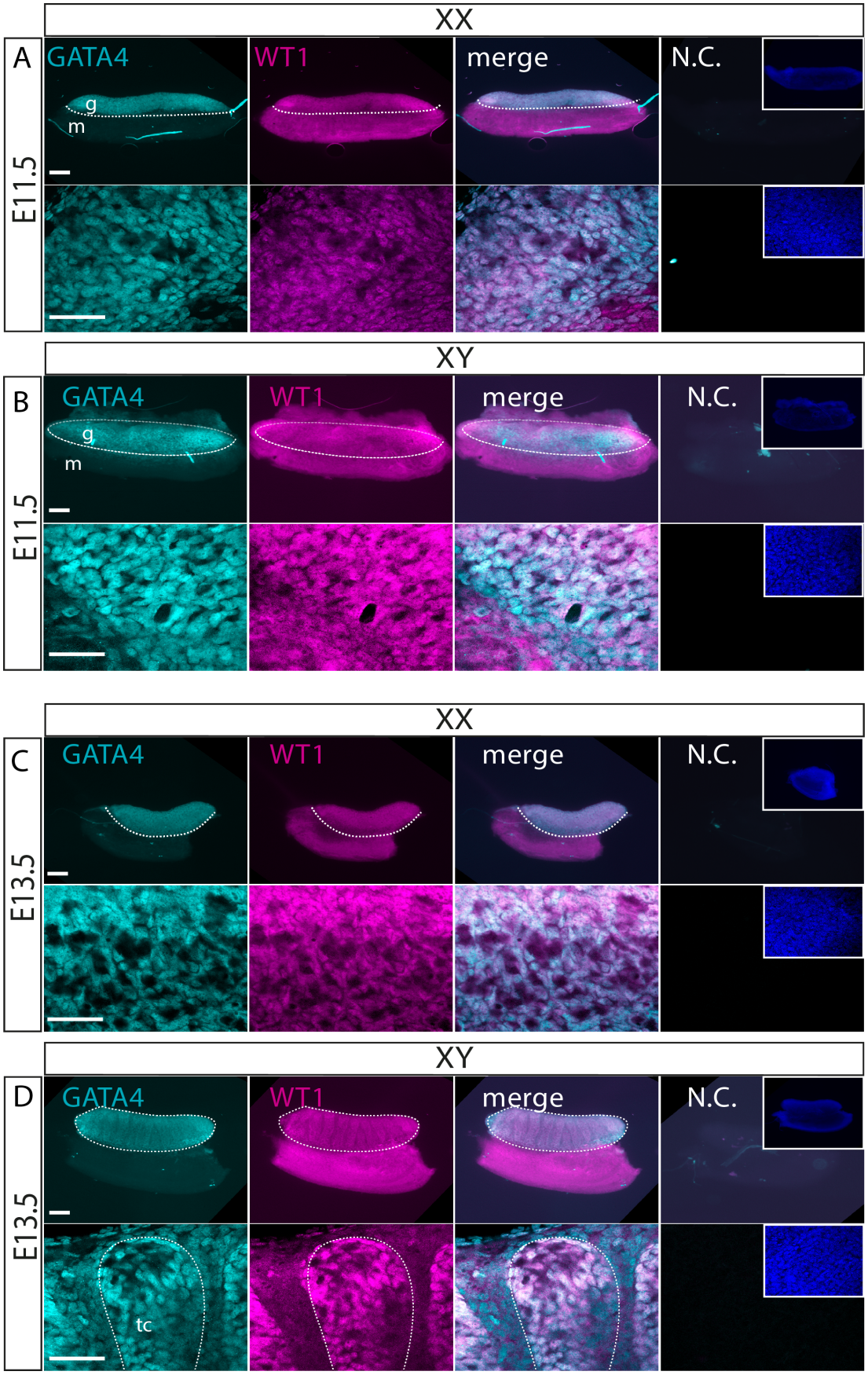
XX
A
E11.5
GATA4
WT1
merge
N.C.
g
m
XY
B
E11.5
GATA4
WT1
merge
N.C.
g
m
XX
C
E13.5
GATA4
WT1
merge
N.C.
XY
D
E13.5
GATA4
WT1
merge
N.C.
tc

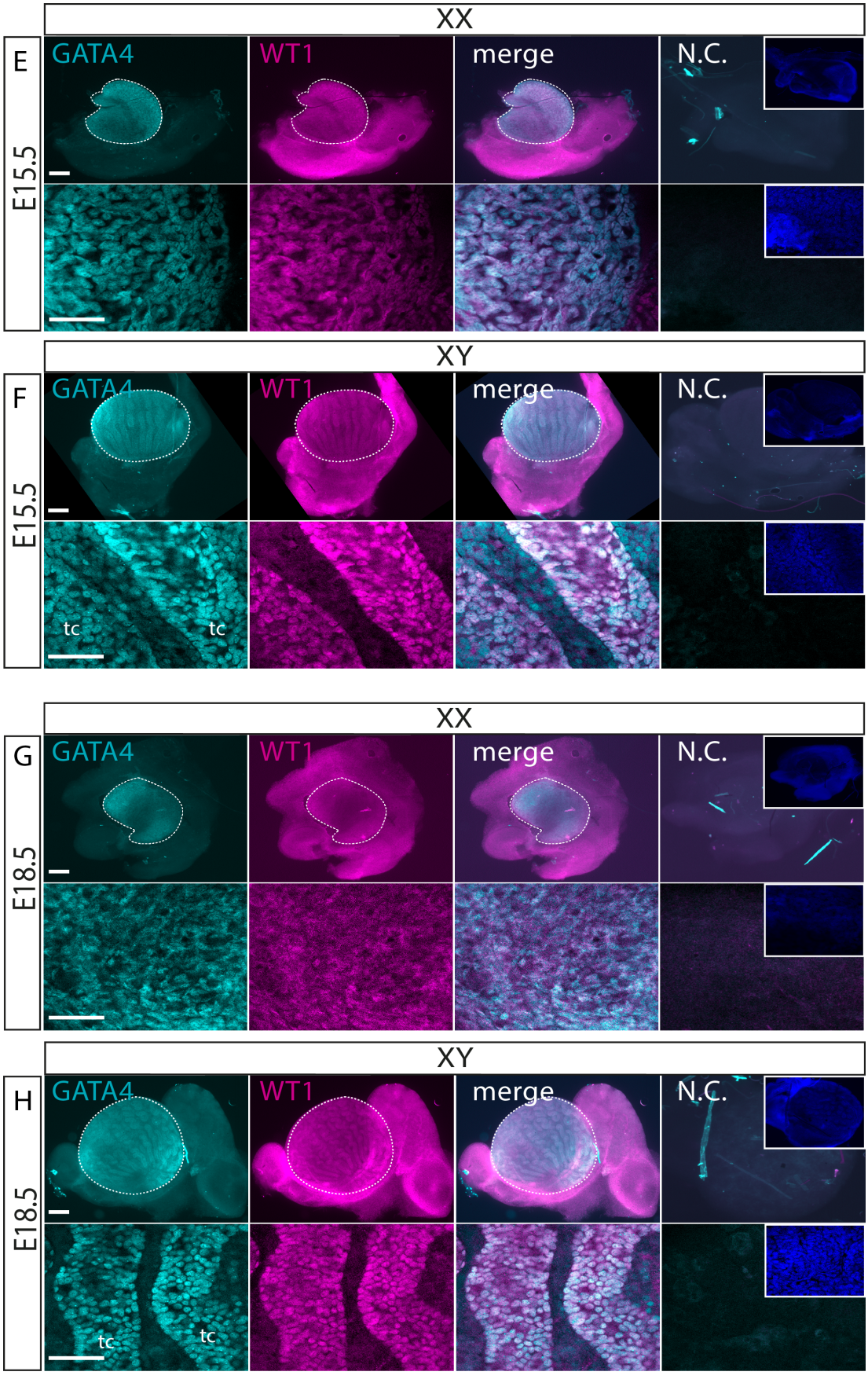
XX
E
E15.5
GATA4
WT1
merge
N.C.
XY
F
E15.5
GATA4
WT1
merge
N.C.
tc
tc
XX
G
E18.5
GATA4
WT1
merge
N.C.
XY
H
E18.5
GATA4
WT1
merge
N.C.
tc
tc

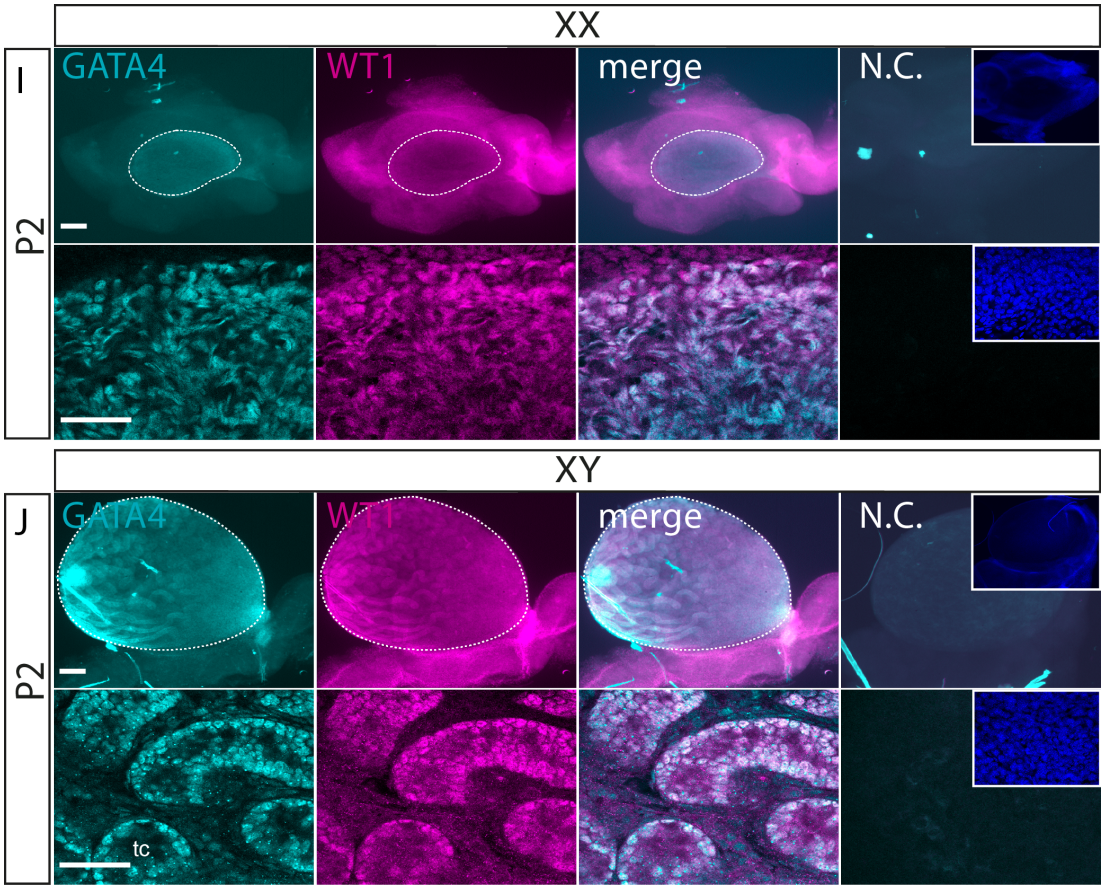


**Figure 2.10: WT1 and GATA4 are co-expressed in testes and ovaries throughout development.**. Gonad/mesonephroi anlagen of genotype XY and XX were dissected from wild type mice at the following stages: (A,B) 11.5 dpc, (C,D) 13.5 dpc, (E,F) 15.5 dpc, (G,H) 18.5 dpc and (I,J) P2 and used for immunohistochemistry with primary antibodies against GATA4 and WT1. Cy3-(WT1) and Dye488-(GATA4) antibodies were used to visualise the primary antibody. The negative control (N.C.) is shown to the right of each panel. DAPI was used for counterstaining cell nuclei. The dashed line represents the gonad. The top panel of either the XX and XY gonad/mesonephros complex depicts representative pictures of the separate channels of an overview image. The bottom panel displays a representative confocal section. GATA4 is observed only in the gonad and Wt1 is observed in the gonad and mesonephros. Nuclear co-expression is observed in XX (A,C,E,G, I) and XY (B,D,F,H,J) throughout development. gonad (g) mesonephros (m), testicular cords (tc), scale bar: overview images: 200$\mu$m; confocal sections: 100$\mu$m.

scattered throughout the gonad. Co-expression was detected only in cells of the seminiferous tubules (Figure 2.10 G). Next, stage P2 was examined, and the observed pattern revealed co-expression of WT1 and GATA4 within the ovary and testis (Figure 2.10 I,J). Moreover, WT1 and GATA4 are observed to be as well co-expressed during adulthood. Immunostainings of the testicular structure (Figure 2.11 A) revealed that GATA4 and WT1 are co-expressed at the periphery of the seminiferous tubules. In addition to the adult testis the heart was subject to analysis and identified GATA4 to be scattered throughout the epicardium and the myocardium, whereas WT1 expression is restricted

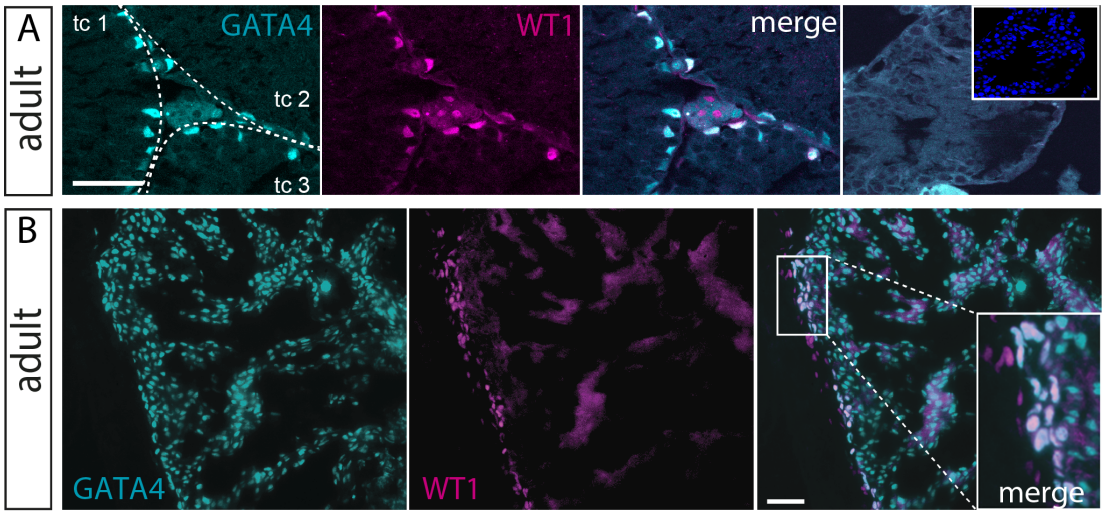


**Figure 2.11: WT1 and GATA4 are co-expressed in adult testes and in the epicardium**. Testis and the heart were dissected from adult wild type mice and post-processed for immunohistochemistry. Primary antibodies against GATA4 and WT1 were used. Cy3-(WT1) and Dye488-(GATA4) antibodies were used to visualise the primary antibody. The negative control (N.C) is shown to the right of each panel. DAPI was used for counterstaining. Negative Control for the heart is not shown. (A) Co-expression in the adult testis is shown by merging the single fluorescent channels. Note that three testicular cords (tc 1, tc 2 and tc 3) are presented.(B) Co-expression of GATA4 and WT1 is shown in the adult heart. GATA4 and WT1 are co-expressed in the epicardium. scale bar: 100$\mu$m.

to the epicardium, the site of co-expression (Figure 2.11 B).

The results herein show that WT1 and GATA4 are co-expressed during gonadal development, and confirm previous studies (37; 150). This in turn strengthens a conceivable functional link between WT1 and GATA4, in terms of acting in a synergistic manner on given target genes, e.g., *Foxl2*.

## 2.4 Proliferation is impaired in the gonad and mesonephros through WT1 and GATA4 vivo-morpholino knockdown

It has been described that WT1 and GATA4 have an impact on cell proliferation (125; 151). It was tempting to hypothesize, whether an effect upon the knockdown of WT1 and GATA4 by vivo-morpholino treatment is associated with changes in the proliferation state within the gonad and mesonephros. In order to address this issue gonad/mesonephroi anlagen were dissected at 12.5 dpc and treated with either *Wt1* or *Gata4* vivo-morpholino. Cell proliferation was assessed in terms of BrdU incorporation into the DNA. The *ex-vivo* organ cultures were incubated for 72 hours. Thereafter, gonads were embedded, cryosectioned and stained using an antibody against BrdU.

### 2.4.1 Proliferation is reduced in ovaries and testes upon WT1 knockdown

Gonads and mesonephroi treated with *Wt1* vivo-morpholino, exhibit impaired cell proliferation in either sex (Figure 2.12 A,B). By comparing *Wt1* vivo-morpholino treated XX gonads, cell proliferation is significantly reduced from 36,0% to 15,6%. Considering the proliferation state in the mesonephros, a significant decline from 38.9% to 22.6% was observed. Furthermore, in XY gonads cell proliferation declines significantly from 26.3% to 14% and in the mesonephros from 45.3% to 19.8%. This concludes that cell proliferation is affected upon vivo-morpholino mediated knockdown of WT1 not only

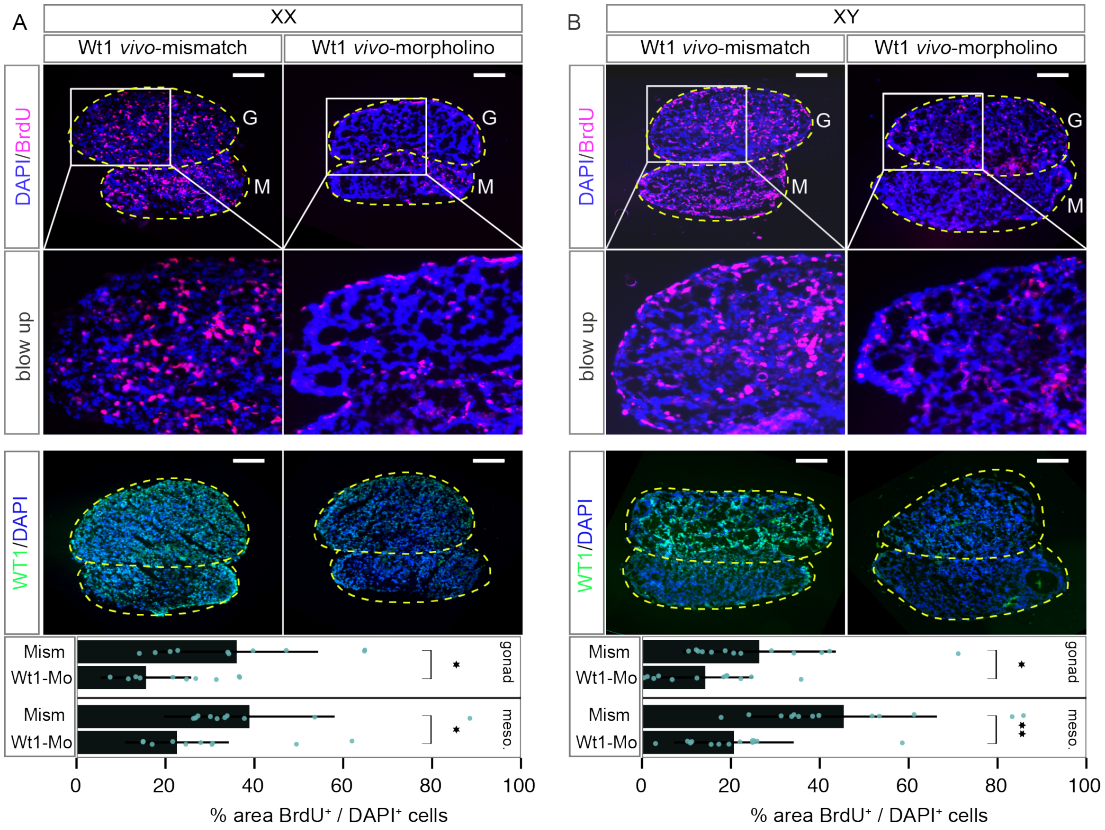


**Figure 2.12: Knockdown of WT1 leads to a significant decrease of proliferation in ovaries, testes and mesonephroi.** Gonad/mesonephroi anlagen were dissected from embryos at 12.5 dpc and cultured using the *ex-vivo* droplet culture technique for 72 hours and BrdU was applied for 24 hours to the media. To assess cell proliferation a BrdU specific antibody was used. The knockdown efficiency was determined by using a WT1 specific antibody. The top and middle panel in A (XX) and B (XY) show a significant reduction in proliferating cells upon antisense inhibition of WT1 in the gonads and mesonephroi. Quantification was performed by counting BrdU positive cells in at least 5 sections of 3 embryos and were normalised to counterstained DAPI cells, as illustrated at the bottom by the bar plots. The sample size is represented by the cyan points. The values are presented as mean SD, *p<0.05, **p<0.01, ***p<0.001; student's t-test. G: gonad; M mesonephros; scale bar: 100$\mu$m

in the gonad but also in the mesonephros.

### 2.4.2 Proliferation is reduced only in testes but not in ovaries upon GATA4 knockdown

Gonads treated with *Gata4* vivo-morpholino exhibit impaired cell proliferation only in XY gonads but not in XX gonads (Figure 2.13 A,B). In particular, XY gonads show a significant decrease in cell proliferation from 25.6% to 6% and the proliferation state in the mesonephros was significantly reduced from 34.9% to 15.3% (Figure 2.13 B).

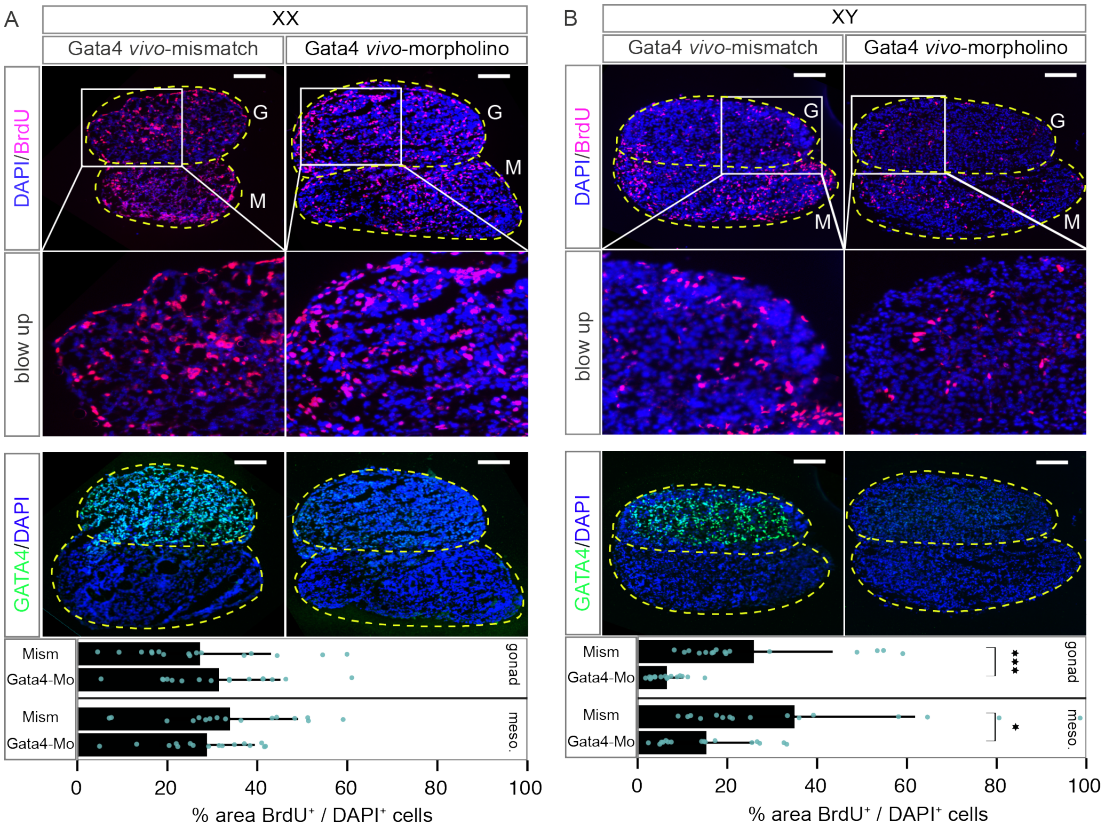


**Figure 2.13: Knockdown of GATA4 leads to a significant decrease of proliferation only in testes and the male mesonephros.** Gonad/mesonephroi anlagen were dissected from 12.5 dpc staged embryos and cultivated using *ex-vivo* for 72 hours. BrdU was added for 24 hours to the media to assess cell proliferation. The knockdown efficiency was determined by using a GATA4 specific antibody, as shown by representative images. The top and middle panel in XY (B) show a significant reduction in proliferating cells upon antisense inhibition of *Gata4* in the gonad and mesonephros of the testis. Inhibition of *Gata4* has no significant effect on proliferation (A). 5 sections of 3 embryos were used for quantification purpose and normalisation was performed by counterstaining DAPI cells, as illustrated in the bar plots. The cyan points represent the sample size. Values are represented as mean SD, *p<0.05, **p<0.01, ***p<0.001. student's t-test. G: gonad; M: mesonephros; scale bar: 100$\mu$m.

## 2.5 Stabilisation of the Wnt pathway in testes by LiCl does not modulate the expression of *Wt1* and *Gata4*

Previous studies have pointed out that Wnt signalling is critical for ovarian development (reviewed in 152). Moreover, data shown in Figure 2.7 and Figure 2.8, suggest that GATA4 may repress *Ctnnb1* expression. LiCl, a Wnt pathway agonist, can be used to diminish the expression of male specific genes and increase the expression of female specific genes within the testis (91; 153). More specifically LiCl inhibits the function of GSK3-$\beta$ (154) and therefore stabilising $\beta$-CATENIN. Within this line it was tempting to hypothesise whether the Wnt pathway modulates the expression of *Wt1* and *Gata4* during male development. Therefore, testes were dissected at 11.25 dpc (16 ts)

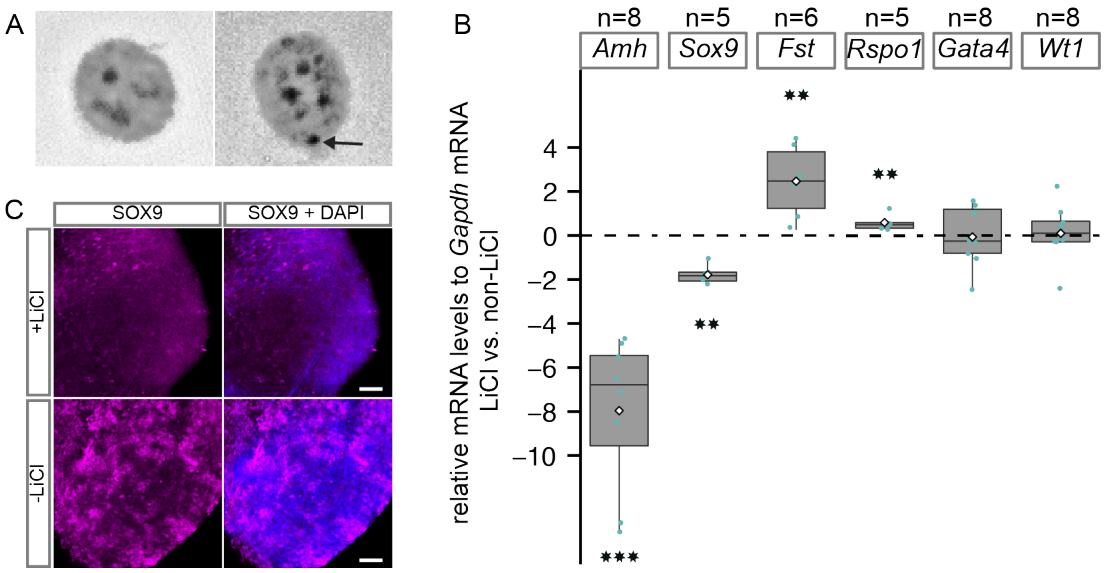


**Figure 2.14: LiCl treatment of testes leads to the up regulation of male specific markers and down regulation of female specific markers.** Testes were dissected at 16-17 ts (11.25 dpc), placed in a 40$\mu$l droplet containing 50mM LiCl and incubated for 24 hours. Thereafter, media was changed and the organs were cultivated for a total of 72 hours. (A) Prior to RT-qPCR analysis the sex was determined by staining isolated cells from the amnion using 1% toluidine-blue solution according to a previously published protocol (155). The inactive X-chromosome was observed as a compact heterochromatic structure at the periphery of the XX cell, known as the Barr body (arrow). (B) From these preparations RNA was extracted and used for RT-qPCR analysis. Male specific markers like *Amh* and *Sox9* were significantly down regulated, whereas the expression of female specific markers, i.e., *Fst* and *Rspo1* was significantly induced. The expression of *Gata4* and *Wt1* is unaltered. Samples were normalised to *Gapdh* and LiCl vs nonLiCl treated samples. Statistical significances are determined by using a paired student's t-test and shown as asterisks: **p<0.01, ***p<0.001. (C) Representative images of SOX9 staining of testis treated with LiCl compared to non-LiCl treated ones. Cultured gonads in LiCl or non-LiCl were used for whole mount immunofluorescence staining and stained with SOX9 and DAPI. A marked down regulation of SOX9 was observed as compared to the control. Scale: 75$\mu$m.

and cultivated *ex-vivo* in hanging droplets. Sex-genotyping was performed by toluidine staining of the inactive X-chromosome in female cells, which is present at the periphery and known as the Barr body (Figure 2.14 A) (155). One gonad was treated with DMEM media supplemented with 50mM LiCl for 24 hours and the contralateral gonad served as a control. Thereafter, the media was replaced without LiCl and incubation was performed for a total of 72 hours. Gonads were then subject to RT-qPCR analysis as well as SOX9 immunostaining. Results from this experiment confirmed on the one hand that the testis specific genes *Amh* and *Sox9* were significantly down regulated to 0.04% and 29.0%, respectively. On the other hand the ovarian promoting genes *Fst* and *Rspo1* were significantly up regulated to 6-fold and 1.7-fold, respectively. This is in line with previous studies (91; 153). In addition, the down regulation of the male specific marker, SOX9, was observed by immunostaining (Figure 2.14 B, C), as shown by others (91; 153). However the expression of *Gata4* and *Wt1* remained unchanged upon LiCl treatment. Therefore, activation of the Wnt pathway has no effect on the expression of *Gata4* and *Wt1*.

# 3

# Discussion

The major scope of this thesis is to dissect the complex interplay between the transcription factors WT1 and GATA4 during sex-determination and differentiation. Importantly, the focus herein is aimed towards the sex-specific analysis to ultimately gather a more complete picture: (i) of whether WT1 is involved in the establishment of a sex-specific signature, (ii) to what extend GATA4 is involved in gonadal development in both sexes, (iii) and in how far WT1 and GATA4 are intertwined in terms of regulating common genes. First, the morphology as well as the gene expression status in germline *Wt1* deficient mice was analysed. In order to examine the functional relationship between WT1 and GATA4 during the sex differentiation phase, a novel approach was applied that comprises the combination of a hanging droplet culture technique with an antisense silencing approach using vivo-morpholinos directed against WT1 and GATA4. Furthermore, cell proliferation within the gonad and the mesonephros was assessed, the Wnt pathway was stabilised in testes using LiCl in order to investigate whether Wnt signalling modulates the mRNA levels of *Wt1* or *Gata4*.

## 3.1 The transcription factor WT1 contributes to the establishment of a sex-specific genetic signature

It is important to note that previous studies analysing germline *Wt1* deficient mice did not differentiate between females and males (108). It might not have been of concern when the analysis was performed prior to sex determination, at the time between 10.75 dpc and 11.0 dpc (108) but it matters after 12.5 dpc when sex-differentiation proceeds. In order to grasp a clearer picture of the potential sex-specific function of WT1 during sex differentiation, it was of great importance to differentiate between the sexes (Figure

2.2). Germline *Wt1* deficient mice at stage 13.5 dpc were analysed by RT-qPCR. The results herein revealed a loss of the sex specific signature which is in line with the known role of WT1 regulating *Sry* expression (48; 49). Genes such as *Dax1, Sf1, Gata4, Amhr2*, and *Star* were significantly reduced in either sex whereas genes such as *Ctnnb1, Fst, Foxl2, Sox9* and *Amh* were down regulated in both male and female (Figure 2.2). For most analysed genes a direct link to WT1 has been shown previously by others, in particular for *Dax1* (103), *Sf1* (31), *Amhr2* (108), *Star* (106), *Ctnnb1* (107), and *Amh* (49). These studies provided important biological insights into the transcriptional regulation mediated by WT1. For most genes such as *Dax1, Gata4, Amhr2, Star, Sox9, Ctnnb1*, and *Amh* the evidence for a direct regulation is primarily based on *in-vitro* assays and therefore remains to be validated in *in-vivo*. Furthermore, notable is the significant down regulation of the *Foxl2* and *Fst* genes, which were identified in this thesis as new potential WT1 target genes. Whether the observed effect is direct or indirect necessitates further experiments encompassing ChIP and reporter gene assays. In addition, *Foxl2* was also significantly down regulated in *ex-vivo* cultured gonads upon the knockdown of *Wt1* using antisense vivo-morpholinos. In contrast, the down regulation of the *Fst* gene was not observed by using the vivo-morpholino approach against *Wt1* (Figure 2.6). This suggests that the downregulation of the *Fst* gene is a secondary consequence of the perturbed morphology of the *Wt1* deficient gonads (Figure 2.1) and the increase apoptosis rate (47). Given that WT1 regulates the *Sry* gene (47; 48; 49), the observed effects possibly mimic the consequence of the down regulation of the *Sry* gene upon the loss of WT1, which consequently culminates in differentiation defects of Sertoli cells (48).

## 3.2 Gonadal differentiation involves a complex cooperation between the transcription factors WT1 and GATA4

### 3.2.1 The *ex-vivo* droplet culture system combined with vivo-morpholino treatment is an effective tool to study *Wt1 / Gata4* gene function beyond the stage of sex determination

Investigating the function of WT1 after sex determination, is hampered by the lethal phenotype of *Wt1* deficient mice (32). This makes later time points unaccessible for investigation. However, this problem could be circumvented by making use of conditional transgenic mice. This system is remarkably useful and revealed fundamental insight into the biological relevance of various factors but it also depends strongly on the transcriptional network of transcription factors that modulate promoters/enhancer

regions that drive transgene expression in conditional transgenic mice. For example, Gao *et al.* deleted *Wt1* in a tissue specific manner by generating a *Wt1*$^{-/flox}$*; Amh-Cre* mouse strain that allows to study the function of WT1 in a testis specific context (104). In order to grasp a clearer picture of the impact of WT1 but also of GATA4 during sex differentiation in either sex I utilised and developed an alternative approach by combining a modified version of the hanging droplet culture technique (91) in conjunction with the application of vivo-morpholinos as an antisense silencing strategy (Figure 2.4). This antisense silencing approach is equally effective in both sexes at the same developmental stage and allows the silencing of multiple genes at the same time point. Using vivo-morpholinos in *ex-vivo* hanging droplet cultured organs represents a novel approach that seems suitable especially in the context of gonadal development.

### 3.2.2 WT1 stabilises the caudal but not the cranial duct system after sex determination

Germline *Wt1* deficient mice show malformations of the caudal mesonephric tubular system, as reported by Sainio *et al.* The authors used mice dissected at 11.0 dpc and could pinpoint that the caudal mesonephric tubules do not develop, whereas the cranial tubular system is present (144). My experiments, described in section 2.3.2 and shown in Figure 2.5, suggest that, by using *ex-vivo* cultured gonad/mesonephroi anlagen – dissected at 12.5 dpc at which stage the tubular duct system is established – WT1 is equally important in the maintenance of the proper development of the caudal mesonephric tubules. Nevertheless, the observed effect could as well be of secondary consequence to the WT1 vivo-morpholino knockdown. One explanation could be that WT1 may regulate a specific factor in the caudal tubules that has no influence in the cranial tubule development, e.g. *Npy* which is expressed caudally but not cranially (156). It could as well be that a factor is expressed in both, the cranial and caudal tubules, but WT1 influences its expression only in the caudal part. The latter might be likely as most factors, such as WNT4, PAX2, PAX8, LHX1, are implicated in mesonephric tubule development and are expressed in both structures (156). This may be supported by the notion that it is known that WT1 could act in a tissue specific context as an activator or repressor, as shown for the *Wnt4* gene (98). Although additional experiments are required in order to derive precise conclusions, data provided by my experiment proposes that WT1 contributes to the maintenance of the caudal tubular system.

### 3.2.3 WT1 is implicated in sex differentiation by establishing a sex specific signature

The main purpose of utilising the vivo-morpholino approach is directed towards the aim to gain greater insight into the functional relevance of WT1 during gonadal sex differentiation. It has been shown that the bipotential gonad embarks on the male pathway under the influence of SRY activity (44), which in turn is active within a narrow window of time ∼10.5 dpc to 11.5 dpc (41; 42). WT1 is a known regulator of *Sry* expression (47; 48; 49). The *Wt1* vivo-morpholino approach led to a significant down regulation of testis specific genes, i.e., *Sf1, Sox9*, and *Amh* (Figure 2.6). These findings suggest that WT1 is required for establishing a sex-specific genetic signature towards testis development. Moreover, the data herein extend the molecular picture of WT1 in respect to gonadal ovarian differentiation. It seems likely that WT1 fulfils an important role in testis and ovary development alike. With regard to ovary development, in both approaches – the vivo-morpholino strategy and in *Wt1* deficient mice – the expression of *Foxl2* and *Dax1* is significantly down regulated (Figure 2.6 and Figure2.2). In terms of *Dax1* this is consistent with a previous report (103). FOXL2 has been ascribed as an important regulator for granulosa cell differentiation. More recently, a report provided evidence that FOXL2 is essential to maintain the ovarian phenotype throughout life time. Upon deleting FOXL2 in adult mice, granulosa cells within the ovary transdifferentiate into a Sertoli cell fate, hence the ovary adopts a testis phenotype (81). The expression of *Foxl2* needs to be turned off in the testis, which is mediated by SOX9 in synergism with ESR1 (81). Furthermore, it has been shown that in the ovary, FOXL2 antagonises the stimulatory effect of WT1(-KTS) in regulating *Sf1* expression. *Sf1* expression is up regulated by WT1(-KTS) (31) in somatic cells within the testis and FOXL2 negatively regulates *Sf1* expression in the somatic cells of the ovary (157). The data herein suggest that WT1 up regulates *Foxl2* – its own competitor – to shut down the expression of *Sf1* in the ovary – hence promoting proper ovarian development. Thus, the results indicate that WT1 is not only required for testis development, but equally important, also engages a crucial role during ovarian development, as shown by the identification of *Foxl2* as a novel potential WT1 target gene. Whether the effect is direct or indirect needs to be proven in future experiments by utilising ChiP on primary gonadal tissue.

### 3.2.4 The transcription factor GATA4 regulates itself and represses *Ctnnb1* equally in both sexes but *Fst* only in the testis

The rationale behind the GATA4 knockdown approach was that it has been shown that WT1/GATA4 interact with each other and co-regulate the expression of *Sry* and

*Amh* (49). In the sole GATA4 knockdown the down regulation of *Star* expression was confirmed as previously shown by others (122). Interestingly, two novel putative GATA4 downstream genes could be identified, namely *Ctnnb1* and *Fst*, both are repressed by GATA4, the former in both sexes and the latter only in the testes.

*Ctnnb1* encodes for $\beta$-catenin that has an essential role in ovarian development but is dispensable for testis development (83; 107). Furthermore, stabilisation of $\beta$-catenin led to a XY to XX sex reversal (91). Within the context of Wnt signalling, the stabilisation of $\beta$-catenin in XY gonads using LiCl, revealed no significant changes in the expression of *Gata4* and *Wt1* were observed, indicating that GATA4 and WT1 may act upstream of the Wnt pathway (Figure 2.14). A report suggests an indirect link between GATA4 and *Ctnnb1* expression, in the context of heart development (158). The authors proposed that *Ctnnb1* expression is primarily affected by NKX2.5, which is a downstream target of GATA4 (158). To conclude, data herein suggests that GATA4 rather fine tunes and sustains basal levels of $\beta$-catenin expression in either sex.

Furthermore, equally interesting was the observed repressive effect of GATA4 on *Fst* expression. This could be a possible explanation for the dimorphic expression pattern observed herein (Figure 2.2) and by others (9; 79), upon comparing wild type ovaries and testes. Both, sole GATA4 antisense silencing and combined knockdown of WT1/GATA4 show an up regulation in *Fst* expression, which indicates that GATA4 exerts a repressive effect. Within this line the following model is proposed (Figure 3.1). Kashimada *et al.* reported that FOXL2 cooperatively interacts with either BMP2 or WNT4, depending on the developmental stage, to activate the expression of *Fst* within the ovary (79).

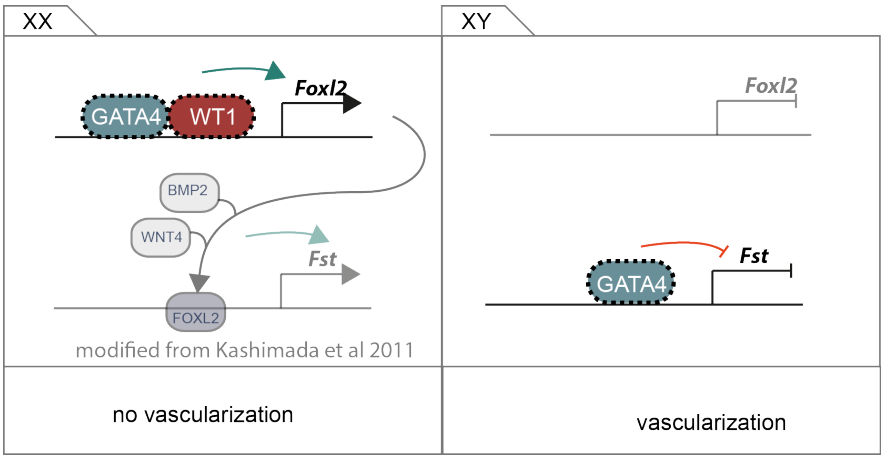


**Figure 3.1: Model for *Fst* suppression by GATA4 in the testis and *Foxl2* activation by GATA4 and WT1 in the ovary.** *Foxl2* and *Fst* show a sex-specific expression pattern. In the testis, GATA4 inhibits *Fst* expression. In the ovary, WT1 and GATA4 are potential activators of *Foxl2* expression. FOXL2 in turn is then able to interact with BMP2 or WNT4 in order to drive *Fst expression*, as reported (157). *Fst* activation within the XX gonad is essential in order to prevent the process of vasculogenesis.

This in turn is associated with the suppression of a vasculature within the ovary (71). The data herein provide the first potential functional link between GATA4 and *Fst* expression within the testis. *Foxl2* expression in the ovary is significantly diminished in *Wt1* deficient mice as well as sole and combined antisense inhibition of WT1 and GATA4 (Figure 2.6 and Figure 2.7). GATA4 was identified as a potential factor that suppresses *Fst* expression within the testis, which in turn contributes to the formation of a prominent functional vasculature. In the ovary, WT1 and GATA4 might synergistically activate *Foxl2*.
Moreover, even though the knockdown of GATA4 proved to be effective, up regulation of *Gata4* transcripts were observed in both, the sole *Gata4* and the combined *Wt1/Gata4* vivo-morpholino approach (Figure 2.7 and Figure 2.8). An auto-regulatory feedback loop of the *Gata4* transcript was previously described, which involves two alternative transcripts, *Gata4 E1a* and *Gata4 E1b* (147; 148). The authors proposed a model which concludes that under normal physiological conditions, GATA4 represses the transcription of the *Gata4 E1b* splice variant. But if GATA4 levels decline, the GATA4 repressive effect is alleviated and *Gata4 E1b* transcription is initiated (147). This model is in line with my observation. The *Gata4 E1b* transcript is strongly up regulated 5-fold testis and only a 2-fold up regulation was observed in the ovary (Figure 2.9). However, the functional relevance of the alternative transcripts is not well defined yet, but the GATA4 E1b transcript could serve as a back-up mechanism that ensures GATA4 levels above a certain threshold (148).

### 3.2.5 WT1 and GATA4 are involved in balancing gene expression towards the fate of either ovary or testis

The rationale behind the combined knockdown approach was based on the fact that WT1/GATA4 cooperatively interact with each other and activate given target genes (49). I hypothesised that WT1/GATA4 cooperatively act on other genes besides AMH and SRY (49). In accordance with the functional dissection of WT1 and GATA4 is that both proteins are co-expressed in the same cell types (Figure 2.10, Figure 2.11 A) (150). The knockdown of both, WT1 and GATA4, in the XX and XY gonad was efficient (Figure 2.4 C). On the mRNA level, the overall expression pattern was rather similar to the one observed for the sole GATA4 knockdown in both sexes (Figure 2.7. Therefore, the combined *Wt1/Gata4* vivo-morpholino treatment may compensate for the down regulation of *Sox9, Sf1* and *Amhr2* in the testis compared to the sole WT1 approach. In the ovary the down regulation of *Dax1* and *Star*, mediated via sole WT1 knockdown, is relieved by GATA4 antisense inhibition but also in the combined approach. The down regulation effect observed for the *Foxl2* transcript was even stronger in the

combined approach, which suggests that WT1 and GATA4 cooperatively activate *Foxl2* transcription. To this end, based on the expression data the following model is proposed with regard to the expression of *Sox9, Sf1* and *Amh* (Figure 3.2). The accessibility of GATA4 to the transcriptional machinery is fine tuned by *Wt1* cis-regulatory elements. In the ovary, FOXL2 prevents or hinders the binding of WT1 to the promoter regions of specific male markers like *Sox9, Sf1* and *Amh*. In the absence of FOXL2, as in the XY

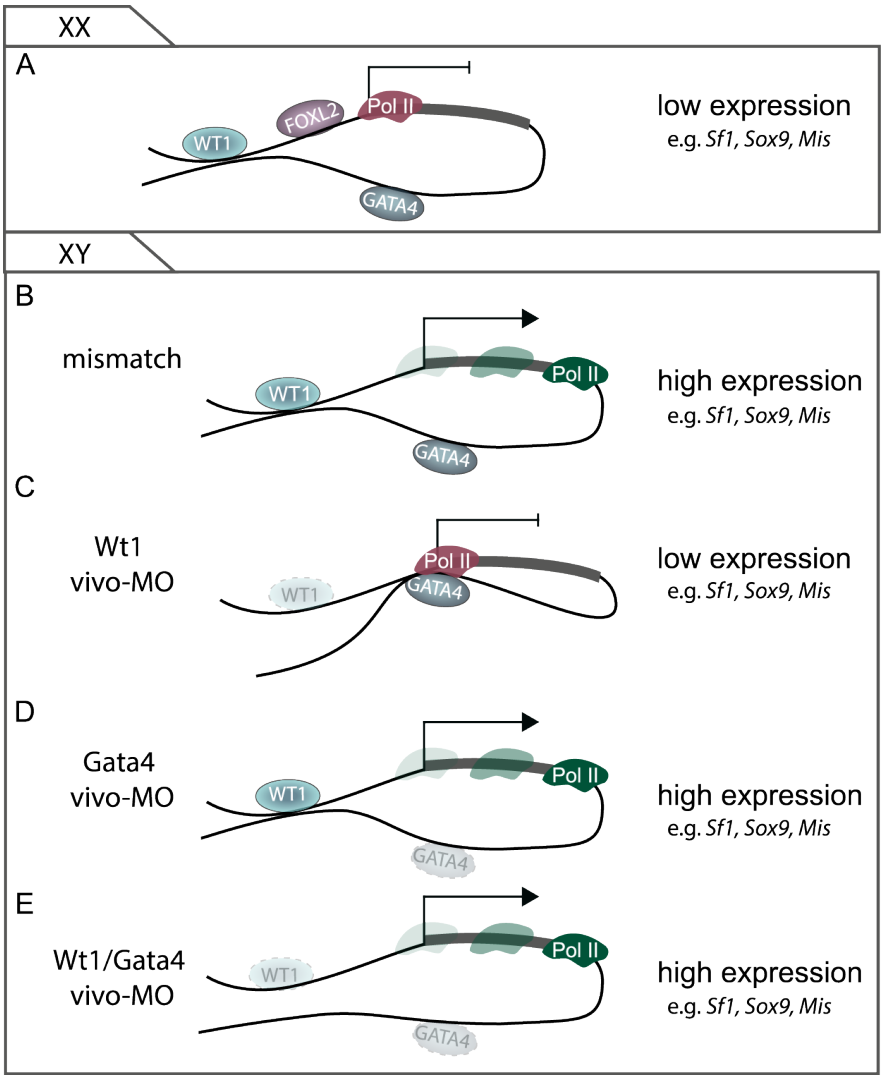


**Figure 3.2: Model that illustrates the potential interplay between WT1, GATA4 and FOXL2 in a sex specific manner.**(A)In the ovary FOXL2 antagonises WT1 and is capable of binding to the promoters of genes such as *Sf1, Sox9* and *Amh*, acting as a transcriptional repressor. (B) The expression of *Foxl2* is undetectable within the testis. WT1 is able to prevent the interaction of GATA4 with the transcriptional initiation complex, thus contributing to the high expression levels of *Sf1, Sox9* and *Amh*. (C) Wt1 antisense silencing makes the interaction of GATA4 with the transcriptional machinery more likely and expression levels drop down to a basal state. (D,E) Knockdown of sole GATA4 or combined with WT1 exerts no effect on gene expression of *Sf1, Sox9* and *Amh*

gonad, WT1 and GATA4 can access specific promoter regions more easily and thereby modulating the expression of genes like *Sox9, Sf1* and *Amh*. Under normal physiological conditions WT1 attenuates the influence of GATA4. Thereby, WT1 takes on a more pronounced role in order to contribute to the high expression levels of *Sox9, Sf1* and *Amh*. The knockdown of WT1 positively influences the interaction of GATA4 with the transcriptional machinery and thereby is able to fine tune the transcriptional activity of *Sox9, Sf1* and *Amh*. The antisense inhibition of GATA4 restores the situation under normal physiological conditions and the expression of *Sox9, Sf1* and *Amh* is not under its influence. Knockdown of both proteins resembles as well the normal conditions in respect to the influence on the expression of genes like *Sox9, Sf1* and *Amh*.

### 3.2.6 WT1 affects cell proliferation in both sexes whereas GATA4 only in the testis

Previous reports provided evidence that WT1 and GATA4 are involved in cell proliferation during development (48; 125; 159). My observations revealed upon subjecting gonads and mesonephroi to *Wt1* vivo-morpholino treatment that XX and XY gonads exhibit a significant reduction in proliferating cells in either organ (see Figure 2.12). Form these results one can conclude that WT1 has a direct effect on the proliferation rate but not only within the XX and XY gonad but also in the mesonephros. Thus, the observed effect is less likely mediated via SRY. This interpretation is based on the notion that the time point gonads were subjected to analysis is past the peak of SRY activity and that the effect was as well observed in the XX gonad and XY mesonephros. The XX gonad lacks the *Sry* gene completely and the XY mesonephros lacks its expression (44). Furthermore, another possible explanation for the observed effect could be the improper regulation of certain paracrine factors as a consequence of the down regulation of WT1, e.g., *Star*, shown in this thesis and by others (106). Paracrine factors – RA or PDGF signalling alike – fulfil an essential role in the development of the gonad as they contribute to cell migration from the mesonephros into gonad. Additionally, it has been reported that WT1 triggers FGF signalling in the kidney and in the gonad (48; 136) and FGF signalling contributes to cell proliferation in the gonad (62).
Very recently a report provided evidence for the importance of GATA4 involved in the thickening of the coelomic epithelium of the genital ridge (37). Experiments, which made use of a conditional knock-out model, namely *Sf1-Cre;Gata4*$^{flx/flx}$, revealed that cell proliferation in the ovary is reduced (125). Results regarding GATA4 antisense silencing within the ovary show that proliferation was not significantly affected (Figure 2.13), hence contradicts this report. However, this could be due to a long term effect what the authors observed in the ovary which could not be revealed by a knockdown

approach using vivo-morpholinos against *Gata4*. It seems difficult to interpret the data observed in this context. One way to examine this effect would be to use a second non-overlapping (with the used one) vivo-morpholino against GATA4 and investigate whether the same results could be obtained. From a physiological perspective one can argue that the proliferation event within the testis underlies a tighter regulation and could be driven forward by additional factors, as the testis is greater in size than the ovary (149). Furthermore, in terms of the *Gata4* vivo-morpholino treatment in the testis, the results show that cell proliferation is affected in the XY gonad and to a lesser extent in the XY mesonephros (Figure 2.13). The observed effect within the mesonephros is somewhat surprising, as GATA4 is only expressed in the gonad (Figure 2.10). This may be a consequence of impaired cell signalling cues from adjacent tissues that have an impact on cell proliferation, e.g., RA signalling (160; 161).
In conclusion, the results herein depict WT1 not only as an essential factor of cell proliferation within the gonad but also emphasises its role in the mesonephros. Data retrieved from the GATA4 vivo-morpholino approach, show its role in the XY gonad, which implies that WT1 and GATA4 contribute to the same effects and this in turn would support the model as suggested (Figure 3.2).

## 3.3 Summary and Outlook

In summary, the thesis describes the complex intertwined regulatory network of WT1 and GATA4 during gonad development. I could show that WT1 engages a fundamental role during the process of sex differentiation, in terms of adjusting a sex specific signature in both sexes, which becomes manifested in the proper morphological appearance of the female and male gonads. While during testis development WT1 binding to regulatory elements reduces the inhibitory effect of GATA4 and thus promoting the expression of male favoured genes such as *Sox9, Sf1* and *Amh*; in the ovary, however, *Foxl2* was identified as a novel putative WT1 target gene that seems to be up regulated by WT1. It appears plausible that FOXL2 initiates a cascade that counterbalances male promoting factors within the ovary, as previously shown for *Sf1* (157). Nevertheless, this model needs to be validated in greater depth in order to draw precise conclusions. The final proof for a direct regulation by WT1 and GATA4 requires the performance of chromatin immunoprecipitation followed by sequencing (ChIP-seq) on primary gonads using specific antibodies against either WT1 and GATA4. Data herein also describe GATA4 as a potential repressor of *Fst* expression and thereby may indirectly contribute to the formation of a prominent vasculature within the testis. Still, whether GATA4 acts directly or indirectly on given target genes is a matter of future investigation, by, e.g., conducting ChIP-seq. However, from a technical point of view, I

provided evidence that the gene targeting approach by using vivo-morpholinos provides a suitable and effective tool especially in terms of gonadal development to study gene function. This approach might be useful in order to validate genome-wide-sequencing data in a timely effective manner.

Putting this into perspective, developmental sexual disorders arise from mutations in essential transcription factors such as WT1 and GATA4. Therefore, unraveling the functional relevance of these factors may contribute in the long run to the patient's case and thereby help them to better understand their situation. As the data herein not only describe but also extend our knowledge of how these factors commit to gonadal development it would be interesting to investigate if these factors are potential therapeutic starting points for common DSDs such as Denys-Drash, Turner, or Frasier syndrome as these are associated with mutations in WT1(162). However, there are still open and enigmatic questions that are arising and are still unanswered but at the same time these questions set the direction for future research.

# 4

# Methods

## 4.1 Animals

### 4.1.1 Mouse strains

Wild type *Wt1*$^{+/+}$ and transgenic *Wt1*$^{+/-}$ mice (C57BL6 strain) (32) were held and crossed at the local mouse facility (Permission no.: T0308/12). The ethical guidelines were followed according to the Animal Protection Law. Mice were anaesthetised using Forene and thereafter killed by cervical dislocation. Mice were disinfected with 70% EtOH. The uterus was excised, immediately placed into ice-cold sterile 1x PBS and kept on ice until embryo dissection.

### 4.1.2 Embryo dissection and staging

Embryos were placed in a 10 cm petri dish containing ice-cold 1x PBS and excavated out from the uterus and extra-embryonic tissue using a Zeiss stereomicroscope and forceps. For staging, the tail somites of embryos at age 11.0 dpc - 12.0 dpc were counted distal to the beginning of the hindlimb (41). Beyond stages 12.5 dpc and older ages, embryos were staged according to the development of the limb (163). Gonads were then isolated using a Zeiss stereomicroscope and forceps and transferred to a 96 well plate using a plunger.

### 4.1.3 Genomic DNA isolation - genotyping of the sex and the *Wt1* locus of *Wt1*$^{+/+}$ and *Wt1*$^{-/-}$ mice by PCR

The embryonic tail was used for sex-genotyping and/or genotyping littermates of crosses of *Wt1*$^{+/-}$ transgenic mice. DNA isolation was performed by adding 100$\mu$l

| Purpose | Cycles | Annealing | Elongation | Polymerase |
|---|---|---|---|---|
| sex-PCR | 38 | 55°C/30sec | 72°C/30sec | AmpliTaq |
| *Wt1*-genotyping | 34 | 54°C / 30sec | 68°C/30sec | Phusion |

**Table 4.1: PCR programs used for sex- and Wt1-genotyping**.

PDNB lysis buffer, supplied with 3$\mu$l proteinase K (15mg/ml) to the tail and incubated at 55°C for 3 hours in a thermoblock. To inactivate proteinase K, samples were heated to 95°C for 5 minutes. Primers used for PCR analysis are listed in Table 4.7. Sex genotyping was performed by PCR amplification of the Y-chromosomal gene *Kdm5d* (140). A 25$\mu$l reaction was setup containing the following: 2$\mu$l genomic DNA, 5$\mu$l 5x buffer, 10$\mu$M fwdPrimer, 10$\mu$M revPrimer, and 0.625U AmpliTaq polymerase (140). In terms of *Wt1* genotyping the PCR reaction (20$\mu$l) was as follows: 4.0$\mu$l 5x Phusion HF Reaction buffer, 0.4$\mu$l dNTPs (10mM), 1$\mu$l Primer WT1-KO-SHA, 1$\mu$l Primer WT1-HO-WTZ, 1$\mu$l Primer WT1-KO-PGK, 0.4U Phusion High Fidelity DNA Polymerase, 0.6$\mu$l DMSO, 11.3$\mu$l H2O, 0.5$\mu$l DNA (32). PCR reactions were run on an UNO-Thermoblock using the PCR programs listed in table (4.1). Thereafter, 6 x OrangeG loading dye was added to the PCR reactions and samples were loaded onto a 1.5% or 2% agarose gel containing SYBR safe added for visualisation purpose.

### 4.1.4 Sex genotyping by staining the inactive X-chromosome in females using Toluidine blue solution

Toluidine-blue staining of amniotic cells was performed when it was critical to gather information of the embryo's sex within a short time, e.g. 30 minutes. This procedure enables one to visualise the heterochromatic inactive X chromosome in females, which is located at the periphery of the cell and known as the Barr Body (164). The procedure was performed according to the following protocol (155). In brief, at the stage of embryo dissection the inner most membrane, the amnion was isolated and placed into a 1.5 ml tube and 1 ml of ice-cold fixative (3:1 dilution of 100% methanol and 100% acetic acid) was added. The tube was inverted 4-6 times. Acetic acid was aspirated, three drops of 60% acetic acid were added using a pasteur pipet, vortexed and topped up to a total of 1.5 ml with 100% acetic acid. Samples were centrifuged at 5000 rpm for 3 minutes. The solution was taken off so that roughly 30-50$\mu$l remained in the tube. Samples were vortexed and 25$\mu$l were placed on a glass slide. 1% toluidine solution was sterile filtered using 0,45$\mu$m filters. A droplet was placed onto a coverslip. The glass slide containing the cells was placed onto the coverslip and the remaining toluidine solution

was removed using whatmann paper. Inspection of the cells was performed under an inverted microscope (Axiovert 35). The cells contained the Barr Body were identified as female cells and hence the embryo of female genotype (155).

## 4.2 Cell culture and organ culture techniques

### 4.2.1 M15 cell line

M15 cells (143) were cultivated in DMEM supplied with 10% FBS at 37°C in a 5% $CO_2$ humidified chamber.

### 4.2.2 siRNA knockdown

The M15 cell line (143), which is derived from the mouse mesonephros, was used for the *Wt1* or *Gata4* siRNA knockdown approach as described previously (165). M15 cells were seeded to 60% confluency in 6 well plates. Antisense inhibition was performed by using a specific pool of four different siRNAs against either *Wt1* (165) or the *Gata4* gene. The control setup was conducted with a pool of four non-targeting siRNAs (siGENOME Non-targeting siRNA). Transfection of the cells was performed using DharmaFECT 1 according to the manufacturer's protocol. For one approach 50pmol of siRNA was used. Cells were cultured for additional 48 hours at 37°C in a 5% $CO_2$ humidified chamber. Thereafter, RNA and protein extractions were prepared as described in section 4.3.1 and 4.3.4.

### 4.2.3 *Ex-vivo* droplet organ culture

The *ex-vivo* droplet organ culture was established as a modified version as published by Maatouk et al (91). The gonads were dissected as described in section 4.1.2 and immediately placed into a 96 well plate containing 100$\mu$l DMEM media supplied with 10% FBS at RT until the dissection procedure was finished. Thereafter the gonads were transferred into 40$\mu$l hanging droplets in the lid of a 24 well plate with 1 ml cell-culture-sterile 1 x PBS added in each well.

### 4.2.4 Vivo-morpholino application

For the sole and combined WT1/GATA4 knockdown the appropriate vivo-morpholino concentrations were prepared in DMEM media supplied with 10% FBS, 100 IU/ml penicillin and 100$\mu$g/ml streptomycin. The vivo-morpholinos were added to the media at a concentration of 10$\mu$M and in case of the combined approach each vivo-morpholino

was added at a concentration of 7.5$\mu$M. One gonad of the embryo was used for the vivo-morpholino knockdown and the corresponding contralateral gonad was used as a control with the mismatch vivo-morpholino. Organ cultures were incubated 72 hours at 37°C in a 5% $CO_2$ humidified chamber and subsequently post-processed accordingly.

### 4.2.5 BrdU treatment

For analysis of cell proliferation 10$\mu$M BrdU was applied to the droplet culture after 48 hours of cultivation, for additional 24 hours. Gonads were fixed in 10% (v/v) formalin for 25 minutes. Formalin was aspirated and preparations were washed once with $NH_4Cl$ and then incubated for 20 minutes in $NH_4Cl$. Organs were embedded in cryomolds with Tissue-Tek®, deep frozen on dry ice and stored at -80°C until cyrosectioning.
From the samples 8$\mu$m cryosections were prepared by a cryostat with temperature settings adjusted at -20°C. Sections were cooked in a microwave oven for 7 minutes in 1 x citrate buffer. For procession, sections were circled using a barrier pen. Blocking was performed for 10 minutes at RT using serum-free DakoCytomation protein block. To visualise proliferating cells, a biotinylated antibody against BrdU (51-75512L) was used concomitantly with a WT1 (2797-1) or GATA4 (sc-1237) antibody, diluted 1:100 in Antibody Diluent Solution. Incubation was performed for 1 hour at RT followed by three washing steps in 1x PBS/Tween20, each 5 minutes. To detect the primary BrdU antibody, Strepdavidin-Cy3 was used at 1:100 dilution prepared in Antibody Diluent Solution. The secondary antibodies for visualisation of either WT1 or GATA4 are described under section 4.3.6. Slides were washed three times in 1x PBS/Tween20. DAPI was used for counterstaining the cell nuclei followed by additional three washing steps in 1x PBS/Tween20, a 5 minutes. Sections were mounted using the Vectashield® mounting medium.

## 4.3 Molecular biology techniques

### 4.3.1 RNA isolation

RNA extraction of M15 cells was performed using TRIzol® according to the manufacturer's protocol. The DNA pellet was resuspended in RNAse-free $H_2O$. Concentration was measured with NanoDrop 2000. RNA isolation of *ex vivo* organ cultures as well as gonads of *Wt1*$^{-/-}$ was conducted with the RNEasy® Micro Kits according to the manufacturer's protocol using Qiashredder columns for tissue homogenisation. RNA was eluted in 14$\mu$l RNAse-free $H_2O$.

### 4.3.2 cDNA - reverse transcription

For cDNA conversion of M15 cell RNA 2$\mu$g were used. 11$\mu$l of single gonad RNA were used to cDNA reverse transcription. First strand synthesis was performed with the appropriate RNA amounts and 1$\mu$l Oligo(dT)12-18 (50$\mu$M), in the initial step. The PCR program was started and after a 65°C step for 5 minutes, a 1 minute 4°C step followed during which 4$\mu$l 5x RT buffer, 1$\mu$l dNTPs (10$\mu$M) and 1$\mu$l DTT (0.1M) was added up to 10$\mu$l. The reaction was heated to 42°C and 1$\mu$l superscript® III (200U/$\mu$l) was applied and incubated at 50°C for 50 minutes followed by 70°C for 15 minutes.

### 4.3.3 Reverse transcriptase - quantitative real time PCR

The cDNA samples used for RT-qPCR were diluted 1:10 in RNase free $H_2O$ and 2$\mu$l were used for RT-qPCR. All reactions were SYBR Green assays and ran on a StepOnePlus Real-Time PCR Systems machine. The RT-qPCR program used is listed under Table 4.1. One 10$\mu$l approach contains 2$\mu$l cDNA (1:10 diluted in RNAse-free $H_2O$), 50nM primer and 0.5 Volume 2x SYBR Green PCR Master Mix. All reactions were performed as duplicates and a $H_2O$ negative control was run concomitantly. The herein used primers are listed in Table 4.7. Primer specificity was assessed upon the inspection of the melting curves and a sample was run on an agarose gel. Primers were considered as specific if a single clear peak was observed and a single band detected on the agarose gel. Melting curves were generated during the end of each run: a gradual increase of the temperature from 60-90°C, according to a temperature change of 0.3°C every 15 seconds followed by concomitantly fluorescence intensity measurement. For normalisation purpose and calculation of the relative expression levels, the Ct value of the housekeeping gene, either *Gapdh* or *Sdha*, was subtracted from the Ct value of the gene of interest. The differences in the mRNA expression level, between the treated sample and the control sample, was calculated by using the $2^{\Delta\Delta Ct}$ method. The changes are considered as fold changes.

### 4.3.4 Protein extraction

M15 cells were washed twice with 1x PBS prior to protein extraction. 300$\mu$l of Laemmli buffer were applied in each well and incubated for 5 minutes at RT. *Ex vivo* cultured gonads were immediately transferred to a 1.5ml tube containing 32$\mu$l Laemmli buffer. Cells as well as gonads were sonicated. Thereafter samples were heated on 95°C in a thermoblock for 5 minutes for protein denaturation. Total protein concentration was determined after the Warburg-Christian equation (166). The OD260 and OD280 was determined using a spectrophotometer.

### 4.3.5 SDS-Page and immunoblotting

SDS page was performed with 20$\mu$g of total protein isolated from M15 cells and in case of *ex vivo* gonad cultures 20$\mu$l of total protein were used. Samples were mixed with 5$\mu$l bromophenol blue as a loading dye and subsequently loaded into the slots of the stacking gel. The chamber was filled with 1x SDS running buffer. Samples were ran at 80 volts samples they allocated at the separation gel. Separation of the proteins was conducted on an 10% denaturing polyacrylamide gel. On all gels a separation marker (Precision Plus Protein Western C Standart) was loaded and ran concomitantly. Then gels were disassembled and protein was transferred to a polyvinylidene difluoride membrane. Therefore, whatman paper was soaked in 1x blotting buffer for 5 minutes. The polyvinylidene difluoride membrane was activated with methanol, followed by a washing step in distilled $H_2O$ and placed for 2 minutes in blotting buffer. Blotting stack was assembled and the protein transfer was performed with a Trans-Blot® SD semidry device at constant 15 volt using 1x blotting buffer. In order to prevent unspecific antibody binding to the membrane, blocking was performed by using 5% powdered milk, solved in 1x TBST. Blocking was conducted for 1 hour. Thereafter, the appropriate antibody was prepared in 2.5% powdered milk and incubation followed at 4°C overnight. The membrane was washed three times for 5 minutes in 1x TBST and subsequently incubated for 1 hour with the secondary antibody diluted in 1x TBST. Thereafter, the membrane was washed three times in 1x TBST. Signal detection was carried using Film SuperRX with a secondary peroxidase antibody and the Western Lightning™ Plus ECL reagents. For detection with another primary antibody the membrane was stripped using 0.2 N NaOH and incubated for 10 minutes at RT, rinsed with distilled $H_20$ and incubated for additional 5 minutes in 1x TBST. Blocking was conducted in 5% milk in 1x TBST followed by antibody incubation as described above.

### 4.3.6 Whole-Mount immunohistochemistry

For co-expression analysis, assessment of duct development and LiCl treatment, gonads of appropriate stages were dissected and after the respective treatment, used for whole-mount immunohistochemistry. The gonads were placed in 1.5 ml tubes, and fixed for 20 minutes in 10% (v/v) formalin. Then washed once in quenching solution followed by an additional incubation period of 30 minutes in quenching solution. Gonads were blocked overnight at 4°C in blocking solution. The next day the blocking solution was aspirated. For co-expression analysis, antibodies, rabbit anti-WT1 (2797-1) and goat anti-GATA4 (sc-1237), were diluted 1:100 in Antibody Diluent Solution solution, applied to the gonads and incubated overnight on 4°C. Three washing steps were performed with blocking solution. In order to visualise the binding of the primary antibody, incu-

bation with the following secondary antibodies overnight at 4°C was conducted: Alexa DyLight™ 488 donkey anti-goat and Cy3-AffiniPure donkey anti-rabbit. In case of the LiCl treated samples, primary antibody rabbit anti-SOX9 (sc-20095; 1:100) and the secondary antibody Cy3-AffiniPure donkey anti-rabbit, were used. For assessing duct development, gonads were treated with *Wt1* vivo-morpholino or mismatch control as described previously (Section 4.2.4). For whole-mount immunohistochemistry the following primary antibodies were used: rabbit anti-PAX2 (PRB-276P; 1:100) and goat anti-GATA4 (sc-1237; 1:100). Then the following secondary antibodies were applied: Alexa DyLight™ 488 donkey anti-rabbit and Cy3-AffiniPure donkey anti-goat. Samples were washed three times with blocking solution. Counterstaining of the cell nuclei was performed using DAPI overnight at 4°C. After three washing steps in blocking solution samples were mounted using Vectashield™.

## 4.4 Microscope adjustments and image acquisition

For co-expression analysis, assessment of duct development and LiCl treated samples a Leica DM 2500 confocal microscope equipped with the LAS AF Lite software was used. Images were acquired with an ACS APO 40.0 x 1.15 oil objective that holds an numerical aperture of 1.5 and a refraction index of 1.52. Images were of 8 bit resolution. Overview images were acquired using an epifluorescence microscope (Axiovert100) which was connected to a digital camera (Diagnostic Instruments). The microscope (Axiovert100) was equipped with the Metamorph software and images were saved in tif format of 12 bit resolution. Sections of the proliferation BrdU-assay were imaged using an upright epifluorescence microscope (Olympus BX61) with a UPLFLN 20 x dry objective. The microscope was equipped with a motorised stage and images acquired were of 8 bit resolution. For all experiments the post-process procedure between control and sample was the same. In brief, RGB Images were split in individual channels using Fiji (167) and overlay images were produced via the action feature in Adobe Photoshop. If adjustments were made they were performed on the whole image and were equally applied between the control and the sample. For the BrdU experiment, the semi-quantification analysis was performed on the raw images after splitting the channels using Fiji (167). Within the gonad and the mesonephros a region of interest (ROI) was defined which served for quantification purpose. The empty green channel was discarded and the red (BrdU) and the blue (DAPI) channels were analysed using a custom macro feature within Fiji (167). In short - the ROI was chosen and the images cropped. Images were filtered using an unsharp mask-, medium- and maximum filter with the default radius of 2 pixels. Background noise was subtracted and a threshold of 50 was set. This threshold was the same throughout the samples and the controls.

The cell area of BrdU-positive and total DAPI-positive cells was then measured. The BrdU positive area was normalised to the total DAPI-positive area.

### 4.4.1 Graphics and statistics

Statistics (student's ttest and summary statistics) were calculated in R (168). SPSS Statistics 2.0 (IBM) was used for ANOVA with a post-hoc Tukey Test. Basic plots were prepared using the ggplot2 package (169). Final adjustments and figure layout was done using Adobe Illustrator.

## 4.5 Equipment - Solutions - Materials - Chemicals

| Device | Company |
|---|---|
| Camera | Diagnostic Instruments |
| Camera RT power supply | SPOT Image Solutions |
| Cell Culture Bench Herasafe | Thermo Fischer Scientific |
| Centrifuge | Eppendorf |
| Centrifuge | Roth |
| Centrifuge (Universal RF) | Hettichy |
| Cryostat Jung CM 3000 | Leica Biosystems |
| Fluorescence microscope Axiovert100 | Zeiss |
| Forceps (Dumont#55) | Aesculap |
| Incubator | Binder |
| Labsonic Ultrasonic homogenizer | Heidolph |
| Leica DM2500 confocal laser microscope | Leica |
| Light Cycler PCR StepOnePlus | Life Technologies |
| Light Source | VWR |
| Luminometer | Berthold Technology |
| Metall Box | Roth |
| Microscope Axiovert35 | Zeiss |
| Microscope lamp | Zeiss |
| Microwave | Whirlpool Corporation |
| Mini Rocker Shaker | peQlab |
| Motorised stage (H1P1BX, serial no. 66404) | Prior Scientific UK |
| NanoDrop 2000 | Thermo Fischer Scientific |
| PCR maschine | Applied Biosystems |
| PCR maschine UNO-Thermoblock | Biometra |
| Precision Weight Balance | Sartorious |
| Safe ImagerTM | Life Technologies |
| Shaker Polymax 1040 | Heidolph |
| Stereomicroscope | Zeiss |
| Stirrer | Heidolph |
| Thermoblock | Biometra |
| Thermostat TCR100 | Roth |
| Trans-BlotR SD SemiDry | Bio-Rad Laboratories |
| Vortex-2-Genie | Scientific Industries |
| Western Blot device | BioRad |
| sonifier(Labsonic) | B. Braun, Melsungen |
| spectrophotometer DU 730 | Beckman Coulter |

**Table 4.2: Equipment**

| Working solutions | Ingredients | Stock |
|---|---|---|
| 1% Toluidine Blue Solution | 0.1g Toluidine dissolved in 100ml distilled $H_2O$ | |
| 1x Blottingpuffer | 10mM 6-aminohexanoic acid, 10% (v/v) methanol | 10 |
| 1x Citrate buffer | 1.8mM citric acid, 8.2mM trisodium citrate, 0.05% (v/v) Tween 20, pH 6.0 | 10 |
| 1x DNA 60mM OrangeG | 10mM Tris-HCl, 0.15%OrangeG, 0.03% Xylene cyanol 60% Glycerine, 60mM EDTA, $H_2O$ | 6 |
| 1x PBS | 0.2g/l KCl, 0.2g/l $KH_2PO_4$, 8g/l NaCl, 1.15g/l $Na_2HPO_4$ | 10 |
| 1x PBS/Tween20 | 1x PBS, 0.2%Tween20 | |
| 1x SDS running buffer | 0.25M Tris-Base, 1.92M Glycine 1% (w/v) SDS (pH 8.3) | 10 |
| 5x TBE | 54g/l Tris-HCl; 27,5g/l Boric acid; 10mM EDTA | 10 |
| Ammonuiumchloride | 1x PBS; 50mM ammoniumchloride | - |
| Blocking solution | 1x PBS, 0.2 % bovine serum albumin, 0.05 % TritonX-100 | - - |
| Fixative ice-cold | 3:1 dilution of 100% methanol and 100% acetic acid | - |
| Laemmli-buffer | 50mM Tris-HCl (pH 6.8); 4M urea acid, 1% (w/v) SDS 7.5mM DTT | - |
| PBND-Puffer | 50mM KCl, 10mM Tris (pH 8.3), 2.5mM $MgCl_2$, 0.1mg/ml Gelatine, 0.45% Tween20 300mg/ml Proteinase K, 0.45% Nonidet-P40 | - |
| Polyacrylamid-separation gel | 0.25 Vol acrylamide/bisacrylamide (w/v: 30/0.8), 0.25 Vol Separation buffer 0.5$\mu$l/ml TEMED 5$\mu$l/ml APS | - |
| Polyacrylamid-stacking gel | 0.11 Vol acrylamide/bisacrylamide (w/v, 30/0.8), 0.125 Vol Stacking gel buffer 1$\mu$l/ml TEMED, 10$\mu$l/ml APS | - |
| Quenching solution | 1x PBS / 50mM $NH_4Cl$ | - |

**Table 4.3: Solutions**

| Working solutions | Ingredients | Stock |
|---|---|---|
| Separation buffer | 1.5M Tris-HCl, 0.4% (w/v) SDS (pH 8.8) | - |
| Stacking gel buffer | 1M Tris-HCl, 0.8% (w/v) SDS (pH 6.8) | - |
| TBST-buffer | 20mM Tris-Base, 137mM NaCl, 0.05% Tween20 (pH 7.6) | - |

**Table 4.3: Solutions (continued)**

| Cell line / Mouse strains | Company | |
|---|---|---|
| M15 cell line (143) | Christoph Englert Lab | |
| *Wt1*$^{+/+}$ C57BL6 | The Jackson Laboratory | |
| *Wt1*$^{+/-}$ C57BL6 (32) | The Jackson Laboratory | |
| **Materials and chemicals** | **Company** | **Cat. no.** |
| 10mM dNTP | Biolone | BIO-39044 |
| APS | Roth | 9592.3 |
| Acetic Acid | Roth | X895 |
| Acrylamid/Bisacrylamid | Roth | 3029.1 |
| Agarose | Roth | 2267.4 |
| Ammonium Chloride | Sigma | A0171-100G |
| AmpliTaq Gold® | Invitrogen | N808-0152 |
| Antibody Diluent Solution | Invitrogen | 003218 |
| Aquatex | Merck | 1.08562.0050 |
| Barrier Pen | Dako | 52002 |
| Boric acid | Merck | 1.00165.1000 |
| BrdU | Roth | 3743.1 |
| Bromphenol Blue | Biomol | 50206 |

**Table 4.4: Materials, Chemicals and Kits**

| Materials and chemicals | Company | Cat. no. |
|---|---|---|
| Coverslips | Roth | H878 |
| DAPI | Sigma | H3342 |
| DMEM high Glucose + stabile L-Glutamin | PPA Laboratories | E15-009 |
| DTT | Roth | 6908.1 |
| DharmaFECT1® | Thermo Fischer Scientific | T-2001-02 |
| EtOH | Sigma Aldrich | 32205 |
| FBS Hyclone | Thermo Fischer Scientific | CH30160.03 |
| FastStart SYBR Green Master | Roche | 04673492001 |
| Film SuperRX | Fujifilm | 4741019236 |
| Forene 100% | Abbott | 2594.00.00 |
| Formalin | JTBaker | 3933 |
| Isoproanol | Merck | 8.18766.1000 |
| Kodak RP X-OMAT Developer | Kodak | 5274394 |
| Kodak RP X-OMAT fixative | Kodak | 5224381 |
| L-Glutamine | PPA Laboratories | M11-004 |
| LiCl | Merck | 105679 |
| Mercaptoethanol | Roth | 4227.1 |
| Methanol | JTBaker | 8045 |
| Nail polish | Rossmann | - |
| Nonidet-P40 | Roche | 1344100 |
| Oligo(d)T - Primer | New England Biolabs | 18418012 |
| Pasteur pipettes | Roth | 4518 |
| Penicillin-Streptomycin | PAA Laboratories | 15140-148 |
| Phusion HF Reaction buffer | New England Biolabs | NEB B0518 S |
| Phusion® High Fidelity Polymerase | New England Biolabs | M0530S |
| Polyvinylidendifluorid-membrane | Roth | T830.1 |
| Potassium chloride(KCl) | Roth | P0117.1 |
| Powdered Milk | Roth | T145.2 |
| Precision Plus Protein Western Staandard | Bio Rad | 161-0376 |
| Protein Block Serum - free | Dako | X0909 |
| RNase-free $H_2O$ | Quiagen | 129112 |
| Roti®-Liquid-Barriere-Marker | Roth | AN91.1 |
| SYBER Safe | Life Technologies | P/N 533102 |
| Superfrost-Glassslides® | Menzel Glr | J1800AMNZ |
| TEMED | Roth | 2367.3 |
| Tissue-Tek O.C.T. compound | Sakura Finetek | 4583 |
| Toluidine-blue O | SigmaAldrich | T3260 |
| Tris-HCl Base | Roth | 9090.3 |
| TritonX100 | Roth | 3051 |
| Trizol®Reagent | Life Technologies | 15596018 |
| Trypsin/ EDTA | BioWest | X0930-100 |
| Tween-20 | Serva | 37470.01 |

**Table 4.4: Materials, Chemicals and Kits (continued)**

| Materials and chemicals | Company | Cat. no. |
|---|---|---|
| Vectashield | Vector Laboratories | VEC-H-1000 |
| Whatman® Blotting paper | GE Healthcare | 3030917 |
| **vivo-morpholino/siRNA** | | |
| Gata4 vivo-morpholino | Genetools | - |
| Gata4 mismatch vivo-morpholino | Genetools | - |
| Gata4 siRNA | Thermo Scientific Dharmacon® | L-040759-01 |
| Wt1 vivo-morpholino | Genetools | - |
| Wt1 mismatch vivo-morpholino | Genetools | - |
| Wt1-siRNA pool | Thermo Scientific Dharmacon® | L-040686-01-0005 |
| ON-Target SMARTpool siGENOME Control Pool Non-targeting siRNA | Thermo Scientific Dharmacon® | D-001206-14-05 |
| **Kits** | | |
| AmpliTaqGold® DNA Polymerase | Invitrogen | 4338856 |
| DharmaFECT1® | GE Healthcare | T-2001-01 |
| RNEasy Micro Kits | Qiagen | 74004 |
| SuperScript® Reverse Transcriptase | Invitrogen | 18080044 |
| Western Lightning Plus ECL | PerkinElmer | NEL105001EA |

**Table 4.4: Materials, Chemicals and Kits (continued)**

| Name | Isotype | Company<br>Cat. no. | Dilution<br>Application |
|---|---|---|---|
| BrdU | mouse-biotinylated | BD Pharmingen<br>51-75512L | 1:100 (IHC*) |
| GATA4 (C-20) | goat IgG<br>polyclonal | Santa Cruz<br>sc-1237 | 1:500 (IHC*)<br>1:5000(IB*) |
| pan-Aktin | mouse IgG<br>monoclonal | Millipore<br>MAB1501R | 1:6000 (IB*) |
| PAX2 | rabbit IgG<br>polyclonal | BAbCO<br>PRB-276P | 1:100 (IHC*) |
| SOX9 (H-90) | rabbit IgG<br>polyclonal | Santa Cruz<br>sc-20095 | 1:100 (IHC*) |
| WT1 (C-19) | rabbit IgG<br>polyclonal | Santa Cruz<br>sc-192 | 1:200 (IHC*)<br>1:400 (IB*) |
| WT1 (Epitomics) | rabbit IgG<br>monoclonal | Epitomics<br>2797-1 | 1:200 (IHC*) |

* IB: Immunoblot; IHC: Immunohistochemistry

**Table 4.5: Primary antibodies**

| Name | Isotype | Company Cat.no | Dilution Application |
|---|---|---|---|
| IgG-HRP | rabbit IgG | Santa Cruz sc-2313 | 1:20000 (IB*) |
| IgG-HRP | goat IgG | Santa Cruz sc-2304 | 1:30000 (IB*) |
| IgG-HRP | mouse IgG | Santa Cruz sc-2005 | 1:30000 (IB*) |
| Precision-Protein-Marker | StrepTactin-HPR | Bio-Rad 161-0380 | 1:10000 (IB*) |
| DyLight$^{TM}$488 | donkey anti-goat | Jackson 705-545-003 | 1:100 (IHC*) |
| DyLight$^{TM}$488 | donkey anti-rabbit | Jackson 711-485-152 | 1:100 (IHC*) |
| Cy3 | donkey anti-goat | Jackson 705-166-147 | 1:200 (IHC*) |
| Cy3 | donkey anti-rabbit | Jackson 711-165-152 | 1:100 (IHC*) |
| Streptavidine-Cy3 | - | Sigma Aldrich S6402 | 1:100 (IHC*) |

* IB: Immunoblot; IHC: Immunohistochemistry

**Table 4.6: Secondary antibodies and immunoblot standard**

| Gene | Forward primer<br>Reverse primer | Acc. no<br>Application |
|---|---|---|
| *Amh* | GGGCCTGGCTAGGGGAGACTG<br>CCCGCTGGGAAGTCCACGGTT | NM_007445<br>RT-qPCR |
| *Amhr2* | CGCTTTATCACTGCTGGC<br>CTTCCCGAATGAGCACAT | NM_144547.2<br>RT-qPCR |
| *Ctnnb1* | CGCCGCTTATAAATCGCTCC<br>CAGGTCAGCTTGAGTAGCCA | NM_007614.3<br>RT-qPCR |
| *Dax1* | TGCTTGAGTTGGCCCAAGAT<br>AGGATCTGCTGGGTTCTCCA | NM_007430.4<br>RT-qPCR |
| *Foxl2* | AGCCGGCTTTTGTCATGATGG<br>AGGTTGTGGCGGATGCTATT | NM_012020.2<br>RT-qPCR |
| *Fst* | AGTGACTTACTCCAGCGCCT<br>CCGTTTCTTCCGAGATGGAGTT | NM_008046.2<br>RT-qPCR |
| *Gapdh* | ACGACCCCTTCATTGACCTCA<br>TTTGGCTCCACCCTTCAAGTG | NM_002046.5<br>RT-qPCR |
| *Gata4* | GATGGGACGGGACACTACCTG<br>ACCTGCTGGCGTCTTAGATTT | NM_008092<br>RT-qPCR |
| *Gata4 E1a* | TCCGCGGACTCACGGAGATC<br>TTGCTCCAGAAATCGTGCGGG | NM_008092<br>RT-qPCR |
| *Gata4 E1b* | ACAGGCTGGAATCTCTGGGCCT<br>TTGCTCCAGAAATCGTGCGGG | NM_008092<br>RT-qPCR |
| *Kdm5d* | CTGAAGCTTTTGGCTTTGAG<br>CCACTGCCAAATTCTTTGG | -<br>Sex - PCR (140) |
| *Sdha* | ACCGGCTTGGAGCAAATTCT<br>TCCAAACCATTCCCCTGTCG | NM_023281.1<br>RT-qPCR |
| *Sf1* | CTGCCGCTTCCAGAAGTGCCT<br>GAGATGGGGCTCCAAAGTCAC | NM_139051<br>RT-qPCR |
| *Sox9* | ACGCGGAGCTCAGCAAGACTC<br>GGTCGGCGGACCCTGAGATTG | NM_011448.4<br>RT-qPCR |
| *Star* | TGGATGGGTCAAGTTCGACG<br>CTCTGCAGGACCTTGATCTCC | NM_011485<br>RT-qPCR |
| *Wt1* | TGCCCTTCTGTCCATTTCACT<br>GATGTTCCCCAATGCGCCCTA | NM_144783<br>RT-qPCR |
| WT1-KO-PGK<br>WT1-KO-SHA<br>WT1-HO-WTZ | CTACCGGTGGATGTGGAATGTGT<br>TCCCGAACAATTTCACCTTGAATC<br>AGCCTAACTTTGGGGCTTATCTCC | -<br>KO - PCR |

* Primers are listed in 5' - 3' direction;

**Table 4.7: Primers**

# 5

# Appendix

| gene<br>sex | genotype | mean<br>$Ct^{\Delta}$ | 1*<br>% | 2*<br>% | 3*<br>% | 4*<br>% | 5*<br>% |
|---|---|---|---|---|---|---|---|
| *Amh* | | | | | | | |
| XX | WT | 15.43 | 41.01 | 0.02 | 87.06 | 0.01 | $+42*10^4$ |
| XX | KO | 16.72 | | | | | |
| XY | WT | 3.36 | | | | | |
| XY | KO | 15.63 | | | | | |
| *Amhr2* | | | | | | | |
| XX | WT | 3.31 | 0.27 | 0.52 | 0.14 | 1.03 | 26.54 |
| XX | KO | 11.82 | | | | | |
| XY | WT | 5.22 | | | | | |
| XY | KO | 12.82 | | | | | |
| *Ctnnb1* | | | | | | | |
| XX | WT | 11.97 | 46.01 | 469.13 | 65.52 | 329.44 | 13.97 |
| XX | KO | 13.09 | | | | | |
| XY | WT | 14.81 | | | | | |
| XY | KO | 12.58 | | | | | |
| *Dax1* | | | | | | | |
| XX | WT | 4.90 | 8.65 | 8.63 | 2.60 | 28.72 | 30.11 |
| XX | KO | 8.43 | | | | | |
| XY | Wt | 6.63 | | | | | |
| XY | KO | 10.16 | | | | | |

**Table 5.1:** Gene expression analysis of *Wt1* deficient mice.

| gene<br>sex | genotype | mean<br>$Ct^{\Delta}$ | 1*<br>% | 2*<br>% | 3*<br>% | 4*<br>% | 5*<br>% |
|---|---|---|---|---|---|---|---|
| *Foxl2* | | | | | | | |
| XX | WT | 11.04 | 2.92 | - | - | - | - |
| XX | KO | 16.14 | | | | | |
| *Fst* | | | | | | | |
| XX | WT | 4.03 | 12.07 | 114.16 | 12.74 | 108.07 | 11.16 |
| XX | KO | 7.08 | | | | | |
| XY | WT | 7.20 | | | | | |
| XY | KO | 7.00 | | | | | |
| *Gata4* | | | | | | | |
| XX | WT | 7.28 | 16.65 | 12.49 | 17.75 | 11.72 | 142.11 |
| XX | KO | 9.87 | | | | | |
| XY | WT | 6.77 | | | | | |
| XY | KO | 9.78 | | | | | |
| *Sf1* | | | | | | | |
| XX | WT | 5.11 | 1.67 | 0.44 | 0.20 | 3.69 | 45.19 |
| XX | KO | 11.02 | | | | | |
| XY | WT | 6.26 | | | | | |
| XY | KO | 14.09 | | | | | |
| *Sox9* | | | | | | | |
| XX | WT | 6.34 | 232.95 | 45.25 | 283.24 | 37.22 | 625.93 |
| XX | KO | 5.12 | | | | | |
| XY | WT | 3.69 | | | | | |
| XY | KO | 4.84 | | | | | |
| *Star* | | | | | | | |
| XX | WT | 5.63 | 13.52 | 24.97 | 31.40 | 10.75 | 125.79 |
| XX | KO | 8.52 | | | | | |
| XY | WT | 5.30 | | | | | |
| XY | KO | 7.30 | | | | | |

* From $\Delta\Delta$Ct the fold increase was calculated and is shown as percent values.
Genotypes are as follows:

1. $Wt1^{+/+}$ XX - $Wt1^{-/-}$ XX
2. $Wt1^{+/+}$ XY - $Wt1^{-/-}$ XY
3. $Wt1^{+/+}$ XX - $Wt1^{-/-}$ XY
4. $Wt1^{+/+}$ XY - $Wt1^{-/-}$ XX
5. $Wt1^{+/+}$ XX - $Wt1^{+/+}$ XY

| gene | values | **Wt1** | | **Gata4** | | **Wt1 /** | **Gata4** |
|---|---|---|---|---|---|---|---|
| | | XX | XY | XX | XY | XX | XY |
| *Amh* | % | 37.39 | 27.32 | 11.71 | 102.21 | 8.92 | 23.56 |
| *Amhr2* | % | 68.18 | 26.16 | 58.71 | 127.77 | 44.27 | 63.24 |
| *Ctnnb1* | % | 126.44 | 164.05 | 553.28 | 562.95 | 361.43 | 540.69 |
| *Dax1* | % | 47.50 | 95.73 | 165.98 | 121.87 | 89.08 | 147.12 |
| *Foxl2* | % | 70.89 | - | 54.89 | - | 20.11 | - |
| *Fst* | % | 94.63 | 73.11 | 46.03 | 290.73 | 128.83 | 204.68 |
| *Gata4* | % | 94.91 | 62.25 | 278.77 | 340.68 | 199.37 | 278.00 |
| *Sf1* | % | 145.83 | 64.64 | 76.10 | 125.68 | 172.81 | 94.57 |
| *Sox9* | % | 111.98 | 53.37 | 74.49 | 132.70 | 147.96 | 89.08 |
| *Star* | % | 43.46 | 38.04 | 58.77 | 54.88 | 66.52 | 49.71 |
| *Wt1* | % | 100.07 | 137.37 | 125.79 | 107.72 | 119.91 | 185.83 |

**Table 5.2:** Gene expression analysis of vivo-morpholino treated organs. From $\Delta\Delta$Ct the fold increase was calculated and is shown as percent values

# 6

# Abstract

Aberrant regulation of given key factors involved in gonad development is the cause of a variety of syndromes associated with disorders of sexual development (DSDs). WT1 and GATA4 are two transcription factors that are implicated and essential for the proper development of the gonad. The functional relevance of WT1 and GATA4 during sex determination is well described. But knowledge in terms of their contribution to the female and male gonad during the sex differentiation phase remains somewhat elusive. This states the central focus of this thesis. In order to address this issue, gonads of wild type *Wt1*$^{+/+}$ and *Wt1*$^{-/-}$ deficient mice were compared in terms of morphology and gene expression status. Further, I established an *ex-vivo* organ culture system that combines the hanging droplet culture technique and an antisense oligonucleotide strategy using vivo-morpholinos against *Wt1* and *Gata4*. This system allows the analysis of the morphology and the gene expression status in single gonadal organ cultures. The data show that WT1 is required to establish a sex specific signature in both sexes. The knockdown of WT1 in *ex-vivo* cultures results in the down regulation of testis specific genes, e.g., *Amh, Amhr2, Sf1* and *Sox9* and ovarian promoting genes, e.g., *Dax1* and *Foxl2*. Thereby, *Foxl2* was identified as a potential WT1 target gene. Antisense silencing of GATA4 led to the up regulation of *Fst* and *Ctnnb1*, which are identified as potential GATA4 target genes, that are repressed by GATA4. Interestingly, changes that were observed in the sole knockdown approach were prevented by the combined knockdown of WT1 and GATA4. This concludes a complex interplay between WT1 and GATA4 that control gonadal gene expression. Furthermore, *Wt1* vivo-morpholino silencing affected the proliferation state of gonadal and mesonephric cells in both sexes. Treated gonads with *Gata4* vivo-morpholino exhibit proliferation defects only in the male gonad and mesonephros, whereas the female organ was unaffected. In addition, I could demonstrate that modulation of the Wnt signalling cascade does not interfere with

the expression of *Wt1* and *Gata4*, which suggests that WT1 and GATA4 act upstream of the Wnt pathway. In summary, I could show that WT1 and GATA4 are equally important during sex differentiation of the female and male gonad by contributing to a sex specific expression pattern.

# 7

# Zusammenfassung

Die abnorme Regulation bestimmter Faktoren, die bei der Gonadenentwicklung eine wichtige Rolle spielen, ist die Ursache für eine Vielzahl an Syndromen, die mit "disorders of sexual development (DSDs)", assoziiert sind. WT1 und GATA4 sind zwei wichtige Transkriptionsfaktoren während der Gonadenentwicklung. Die funktionelle Relevanz beider Faktoren ist während der Geschlechtsfestlegung gut erforscht. Das Wissen hingegen über deren Beitrag zur Entwicklung der weiblichen und männlichen Gonade im Laufe der Geschlechtsdifferenzierung verblieb etwas flüchtig. Dies konstantiert den zentralen Fokus der Doktorarbeit. Um diese Aufgabe zu bearbeiten, wurden die Gonaden von Wildtyp $Wt1^{+/+}$ und $Wt1^{-/-}$ defizienter Mausembryonen miteinander, im Bezug auf die Morphologie und Genexpression, verglichen. Weiters etablierte ich ein *ex-vivo* Organkultursystem, welches sich aus einer hängenden Tröpfchenkultur und dem Einsatz von vivo-morpholinos gegen WT1 und GATA4 gerichtet, zusammensetzt. Dieses System ermöglicht die Analyse der Genexpression und Morphologie in einzelnen Gonadenkulturen. Die Daten zeigen, dass WT1 für eine sex-spezifische Signatur in beiden Geschlechter eine wichtige Rolle spielt. Der Knockdown von WT1 in *ex-vivo* Organkulturen bringt eine Abnahme in der Expression männlicher Gene, das heisst, *Amh, Amhr2, Sf1* und *Sox9* sowie weiblicher Gene, das heisst, *Dax1* und *Foxl2*, mit sich. Dabei wurde *Foxl2* als potentielles WT1 Zielgen identifiziert. Der GATA4 Knockdown führte zu einer Hochregulierung von *Fst* und *Ctnnb1*, welche somit als potentielle GATA4 Zielgene identifiziert werden konnten. Interessanterweise sind Veränderungen die im WT1 Einzelknockdown verzeichnet wurden, durch den kombinierten Knockdown von WT1/GATA4 kompensiert worden. Dies lässt folgern, dass WT1 und GATA4 in einem komplexen Zusammenspiel die gonadale Genexpression steuern. Darüberhinaus bewirkte der WT1 Knockdown in beiden Geschlechtern eine Abnahme in der Proliferation gonadaler und mesonephros-spezifscher Zellen. Gonaden, die mit *Gata4*

vivo-morpholino behandelt wurden, weissen ausschliesslich auf eine Proliferationsabnahme in der männlichen Gonade und dem Mesonephros hin, wohingegen die Proliferation im weibliche Organ unbeeinflusst blieb. Zusätzlich konnte ich zeigen, dass eine Modulation des Wnt Signalwegs die Expression von *Wt1* und *Gata4* nicht beeinflusst. Die lässt die Annahme zu, dass möglicherweise WT1 und GATA4 dem Wnt Signalweg vorangeschaltet sind. Zusammenfassend konnte ich zeigen, dass WT1 und GATA4 eine ebenso wichtige Rolle während der Geschlechtsdifferenzierungs-phase der weiblichen sowie der männlichen Gonade einnehmen, und einen wichtigen Beitrag zu einer Geschlechts-spezifischen Signatur beisteuern.

# Bibliography


[1] Dagmar Wilhelm, Stephen Palmer, and Peter Koopman. Sex Determination and Gonadal Development in Mammals. *Physiol. Rev.*, pages 1–28, 2007.

[2] J Gubbay, J Collignon, P Koopman, B Capel, A Economou, A Münsterberg, N Vivian, P Goodfellow, and R Lovell-Badge. A gene mapping to the sex-determining region of the mouse Y chromosome is a member of a novel family of embryonically expressed genes. *Nature*, 346(6281):245–50, July 1990.

[3] A H Sinclair, P Berta, M S Palmer, J R Hawkins, B L Griffiths, M J Smith, J W Foster, A M Frischauf, R Lovell-Badge, and P N Goodfellow. A gene from the human sex-determining region encodes a protein with homology to a conserved DNA-binding motif. *Nature*, 346(6281):240–4, July 1990.

[4] P N Goodfellow and R Lovell-Badge. SRY and sex determination in mammals. *Annu. Rev. Genet.*, 27:71–92, January 1993.

[5] Stefanie Eggers, Thomas Ohnesorg, and Andrew Sinclair. Genetic regulation of mammalian gonad development. *Nat. Rev. Endocrinol.*, 10(11):673–683, November 2014.

[6] Valerie A Arboleda, David E Sandberg, and Eric Vilain. DSDs: genetics, underlying pathologies and psychosexual differentiation. *Nat. Rev. Endocrinol.*, 10(10):603–15, October 2014.

[7] Ryuji Hiramatsu, Shogo Matoba, Masami Kanai-Azuma, Naoki Tsunekawa, Yuko Katoh-Fukui, Masamichi Kurohmaru, Ken-Ichirou Morohashi, Dagmar Wilhelm, Peter Koopman, and Yoshiakira Kanai. A critical time window of Sry action in gonadal sex determination in mice. *Development*, 136(1):129–38, January 2009.

[8] Steven C Munger, Anirudh Natarajan, Loren L Looger, Uwe Ohler, and Blanche Capel. Fine time course expression analysis identifies cascades of activation and repression and maps a putative regulator of mammalian sex determination. *PLoS Genet.*, 9(7):e1003630, January 2013.

[9] Gerrit J Bouma, Geoffrey T Hart, Linda L Washburn, Andrew K Recknagel, and Eva M Eicher. Using real time RT-PCR analysis to determine multiple gene expression patterns during XX and XY mouse fetal gonad development. *Gene Expr. Patterns*, 5(1):141–9, November 2004.

[10] J Karl and B Capel. Sertoli cells of the mouse testis originate from the coelomic epithelium. *Dev. Biol.*, 203(2):323–33, November 1998.

[11] B Capel. The battle of the sexes. *Mech. Dev.*, 92(1):89–103, March 2000.

[12] Jennifer Brennan and Blanche Capel. One tissue, two fates: molecular genetic events that underlie testis versus ovary development. *Nat. Rev. Genet.*, 5(7):509–21, July 2004.

[13] P Koopman, J Gubbay, N Vivian, P Goodfellow, and R Lovell-Badge. Male development of chromosomally female mice transgenic for Sry. *Nature*, 351(6322):117–21, May 1991.

[14] Kenneth H Albrecht and Eva M Eicher. Evidence that Sry is expressed in pre-Sertoli cells and Sertoli and granulosa cells have a common precursor. *Dev. Biol.*, 240(1):92–107, December 2001.

[15] Jonah Cool, Tony DeFalco, and Blanche Capel. Testis formation in the fetal mouse: dynamic and complex de novo tubulogenesis. *Wiley Interdiscip. Rev. Dev. Biol.*, 1(6):847–59, 2012.

[16] Liesl Nel-Themaat, Chuan-Wei Jang, M David Stewart, Haruhiko Akiyama, Robert S Viger, and Richard R Behringer. Sertoli cell behaviors in developing testis cords and postnatal seminiferous tubules of the mouse. *Biol. Reprod.*, 84(2):342–50, February 2011.

[17] Dagmar Wilhelm and Peter Koopman. The makings of maleness: towards an integrated view of male sexual development. *Nat. Rev. Genet.*, 7(8):620–31, August 2006.

[18] Bluma J Lesch and David C Page. Genetics of germ cell development. *Nat. Rev. Genet.*, 13(11):781–94, November 2012.

[19] Terje Svingen and Peter Koopman. Building the mammalian testis: origins, differentiation, and assembly of the component cell populations. *Genes Dev.*, 27(22):2409–26, November 2013.

[20] Barbara Nicol and Humphrey H-C Yao. Building an ovary: insights into establishment of somatic cell lineages in the mouse. *Sex Dev.*, 8(5):243–51, January 2014.

[21] Lindsey Mork, Danielle M Maatouk, Jill A McMahon, Jin Jin Guo, Pumin Zhang, Andrew P McMahon, and Blanche Capel. Temporal differences in granulosa cell specification in the ovary reflect distinct follicle fates in mice. *Biol. Reprod.*, 86(2):37, February 2012.

[22] Jennifer Schmahl, Kamran Rizzolo, and Philippe Soriano. The PDGF signaling pathway controls multiple steroid-producing lineages. *Genes Dev.*, 22(23):3255–67, December 2008.

[23] Denis A Magoffin. Ovarian theca cell. *Int. J. Biochem. Cell Biol.*, 37(7):1344–9, July 2005.

[24] E K Ungewitter and H H-C Yao. How to make a gonad: cellular mechanisms governing formation of the testes and ovaries. *Sex Dev.*, 7(1-3):7–20, January 2013.

[25] Akio Kobayashi and Richard R Behringer. Developmental genetics of the female reproductive tract in mammals. *Nat. Rev. Genet.*, 4(12):969–80, December 2003.

[26] Ian R Adams and Anne McLaren. Sexually dimorphic development of mouse primordial germ cells: switching from oogenesis to spermatogenesis. *Development*, 129(5):1155–64, March 2002.

[27] J Martineau, K Nordqvist, C Tilmann, R Lovell-Badge, and B Capel. Male-specific cell migration into the developing gonad. *Curr. Biol.*, 7(12):958–68, December 1997.

[28] K. Gilbert, S.F. and Knisely. *Developmental Biology 9th Ed + a Student Handbook in Writing in Biology 3rd Ed.* Sinauer Associates Incorporated, 2010.

[29] Yuka Fujimoto, Satomi S Tanaka, Yasuka L Yamaguchi, Hiroki Kobayashi, Shunsuke Kuroki, Makoto Tachibana, Mai Shinomura, Yoshiakira Kanai, Ken-Ichirou Morohashi, Kiyoshi Kawakami, and Ryuichi Nishinakamura. Homeoproteins Six1 and Six4 regulate male sex determination and mouse gonadal development. *Dev. Cell*, 26(4):416–30, August 2013.

[30] Serge Nef, Sunita Verma-Kurvari, Jussi Merenmies, Jean-Dominique Vassalli, Argiris Efstratiadis, Domenico Accili, and Luis F Parada. Testis determination requires insulin receptor family function in mice. *Nature*, 426(6964):291–5, November 2003.

[31] Dagmar Wilhelm and Christoph Englert. The Wilms tumor suppressor WT1 regulates early gonad development by activation of Sf1. *Genes Dev.*, 16(14):1839–51, July 2002.

[32] J A Kreidberg, H Sariola, J M Loring, M Maeda, J Pelletier, D Housman, and R Jaenisch. WT-1 is required for early kidney development. *Cell*, 74(4):679–91, August 1993.

[33] O S Birk, D E Casiano, C A Wassif, T Cogliati, L Zhao, Y Zhao, A Grinberg, S Huang, J A Kreidberg, K L Parker, F D Porter, and H Westphal. The LIM homeobox gene Lhx9 is essential for mouse gonad formation. *Nature*, 403(6772):909–13, February 2000.

[34] Y Katoh-Fukui, R Tsuchiya, T Shiroishi, Y Nakahara, N Hashimoto, K Noguchi, and T Higashinakagawa. Male-to-female sex reversal in M33 mutant mice. *Nature*, 393(6686):688–92, June 1998.

[35] N Miyamoto, M Yoshida, S Kuratani, I Matsuo, and S Aizawa. Defects of urogenital development in mice lacking Emx2. *Development*, 124(9):1653–64, May 1997.

[36] Sergei G Tevosian, Kenneth H Albrecht, John D Crispino, Yuko Fujiwara, Eva M Eicher, and Stuart H Orkin. Gonadal differentiation, sex determination and normal Sry expression in mice require direct interaction between transcription partners GATA4 and FOG2. *Development*, 129(19):4627–34, October 2002.

[37] Yueh-Chiang Hu, Leah M Okumura, and David C Page. Gata4 is required for formation of the genital ridge in mice. *PLoS Genet.*, 9(7):e1003629, July 2013.

[38] M Bullejos and P Koopman. Spatially dynamic expression of Sry in mouse genital ridges. *Dev. Dyn.*, 221(2):201–5, June 2001.

[39] Dagmar Wilhelm, Fred Martinson, Stephen Bradford, Megan J Wilson, Alexander N Combes, Annemiek Beverdam, Josephine Bowles, Hirofumi Mizusaki, and Peter Koopman. Sertoli cell differentiation is induced both cell-autonomously and through prostaglandin signaling during mammalian sex determination. *Dev. Biol.*, 287(1):111–24, November 2005.

[40] P Koopman, A Münsterberg, B Capel, N Vivian, and R Lovell-Badge. Expression of a candidate sex-determining gene during mouse testis differentiation. *Nature*, 348(6300):450–2, November 1990.

[41] A Hacker, B Capel, P Goodfellow, and R Lovell-Badge. Expression of Sry, the mouse sex determining gene. *Development*, 121(6):1603–14, June 1995.

[42] Y W Jeske, J Bowles, A Greenfield, and P Koopman. Expression of a linear Sry transcript in the mouse genital ridge. *Nat. Genet.*, 10(4):480–2, August 1995.

[43] Louisa M Ludbrook and Vincent R Harley. Sex determination: a 'window' of DAX1 activity. *Trends Endocrinol. Metab.*, 15(3):116–21, April 2004.

[44] Christian Larney, Timothy L Bailey, and Peter Koopman. Switching on sex: transcriptional regulation of the testis-determining gene Sry. *Development*, 141(11):2195–205, June 2014.

[45] P de Santa Barbara, C Méjean, B Moniot, M H Malclès, P Berta, and B Boizet-Bonhoure. Steroidogenic factor-1 contributes to the cyclic-adenosine monophosphate down-regulation of human SRY gene expression. *Biol. Reprod.*, 64(3):775–83, March 2001.

[46] Frank William Buaas, Pierre Val, and Amanda Swain. The transcription co-factor CITED2 functions during sex determination and early gonad development. *Hum. Mol. Genet.*, 18(16):2989–3001, August 2009.

[47] A Hammes, J K Guo, G Lutsch, J R Leheste, D Landrock, U Ziegler, M C Gubler, and A Schedl. Two splice variants of the Wilms' tumor 1 gene have distinct functions during sex determination and nephron formation. *Cell*, 106(3):319–29, August 2001.

[48] Stephen T Bradford, Dagmar Wilhelm, Roberto Bandiera, Valerie Vidal, Andreas Schedl, and Peter Koopman. A cell-autonomous role for WT1 in regulating Sry in vivo. *Hum. Mol. Genet.*, 18(18):3429–38, September 2009.

[49] Yoko Miyamoto, Hiroaki Taniguchi, Frédéric Hamel, David W Silversides, and Robert S Viger. A GATA4/WT1 cooperation regulates transcription of genes required for mammalian sex determination and differentiation. *BMC Mol. Biol.*, 9:44, January 2008.

[50] A Hossain and G F Saunders. The human sex-determining gene SRY is a direct target of WT1. *J. Biol. Chem.*, 276(20):16817–23, May 2001.

[51] Mathias S Gierl, Wolfram H Gruhn, Annika von Seggern, Nicole Maltry, and Christof Niehrs. GADD45G Functions in Male Sex Determination by Promoting p38 Signaling and Sry Expression. *Dev. Cell*, October 2012.

[52] Shunsuke Kuroki, Shogo Matoba, Mika Akiyoshi, Yasuko Matsumura, Hitoshi Miyachi, Nathan Mise, Kuniya Abe, Atsuo Ogura, Dagmar Wilhelm, Peter Koopman, Masami Nozaki, Yoshiakira Kanai, Yoichi Shinkai, and Makoto Tachibana. Epigenetic regulation of mouse sex determination by the histone demethylase Jmjd1a. *Science*, 341(6150):1106–9, September 2013.

[53] Makoto Ono and Vincent R Harley. Disorders of sex development: new genes, new concepts. *Nat. Rev. Endocrinol.*, 9(2):79–91, February 2013.

[54] Ryohei Sekido and Robin Lovell-Badge. Sex determination involves synergistic action of SRY and SF1 on a specific Sox9 enhancer. *Nature*, 453(7197):930–4, June 2008.

[55] S Mansour, C M Hall, M E Pembrey, and I D Young. A clinical and genetic study of campomelic dysplasia. *J. Med. Genet.*, 32(6):415–20, June 1995.

[56] Marie-Christine Chaboissier, Akio Kobayashi, Valerie I P Vidal, Susanne Lützkendorf, Henk J G van de Kant, Michael Wegner, Dirk G de Rooij, Richard R Behringer, and Andreas Schedl. Functional analysis of Sox8 and Sox9 during sex determination in the mouse. *Development*, 131(9):1891–901, May 2004.

[57] Francisco Barrionuevo, Stefan Bagheri-Fam, Jürgen Klattig, Ralf Kist, Makoto M Taketo, Christoph Englert, and Gerd Scherer. Homozygous inactivation of Sox9 causes complete XY sex reversal in mice. *Biol. Reprod.*, 74(1):195–201, January 2006.

[58] C E Bishop, D J Whitworth, Y Qin, A I Agoulnik, I U Agoulnik, W R Harrison, R R Behringer, and P A Overbeek. A transgenic insertion upstream of sox9 is associated with dominant XX sex reversal in the mouse. *Nat. Genet.*, 26(4):490–4, December 2000.

[59] V P Vidal, M C Chaboissier, D G de Rooij, and A Schedl. Sox9 induces testis development in XX transgenic mice. *Nat. Genet.*, 28(3):216–7, July 2001.

[60] Ryohei Sekido and Robin Lovell-Badge. Sex determination and SRY: down to a wink and a nudge? *Trends Genet.*, 25(1):19–29, January 2009.

[61] Jennifer Schmahl and Blanche Capel. Cell proliferation is necessary for the determination of male fate in the gonad. *Dev. Biol.*, 258(2):264–76, June 2003.

[62] Jennifer Schmahl, Yuna Kim, Jennifer S Colvin, David M Ornitz, and Blanche Capel. Fgf9 induces proliferation and nuclear localization of FGFR2 in Sertoli

precursors during male sex determination. *Development*, 131(15):3627–36, August 2004.

[63] Yuna Kim, Nathan Bingham, Ryohei Sekido, Keith L Parker, Robin Lovell-Badge, and Blanche Capel. Fibroblast growth factor receptor 2 regulates proliferation and Sertoli differentiation during male sex determination. *Proc. Natl. Acad. Sci. U. S. A.*, 104(42):16558–63, October 2007.

[64] Brigitte Moniot, Faustine Declosmenil, Francisco Barrionuevo, Gerd Scherer, Kosuke Aritake, Safia Malki, Laetitia Marzi, Anne Cohen-Solal, Ina Georg, Jürgen Klattig, Christoph Englert, Yuna Kim, Blanche Capel, Naomi Eguchi, Yoshihiro Urade, Brigitte Boizet-Bonhoure, and Francis Poulat. The PGD2 pathway, independently of FGF9, amplifies SOX9 activity in Sertoli cells during male sexual differentiation. *Development*, 136(11):1813–21, June 2009.

[65] Yunmin Li, Ming Zheng, and Yun-Fai Chris Lau. The sex-determining factors SRY and SOX9 regulate similar target genes and promote testis cord formation during testicular differentiation. *Cell Rep.*, 8(3):723–33, August 2014.

[66] Alexander N Combes, Emmanuelle Lesieur, Vincent R Harley, Andrew H Sinclair, Melissa H Little, Dagmar Wilhelm, and Peter Koopman. Three-dimensional visualization of testis cord morphogenesis, a novel tubulogenic mechanism in development. *Dev. Dyn.*, 238(5):1033–41, May 2009.

[67] B Capel. Patterning the gonad in 4-dimensions. *Anim. Biol. Reprod. ISABR 2008,International Symp. 2nd*, pages 30–33, 2009.

[68] Liesl Nel-Themaat, Tegy J Vadakkan, Ying Wang, Mary E Dickinson, Haruhiko Akiyama, and Richard R Behringer. Morphometric analysis of testis cord formation in Sox9-EGFP mice. *Dev. Dyn.*, 238(5):1100–10, May 2009.

[69] Douglas Coveney, Jonah Cool, Tim Oliver, and Blanche Capel. Four-dimensional analysis of vascularization during primary development of an organ, the gonad. *Proc. Natl. Acad. Sci. U. S. A.*, 105(20):7212–7, May 2008.

[70] Katherine Jeays-Ward, Christine Hoyle, Jennifer Brennan, Mathieu Dandonneau, Graham Alldus, Blanche Capel, and Amanda Swain. Endothelial and steroidogenic cell migration are regulated by WNT4 in the developing mammalian gonad. *Development*, 130(16):3663–70, August 2003.

[71] Humphrey H C Yao, Martin M Matzuk, Carolina J Jorgez, Douglas B Menke, David C Page, Amanda Swain, and Blanche Capel. Follistatin operates down-

stream of Wnt4 in mammalian ovary organogenesis. *Dev. Dyn.*, 230(2):210–5, June 2004.

[72] Andrea J Ross, Christopher Tilman, Humphrey Yao, David MacLaughlin, and Blanche Capel. AMH induces mesonephric cell migration in XX gonads. *Mol. Cell. Endocrinol.*, 211(1-2):1–7, December 2003.

[73] S Nef and L F Parada. Hormones in male sexual development. *Genes Dev.*, 14(24):3075–86, December 2000.

[74] J Klattig and C Englert. The Müllerian duct: recent insights into its development and regression. *Sex Dev.*, 1(5):271–8, January 2007.

[75] Avenel Joseph, Humphrey Yao, and Barry T Hinton. Development and morphogenesis of the Wolffian/epididymal duct, more twists and turns. *Dev. Biol.*, 325(1):6–14, January 2009.

[76] K McElreavey, E Vilain, N Abbas, I Herskowitz, and M Fellous. A regulatory cascade hypothesis for mammalian sex determination: SRY represses a negative regulator of male development. *Proc. Natl. Acad. Sci. U. S. A.*, 90(8):3368–72, April 1993.

[77] Humphrey Hung-Chang Yao, Christopher Tilmann, Guang-Quan Zhao, and Blanche Capel. The battle of the sexes: opposing pathways in sex determination. *Novartis Found. Symp.*, 244:187–98; discussion 198–206, 253–7, January 2002.

[78] Yuna Kim, Akio Kobayashi, Ryohei Sekido, Leo DiNapoli, Jennifer Brennan, Marie-Christine Chaboissier, Francis Poulat, Richard R Behringer, Robin Lovell-Badge, and Blanche Capel. Fgf9 and Wnt4 act as antagonistic signals to regulate mammalian sex determination. *PLoS Biol.*, 4(6):e187, June 2006.

[79] Kenichi Kashimada, Emanuele Pelosi, Huijun Chen, David Schlessinger, Dagmar Wilhelm, and Peter Koopman. FOXL2 and BMP2 act cooperatively to regulate follistatin gene expression during ovarian development. *Endocrinology*, 152(1):272–80, January 2011.

[80] Manuela Uda, Chris Ottolenghi, Laura Crisponi, Jose Elias Garcia, Manila Deiana, Wendy Kimber, Antonino Forabosco, Antonio Cao, David Schlessinger, and Giuseppe Pilia. Foxl2 disruption causes mouse ovarian failure by pervasive blockage of follicle development. *Hum. Mol. Genet.*, 13(11):1171–81, June 2004.

[81] N Henriette Uhlenhaut, Susanne Jakob, Katrin Anlag, Tobias Eisenberger, Ryohei Sekido, Jana Kress, Anna-Corina Treier, Claudia Klugmann, Christian Klasen, Nadine I Holter, Dieter Riethmacher, Günther Schütz, Austin J Cooney, Robin Lovell-Badge, and Mathias Treier. Somatic sex reprogramming of adult ovaries to testes by FOXL2 ablation. *Cell*, 139(6):1130–42, December 2009.

[82] Anne-Amandine Chassot, Stephen T Bradford, Aurélie Auguste, Elodie P Gregoire, Eric Pailhoux, Dirk G de Rooij, Andreas Schedl, and Marie-Christine Chaboissier. WNT4 and RSPO1 together are required for cell proliferation in the early mouse gonad. *Development*, October 2012.

[83] Chia-Feng Liu, Nathan Bingham, Keith Parker, and Humphrey H-C Yao. Sex-specific roles of beta-catenin in mouse gonadal development. *Hum. Mol. Genet.*, 18(3):405–17, February 2009.

[84] Jonah Cool and Blanche Capel. Mixed signals: development of the testis. *Semin. Reprod. Med.*, 27(1):5–13, January 2009.

[85] Stella Tran, Ying Wang, Pankaj Lamba, Xiang Zhou, Ulrich Boehm, and Daniel J Bernard. The CpG island in the murine foxl2 proximal promoter is differentially methylated in primary and immortalized cells. *PLoS One*, 8(10):e76642, January 2013.

[86] Anyi Dai, Haixiang Sun, Ting Fang, Qun Zhang, Shaogen Wu, Yue Jiang, Lijun Ding, Guijun Yan, and Yali Hu. MicroRNA-133b stimulates ovarian estradiol synthesis by targeting Foxl2. *FEBS Lett.*, 587(15):2474–82, August 2013.

[87] Adrien Georges, Aurelie Auguste, Laurianne Bessière, Anne Vanet, Anne-Laure Todeschini, and Reiner A Veitia. FOXL2: a central transcription factor of the ovary. *J. Mol. Endocrinol.*, 52(1):R17–33, February 2014.

[88] Anna Biason-Lauber. WNT4, RSPO1, and FOXL2 in Sex Development. *Semin. Reprod. Med.*, 30(5):387–95, October 2012.

[89] Pietro Parma, Orietta Radi, Valerie Vidal, Marie Christine Chaboissier, Elena Dellambra, Stella Valentini, Liliana Guerra, Andreas Schedl, and Giovanna Camerino. R-spondin1 is essential in sex determination, skin differentiation and malignancy. *Nat. Genet.*, 38(11):1304–9, November 2006.

[90] Anne-Amandine Chassot, Fariba Ranc, Elodie P Gregoire, Hermien L Roepers-Gajadien, Makoto M Taketo, Giovanna Camerino, Dirk G de Rooij, Andreas Schedl, and Marie-Christine Chaboissier. Activation of beta-catenin signaling

by Rspo1 controls differentiation of the mammalian ovary. *Hum. Mol. Genet.*, 17(9):1264–77, May 2008.

[91] Danielle M Maatouk, Leo DiNapoli, Ashley Alvers, Keith L Parker, Makoto M Taketo, and Blanche Capel. Stabilization of beta-catenin in XY gonads causes male-to-female sex-reversal. *Hum. Mol. Genet.*, 17(19):2949–55, October 2008.

[92] Hannah Mandel, Revital Shemer, Zvi U Borochowitz, Marina Okopnik, Carlos Knopf, Margarita Indelman, Arie Drugan, Dov Tiosano, Ruth Gershoni-Baruch, Mordechai Choder, and Eli Sprecher. SERKAL syndrome: an autosomal-recessive disorder caused by a loss-of-function mutation in WNT4. *Am. J. Hum. Genet.*, 82(1):39–47, January 2008.

[93] Samantha A Jameson, Yi-Tzu Lin, and Blanche Capel. Testis development requires the repression of Wnt4 by Fgf signaling. *Dev. Biol.*, June 2012.

[94] Leon Speroff Fritz and Marc A. *Clinical Gynecologic Endocrinology and Infertility.* Lippincott Williams \& Wilkins, 2005.

[95] D A Haber, A J Buckler, T Glaser, K M Call, J Pelletier, R L Sohn, E C Douglass, and D E Housman. An internal deletion within an 11p13 zinc finger gene contributes to the development of Wilms' tumor. *Cell*, 61(7):1257–69, June 1990.

[96] Vicki Huff. Wilms' tumours: about tumour suppressor genes, an oncogene and a chameleon gene. *Nat. Rev. Cancer*, 11(2):111–21, February 2011.

[97] Maria Teresa Discenza and Jerry Pelletier. Insights into the physiological role of WT1 from studies of genetically modified mice. *Physiol. Genomics*, 16(3):287–300, February 2004.

[98] Abdelkader Essafi, Anna Webb, Rachel L Berry, Joan Slight, Sally F Burn, Lee Spraggon, Victor Velecela, Ofelia M Martinez-Estrada, John H Wiltshire, Stefan G E Roberts, David Brownstein, Jamie A Davies, Nicholas D Hastie, and Peter Hohenstein. A wt1-controlled chromatin switching mechanism underpins tissue-specific wnt4 activation and repression. *Dev. Cell*, 21(3):559–74, September 2011.

[99] Peter Hohenstein and Nicholas D Hastie. The many facets of the Wilms' tumour gene, WT1. *Hum. Mol. Genet.*, 15 Spec No:R196–201, October 2006.

[100] D A Haber, R L Sohn, A J Buckler, J Pelletier, K M Call, and D E Housman. Alternative splicing and genomic structure of the Wilms tumor gene WT1. *Proc. Natl. Acad. Sci. U. S. A.*, 88(21):9618–22, November 1991.

[101] Stefan G E Roberts. The modulation of WTI transcription function by cofactors. *Biochem. Soc. Symp.*, 201(73):191–201, January 2006.

[102] Avril A Morrison, Rebecca L Viney, and Michael R Ladomery. The post-transcriptional roles of WT1, a multifunctional zinc-finger protein. *Biochim. Biophys. Acta*, 1785(1):55–62, January 2008.

[103] J Kim, D Prawitt, N Bardeesy, E Torban, C Vicaner, P Goodyer, B Zabel, and J Pelletier. The Wilms' tumor suppressor gene (wt1) product regulates Dax-1 gene expression during gonadal differentiation. *Mol. Cell. Biol.*, 19(3):2289–99, March 1999.

[104] Fei Gao, Sourindra Maiti, Nargis Alam, Zhen Zhang, Jian Min Deng, Richard R Behringer, Charlotte Lécureuil, Florian Guillou, and Vicki Huff. The Wilms tumor gene, Wt1, is required for Sox9 expression and maintenance of tubular architecture in the developing testis. *Proc. Natl. Acad. Sci. U. S. A.*, 103(32):11987–92, August 2006.

[105] Jürgen Klattig, Ralph Sierig, Dagmar Kruspe, Birgit Besenbeck, and Christoph Englert. Wilms' tumor protein Wt1 is an activator of the anti-Müllerian hormone receptor gene Amhr2. *Mol. Cell. Biol.*, 27(12):4355–64, June 2007.

[106] Min Chen, Xiaona Wang, Yanbo Wang, Lianjun Zhang, Binyang Xu, Limin Lv, Xiuhong Cui, Wei Li, and Fei Gao. Wt1 is involved in leydig cell steroid hormone biosynthesis by regulating paracrine factor expression in mice. *Biol. Reprod.*, 90(4):71, April 2014.

[107] Hao Chang, Fei Gao, Florian Guillou, Makoto M Taketo, Vicki Huff, and Richard R Behringer. Wt1 negatively regulates beta-catenin signaling during testis development. *Development*, 135(10):1875–85, May 2008.

[108] J Klattig, R Sierig, D Kruspe, M S Makki, and C Englert. WT1-mediated gene regulation in early urogenital ridge development. *Sex Dev.*, 1(4):238–54, January 2007.

[109] Anwar Hossain and Grady F Saunders. Role of Wilms tumor 1 (WT1) in the transcriptional regulation of the Mullerian-inhibiting substance promoter. *Biol. Reprod.*, 69(6):1808–14, December 2003.

[110] Tessa Peterkin, Abigail Gibson, Matthew Loose, and Roger Patient. The roles of GATA-4, -5 and -6 in vertebrate heart development. *Semin. Cell Dev. Biol.*, 16(1):83–94, February 2005.

[111] Tamara Zaytouni, Evgeni E Efimenko, and Sergei G Tevosian. *GATA transcription factors in the developing reproductive system.*, volume 76. Elsevier Inc., 1 edition, January 2011.

[112] J D Molkentin. The zinc finger-containing transcription factors GATA-4, -5, and -6. Ubiquitously expressed regulators of tissue-specific gene expression. *J. Biol. Chem.*, 275(50):38949–52, December 2000.

[113] Alistair J Watt, Michele A Battle, Jixuan Li, and Stephen A Duncan. GATA4 is essential for formation of the proepicardium and regulates cardiogenesis. *Proc. Natl. Acad. Sci. U. S. A.*, 101(34):12573–8, August 2004.

[114] Chay T Kuo, Edward E Morrisey, Roshani Anandappa, Kirsten Sigrist, Min M Lu, M S Parmacek, C Soudais, and J M Leiden. GATA4 transcription factor is required for ventral morphogenesis and heart tube formation. *Genes Dev.*, 11(8):1048–60, April 1997.

[115] Robert S Viger, Séverine Mazaud Guittot, Mikko Anttonen, David B Wilson, and Markku Heikinheimo. Role of the GATA family of transcription factors in endocrine development, function, and disease. *Mol. Endocrinol.*, 22(4):781–98, April 2008.

[116] Anabel Rojas, William Schachterle, Shan-Mei Xu, Franz Martín, and Brian L Black. Direct transcriptional regulation of Gata4 during early endoderm specification is controlled by FoxA2 binding to an intronic enhancer. *Dev. Biol.*, 346(2):346–55, October 2010.

[117] Anabel Rojas, William Schachterle, Shan-Mei Xu, and Brian L Black. An endoderm-specific transcriptional enhancer from the mouse Gata4 gene requires GATA and homeodomain protein-binding sites for function in vivo. *Dev. Dyn.*, 238(10):2588–98, October 2009.

[118] Anabel Rojas, Sarah De Val, Analeah B Heidt, Shan-Mei Xu, James Bristow, and Brian L Black. Gata4 expression in lateral mesoderm is downstream of BMP4 and is activated directly by Forkhead and GATA transcription factors through a distal enhancer element. *Development*, 132(15):3405–17, August 2005.

[119] William Schachterle, Anabel Rojas, Shan-Mei Xu, and Brian L Black. ETS-dependent regulation of a distal Gata4 cardiac enhancer. *Dev. Biol.*, 361(2):439–49, January 2012.

[120] Séverine Mazaud Guittot, Amélie Tétu, Eric Legault, Nicolas Pilon, David W Silversides, and Robert S Viger. The proximal Gata4 promoter directs reporter

gene expression to sertoli cells during mouse gonadal development. *Biol. Reprod.*, 76(1):85–95, January 2007.

[121] Jacques J Tremblay, Frédéric Hamel, and Robert S Viger. Protein kinase A-dependent cooperation between GATA and CCAAT/enhancer-binding protein transcription factors regulates steroidogenic acute regulatory protein promoter activity. *Endocrinology*, 143(10):3935–45, October 2002.

[122] Boris Thurisch, Shermi Y Liang, Nanette Sarioglu, Lutz Schomburg, Jörg Bungert, and Christof Dame. Transgenic mice expressing small interfering RNA against Gata4 point to a crucial role of Gata4 in the heart and gonads. *J. Mol. Endocrinol.*, 43(4):157–69, October 2009.

[123] R S Viger, C Mertineit, J M Trasler, and M Nemer. Transcription factor GATA-4 is expressed in a sexually dimorphic pattern during mouse gonadal development and is a potent activator of the Müllerian inhibiting substance promoter. *Development*, 125(14):2665–75, July 1998.

[124] Nikolay L Manuylov, Fatima O Smagulova, Lyndsay Leach, and Sergei G Tevosian. Ovarian development in mice requires the GATA4-FOG2 transcription complex. *Development*, 135(22):3731–43, November 2008.

[125] Evgeni Efimenko, Maria B Padua, Nikolay L Manuylov, Shawna C Fox, Deborah A Morse, and Sergei G Tevosian. The transcription factor GATA4 is required for follicular development and normal ovarian function. *Dev. Biol.*, 381(1):144–58, September 2013.

[126] Hicham Bouabe and Klaus Okkenhaug. Gene targeting in mice: a review. *Methods Mol. Biol.*, 1064:315–36, January 2013.

[127] Ryszard Kole, Adrian R Krainer, and Sidney Altman. RNA therapeutics: beyond RNA interference and antisense oligonucleotides. *Nat. Rev. Drug Discov.*, 11(2):125–40, February 2012.

[128] J Summerton and D Weller. Morpholino antisense oligomers: design, preparation, and properties. *Antisense Nucleic Acid Drug Dev.*, 7(3):187–95, June 1997.

[129] J Summerton. Morpholino antisense oligomers: the case for an RNase H-independent structural type. *Biochim. Biophys. Acta*, 1489(1):141–58, December 1999.

[130] Jon D Moulton and Shan Jiang. Gene knockdowns in adult animals: PPMOs and vivo-morpholinos. *Molecules*, 14(3):1304–23, January 2009.

[131] Yong-Fu Li and Paul A Morcos. Design and synthesis of dendritic molecular transporter that achieves efficient in vivo delivery of morpholino antisense oligo. *Bioconjug. Chem.*, 19(7):1464–70, July 2008.

[132] Paul A Morcos, Yongfu Li, and Shan Jiang. Vivo-Morpholinos: a non-peptide transporter delivers Morpholinos into a wide array of mouse tissues. *Biotechniques*, 45(6):613–4, 616, 618 passim, December 2008.

[133] Sunny Hartwig, Jacqueline Ho, Priyanka Pandey, Kenzie Macisaac, Mary Taglienti, Michael Xiang, Gil Alterovitz, Marco Ramoni, Ernest Fraenkel, and Jordan A Kreidberg. Genomic characterization of Wilms' tumor suppressor 1 targets in nephron progenitor cells during kidney development. *Development*, 137(7):1189–203, April 2010.

[134] Charlotte L J Jacobi, Lucas J Rudigier, Holger Scholz, and Karin M Kirschner. Transcriptional regulation by the Wilms tumor protein, Wt1, suggests a role of the metalloproteinase Adamts16 in murine genitourinary development. *J. Biol. Chem.*, 288(26):18811–24, June 2013.

[135] Karin M Kirschner, Julian F W Braun, Charlotte L Jacobi, Lucas J Rudigier, Anja Bondke Persson, and Holger Scholz. Amine oxidase copper-containing 1 (AOC1) is a downstream target gene of the Wilms tumor protein, WT1, during kidney development. *J. Biol. Chem.*, 289(35):24452–62, August 2014.

[136] Fariba Jian Motamedi, Danielle A Badro, Michael Clarkson, M Rita Lecca, Stephen T Bradford, Fabian A Buske, Kathrin Saar, Norbert Hübner, André W Brändli, and Andreas Schedl. WT1 controls antagonistic FGF and BMP-pSMAD pathways in early renal progenitors. *Nat. Commun.*, 5:4444, January 2014.

[137] R R Behringer. The in vivo roles of müllerian-inhibiting substance. *Curr. Top. Dev. Biol.*, 29:171–87, January 1994.

[138] Amalia Sertedaki, Kostas Pantos, Christina Vrettou, Georgia Kokkali, Christina Christofidou, Emmanouel Kanavakis, and Catherine Dacou-Voutetakis. Conception and pregnancy outcome in a patient with 11-bp deletion of the steroidogenic acute regulatory protein gene. *Fertil. Steril.*, 91(3):934.e15–8, March 2009.

[139] A Swain, E Zanaria, A Hacker, R Lovell-Badge, and G Camerino. Mouse Dax1 expression is consistent with a role in sex determination as well as in adrenal and hypothalamus function. *Nat. Genet.*, 12(4):404–9, April 1996.

[140] Steven J Clapcote and John C Roder. Simplex PCR assay for sex determination in mice. *Biotechniques*, 38(5):702, 704, 706, May 2005.

[141] Fei Gao, Jun Zhang, Xiaona Wang, Junling Yang, Dahua Chen, Vicki Huff, and Yi-Xun Liu. Wt1 functions in ovarian follicle development by regulating granulosa cell differentiation. *Hum. Mol. Genet.*, 23(2):333–41, January 2014.

[142] Nicolas Kalfa, Marc Fellous, Brigitte Boizet-Bonhoure, Catherine Patte, Pierre Duvillard, Catherine Pienkowski, Francis Jaubert, Aude Ecochard, and Charles Sultan. Aberrant expression of ovary determining gene FOXL2 in the testis and juvenile granulosa cell tumor in children. *J. Urol.*, 180(4 Suppl):1810–3, October 2008.

[143] S H Larsson, J P Charlieu, K Miyagawa, D Engelkamp, M Rassoulzadegan, A Ross, F Cuzin, V van Heyningen, and N D Hastie. Subnuclear localization of WT1 in splicing or transcription factor domains is regulated by alternative splicing. *Cell*, 81(3):391–401, May 1995.

[144] K Sainio, P Hellstedt, J A Kreidberg, L Saxén, and H Sariola. Differential regulation of two sets of mesonephric tubules by WT-1. *Development*, 124(7):1293–9, April 1997.

[145] T Svingen, C M Spiller, K Kashimada, V R Harley, and P Koopman. Identification of suitable normalizing genes for quantitative real-time RT-PCR analysis of gene expression in fetal mouse gonads. *Sex Dev.*, 3(4):194–204, January 2009.

[146] Sandy von Salisch, Martin Klar, Boris Thurisch, Jörg Bungert, and Christof Dame. Gata4 and Sp1 regulate expression of the erythropoietin receptor in cardiomyocytes. *J. Cell. Mol. Med.*, 15(9):1963–72, September 2011.

[147] Séverine Mazaud Guittot, Marie France Bouchard, Jean-Philippe Robert-Grenon, Claude Robert, Cynthia G Goodyer, David W Silversides, and Robert S Viger. Conserved usage of alternative 5' untranslated exons of the GATA4 gene. *PLoS One*, 4(12):e8454, January 2009.

[148] Séverine Mazaud-Guittot, Bruno Prud'homme, Marie France Bouchard, Francis Bergeron, Caroline Daems, Sergei G Tevosian, and Robert S Viger. GATA4 autoregulates its own expression in mouse gonadal cells via its distal 1b promoter. *Biol. Reprod.*, 90(2):25, February 2014.

[149] U Mittwoch. Males, females and hermaphrodites. An inaugural lecture delivered by Professor Ursula Mittwoch at University College London on 24 October 1985. *Ann. Hum. Genet.*, 50(Pt 2):103–21, May 1986.

[150] Thomas A Natoli, Julia A Alberta, Alex Bortvin, Mary E Taglienti, Douglas B Menke, Jan Loring, Rudolf Jaenisch, David C Page, David E Housman, and

Jordan a Kreidberg. Wt1 functions in the development of germ cells in addition to somatic cell lineages of the testis. *Dev. Biol.*, 268(2):429–40, April 2004.

[151] Nicole Wagner, Kay-Dietrich Wagner, Gunnar Schley, Sarah E Coupland, Heinrich Heimann, Rosemarie Grantyn, and Holger Scholz. The Wilms' tumor suppressor Wt1 is associated with the differentiation of retinoblastoma cells. *Cell Growth Differ.*, 13(7):297–305, July 2002.

[152] Anne-Amandine Chassot, Isabelle Gillot, and Marie-Christine Chaboissier. R-spondin1, WNT4, and the CTNNB1 signaling pathway: strict control over ovarian differentiation. *Reproduction*, 148(6):R97–R110, December 2014.

[153] Pascal Bernard, Janelle Ryan, Helena Sim, Daniel P Czech, Andrew H Sinclair, Peter Koopman, and Vincent R Harley. Wnt signaling in ovarian development inhibits Sf1 activation of Sox9 via the Tesco enhancer. *Endocrinology*, 153(2):901–12, February 2012.

[154] Bradley W Doble and James R Woodgett. GSK-3: tricks of the trade for a multi-tasking kinase. *J. Cell Sci.*, 116(Pt 7):1175–86, April 2003.

[155] Blanche Capel and Jordan Batchvarov. Sex chromatin staining in amnion cells. *CSH Protoc.*, 2008:pdb.prot5079, January 2008.

[156] K M Georgas, H S Chiu, E Lesieur, B A Rumballe, and Melissa H Little. Expression of metanephric nephron-patterning genes in differentiating mesonephric tubules. *Dev. Dyn.*, 240(6):1600–12, June 2011.

[157] Kei Takasawa, Kenichi Kashimada, Emanuele Pelosi, Masatoshi Takagi, Tomohiro Morio, Hiroshi Asahara, David Schlessinger, Shuki Mizutani, and Peter Koopman. FOXL2 transcriptionally represses Sf1 expression by antagonizing WT1 during ovarian development in mice. *FASEB J.*, 28(5):2020–8, May 2014.

[158] Ali M Riazi, Jun K Takeuchi, Lisa K Hornberger, Syed Hassan Zaidi, Fariba Amini, John Coles, Benoit G Bruneau, and Glen S Van Arsdell. NKX2-5 regulates the expression of beta-catenin and GATA4 in ventricular myocytes. *PLoS One*, 4(5):e5698, January 2009.

[159] Kay-Dietrich Wagner, Nicole Wagner, Valerie P I Vidal, Gunnar Schley, Dagmar Wilhelm, Andreas Schedl, Christoph Englert, and Holger Scholz. The Wilms' tumor gene Wt1 is required for normal development of the retina. *EMBO J.*, 21(6):1398–405, March 2002.

[160] Dong Liang, Wenshuang Jia, Jingyun Li, Kui Li, and Qingshun Zhao. Retinoic acid signaling plays a restrictive role in zebrafish primitive myelopoiesis. *PLoS One*, 7(2):e30865, January 2012.

[161] George Wolf. Retinoic acid as cause of cell proliferation or cell growth inhibition depending on activation of one of two different nuclear receptors. *Nutr. Rev.*, 66(1):55–9, January 2008.

[162] Yang-li Dai, Jun-Fen Fu, Fang Hong, Shan Xu, and Zheng Shen. WT1 mutation as a cause of 46 XY DSD and Wilm's tumour: a case report and literature review. *Acta Paediatr.*, 100(7):e39–42, July 2011.

[163] K Theiler. *The House Mouse: Atlas of Embryonic Development*. Springer New York, 1989.

[164] M L Barr and Bertram. A morphological distinction between neurones of the male and female, and the behaviour of the nucleolar satellite during accelerated nucleoprotein synthesis. *Nature*, 163(4148):676, April 1949.

[165] Andreas Steege, Michael Fähling, Alexander Paliege, Anja Bondke, Karin M Kirschner, Peter Martinka, Charlotte Kaps, Andreas Patzak, Pontus B Persson, Bernd J Thiele, Holger Scholz, and Ralf Mrowka. Wilms' tumor protein (-KTS) modulates renin gene transcription. *Kidney Int.*, 74(4):458–66, August 2008.

[166] Christian W Warburg O. Protein estimation by extinction at 260 nm and 280 nm. *Biochem Zeitschrift*, 310:384–392, 1941.

[167] Johannes Schindelin, Ignacio Arganda-Carreras, Erwin Frise, Verena Kaynig, Mark Longair, Tobias Pietzsch, Stephan Preibisch, Curtis Rueden, Stephan Saalfeld, Benjamin Schmid, Jean-Yves Tinevez, Daniel James White, Volker Hartenstein, Kevin Eliceiri, Pavel Tomancak, and Albert Cardona. Fiji: an open-source platform for biological-image analysis. *Nat. Methods*, 9(7):676–82, July 2012.

[168] R Core Team. *R: A Language and Environment for Statistical Computing*. Vienna, Austria, 2014.

[169] Hadley Wickham. *ggplot2: elegant graphics for data analysis*. Springer New York, 2009.

# Selbstständigkeitserklärung

Hiermit erkläre ich, dass ich diese Arbeit selbstständig verfasst und keine anderen als die angegeben Hilfsmittel und Quellen verwendet habe. Ferner versichere ich, dass diese Arbeit in dieser oder ähnlicher Form keiner anderen Prüfungsbehörde vorgelegt wurde.

Lucas Johannes Rudigier

Berlin, March 2015

# Curriculum Vitae

Lucas Johannes Rudigier

*Curriculum Vitae*

For reasons of data protection, the curriculum vitae is not published in the online version